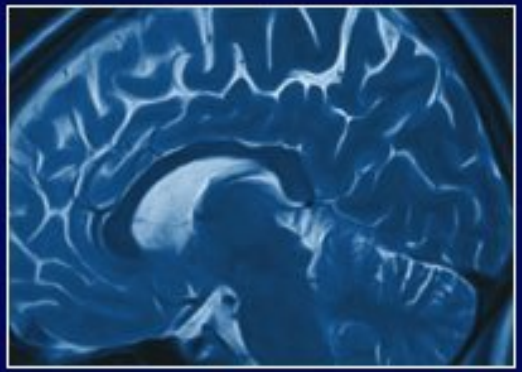

The Waisman Laboratory for Brain Imaging and Behavior

University of Wisconsin SCHOOL OF MEDICINE AND PUBLIC HEALTH

Introduction to DTI Processing and Analysis with MATLAB

Moo K. Chung
Waisman Laboratory for Brain Imaging and Behavior
Department of Biostatistics and Medical Informatics
University of Wisconsin-Madison

www.stat.wisc.edu/~mchung

Waisman Laboratory for Brain Imaging and Behavior, Madison

http://brainimaging.waisman.wisc.edu

Acknowledgements

Jamie Hanson, Nagesh Adluru,
Andrew L. Alexander, Seth Pollack,
Richard J. Davidson

University of Wisconsin-Madison


Seth Pollack


Nagesh Adluru


Moo Chung


Richard Davidson


Jamie Hanson

Abstract

The main challenge in processing DTI is caused by the non-Euclidean nature of diffusion tensor, which is a symmetric and positive definite matrix at each voxel. This requires new computational solutions in smoothing, registering and performing tractography. In this introductory tutorial, publically available MRI and DTI processing and analysis tools will be introduced and the underlying principle will be discussed. MATLAB demonstration for performing simple DTI processing is given. The demonstration is based on methods introduced in Chung et al (2010, Statistics and Its Interface 3:69-80) http://www.stat.wisc.edu/~mchung/papers/chung.2010.SII.pdf.

The MATLAB codes and lecture material will be available through http://brainimaging.waisman.wisc.edu/~chung/DTI/
Students are encouraged to bring their own laptop and follow through the MATLAB demonstration with the instructor.

Diffusion Tensor Imaging

Brain White Matter Fibers

Temporal genu of optic radiation

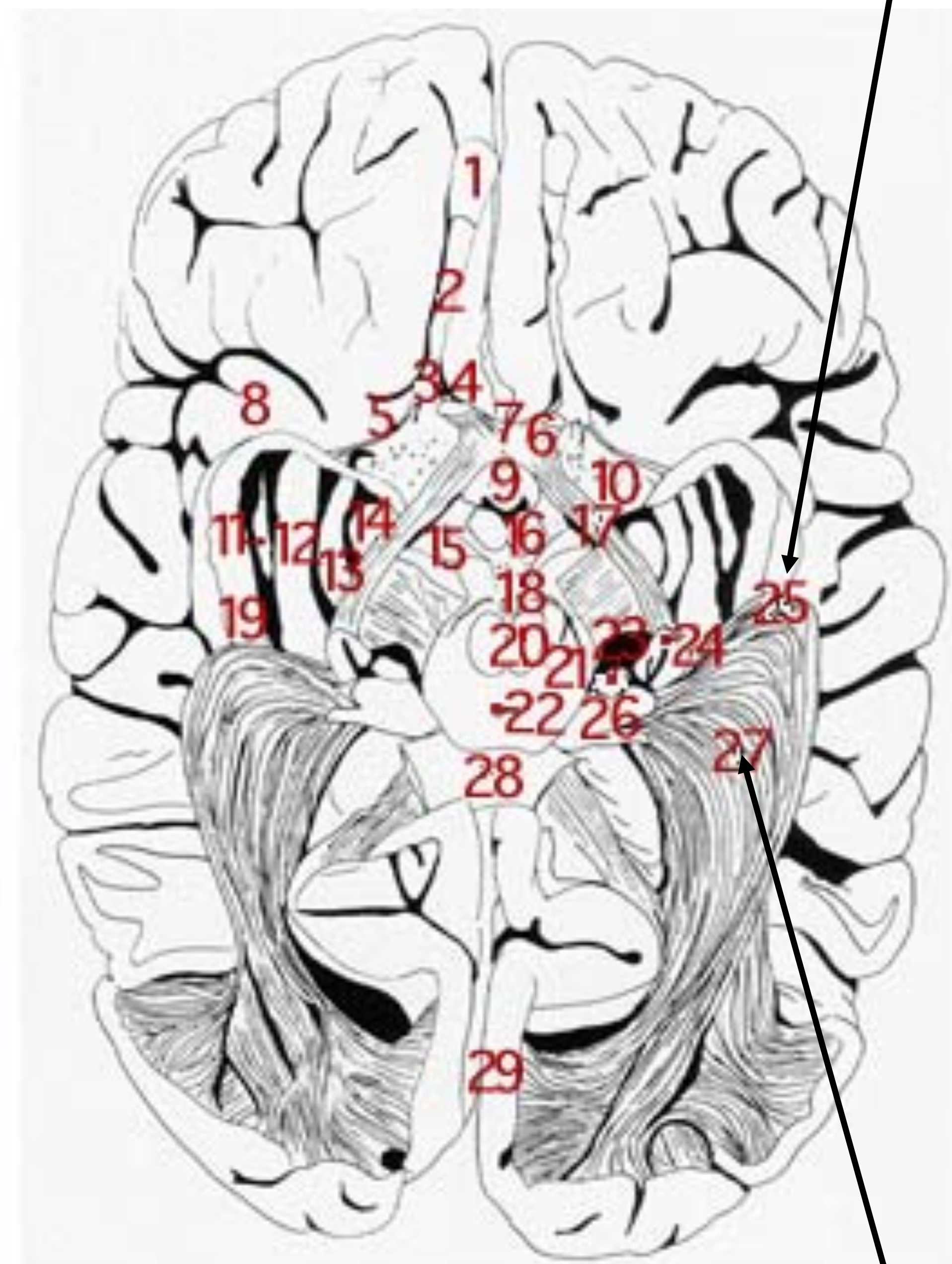

1. Olfactory bulb
2. Olfactory tract
3. Olfactory trigone
4. Medial olfactory stria
5. Lateral olfactory stria
6. Optic nerve

Sagittal stratum

Source: www.vh.org

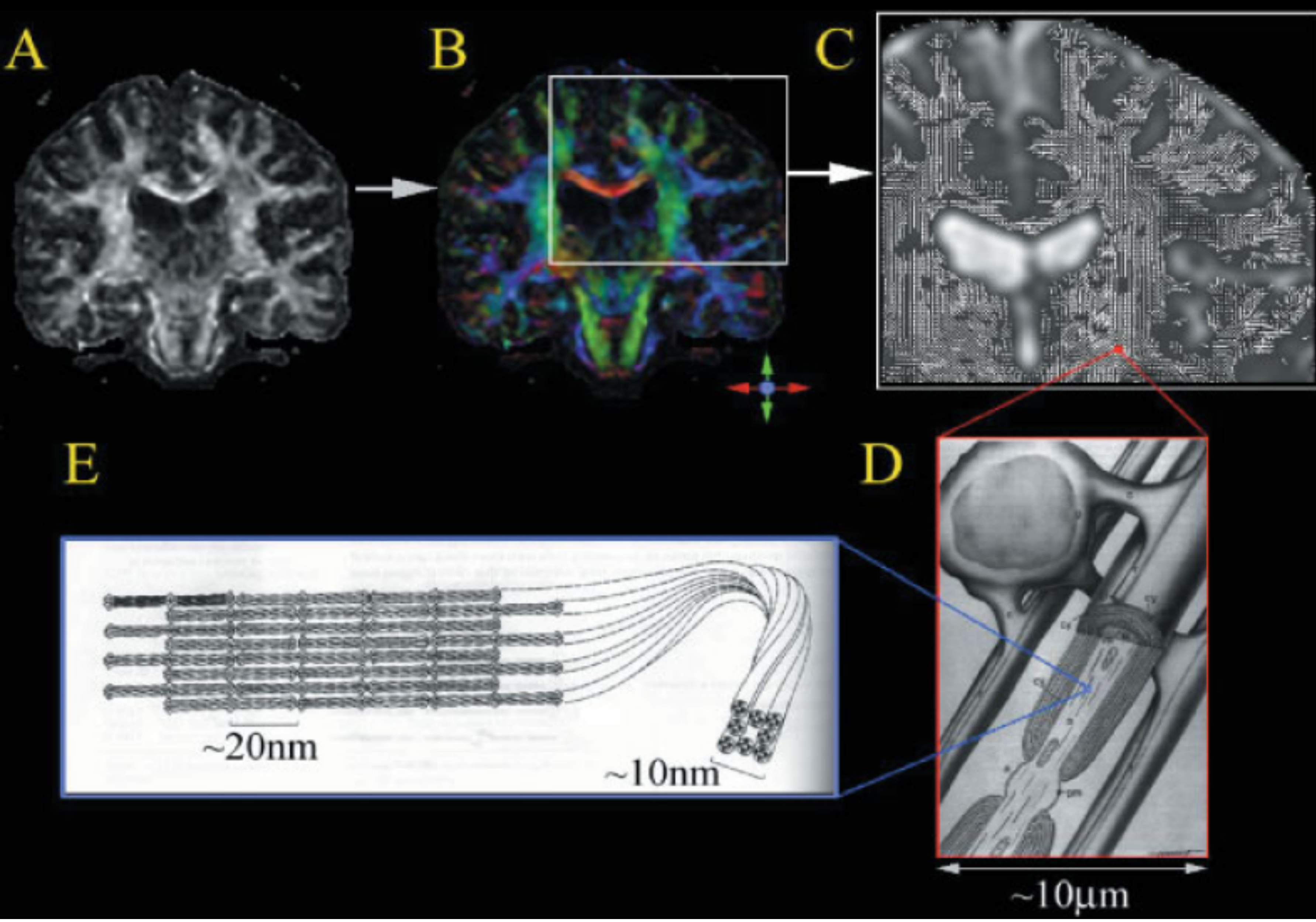

Figure 1. Schematic diagram of the white matter structure and its relationship with the information provided by DTI-based images, such as anisotropy maps (A), have sufficient resolution to segment white and gray matter. By incorporating DTI orientation information, white matter can be parcellated into various tracts using a color-coded map (B) or a vector map (C). The image resolution is sufficient to delineate large white matter tracts, which mostly consist of neuroglia and axons that are largely running parallel. A pixel thus contains bundles of axons and neuroglial cells (D). Note that the size of a pixel (C) is on the order of mm but that the size of the cells (D) is on the order of μm. The axon is filled with neuronal filaments (E) running along its longitudinal axis, which may contribute in superimposing anisotropy on the direction of water diffusion. In the color-coded map, red indicates fibers running along the right–left direction, green inferior–superior, and blue anterior–posterior (perpendicular to the plane). The figures (D) and (E) were reproduced from Carpenter[49] and Alberts *et al.*[64] respectively with permission

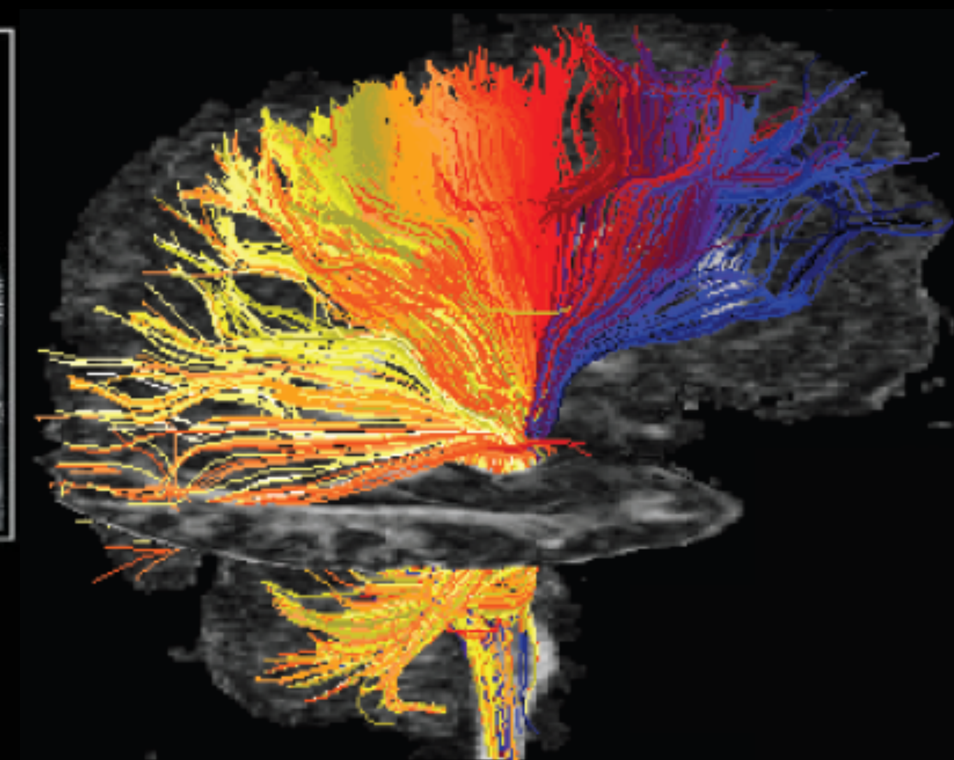

Mori and van Zijl
NMR Biomed 2002

Diffusion Tensor Imaging

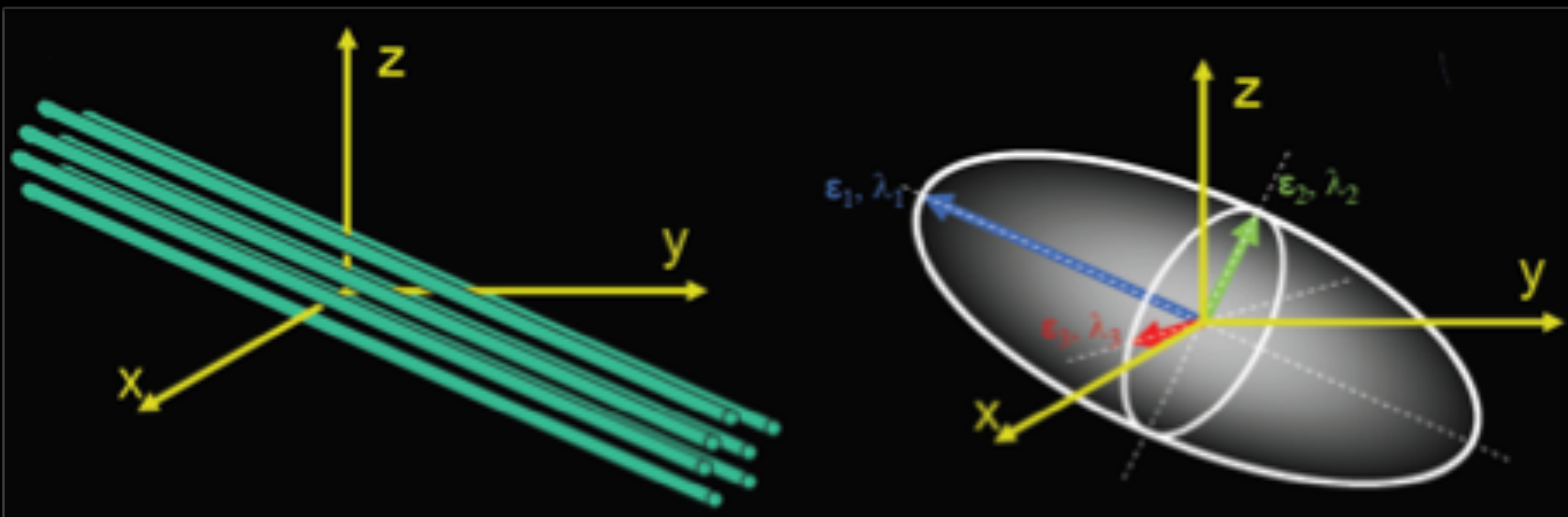

The movement of anisotropic water diffusion can be measured using DTI

↓

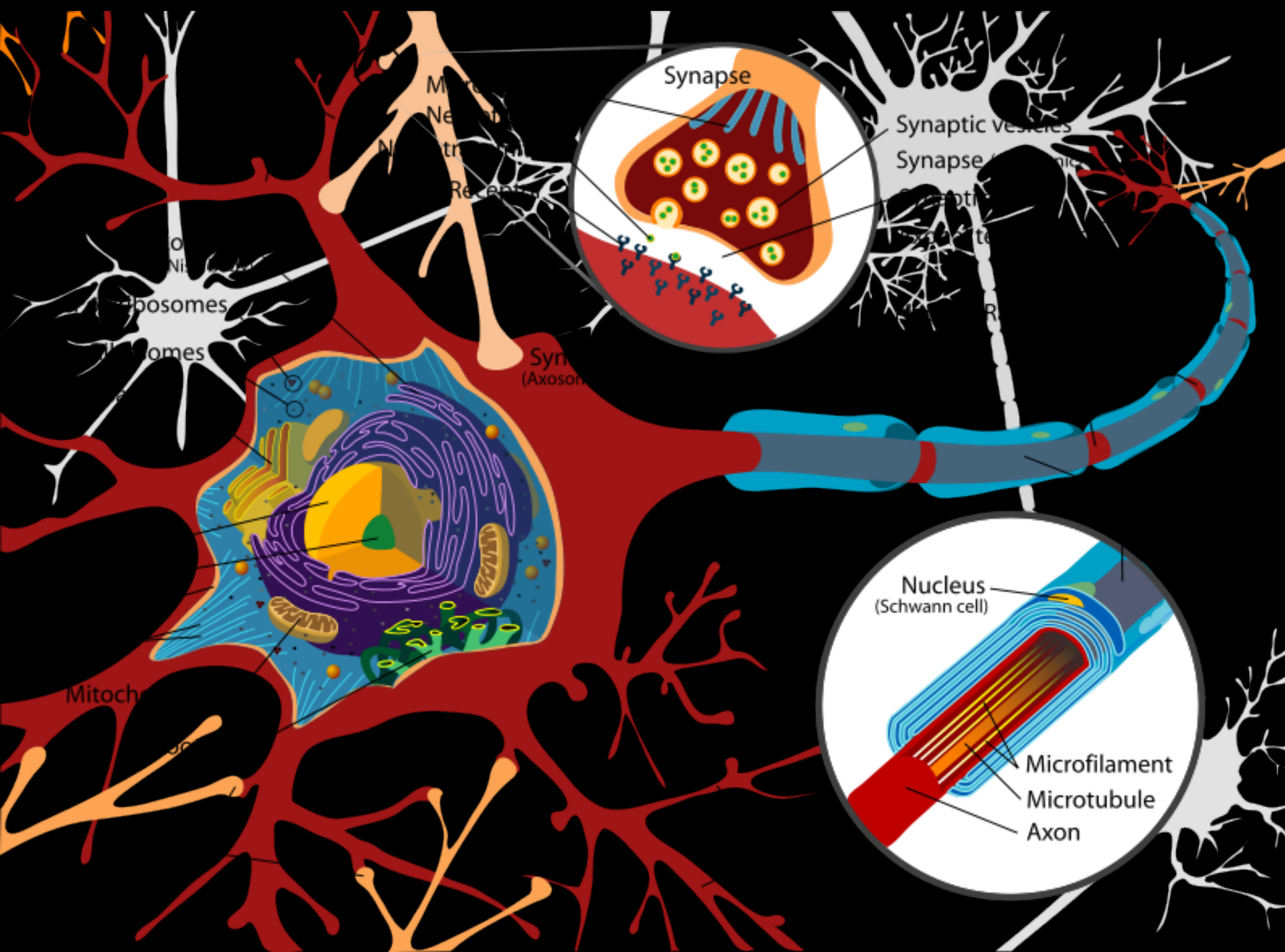

The direction of neuronal filaments in the axon dictates the movement of water diffusion.

Backwardness of human neuroanatomy

Francis Crick and Edward Jones

To interpret the activity of living human brains, their neuroanatomy must be known in detail. New techniques to do this are urgently needed, since most of the methods now used on monkeys cannot be used on humans.

OVER the past 20 years there have been great advances in understanding the neuroanatomy of the macaque monkey, especially its cerebral cortex. We have learned much about the functional parcellation of the monkey's cortex from both anatomical and physiological studies. We know, for example, that rather

Most of the MRI scans used, although of high resolution, are static; they show structure but not activity. Such a scan can picture, for example, exactly how the cerebral cortex is folded in a particular individual but not what part is functionally active. The spatial resolution of classical MRI is now 1 mm or less so that

that for the macaque shown in Fig. 1? And what does the human equivalent of the connectional map of Fig. 2 look like? The shameful answer is that we do not have such detailed maps because, for obvious reasons, most of the experimental methods used on the macaque brain cannot be used on humans.

Crick, F and Jones, E. 1993. Nature 362:109-110

Macaque cortical map

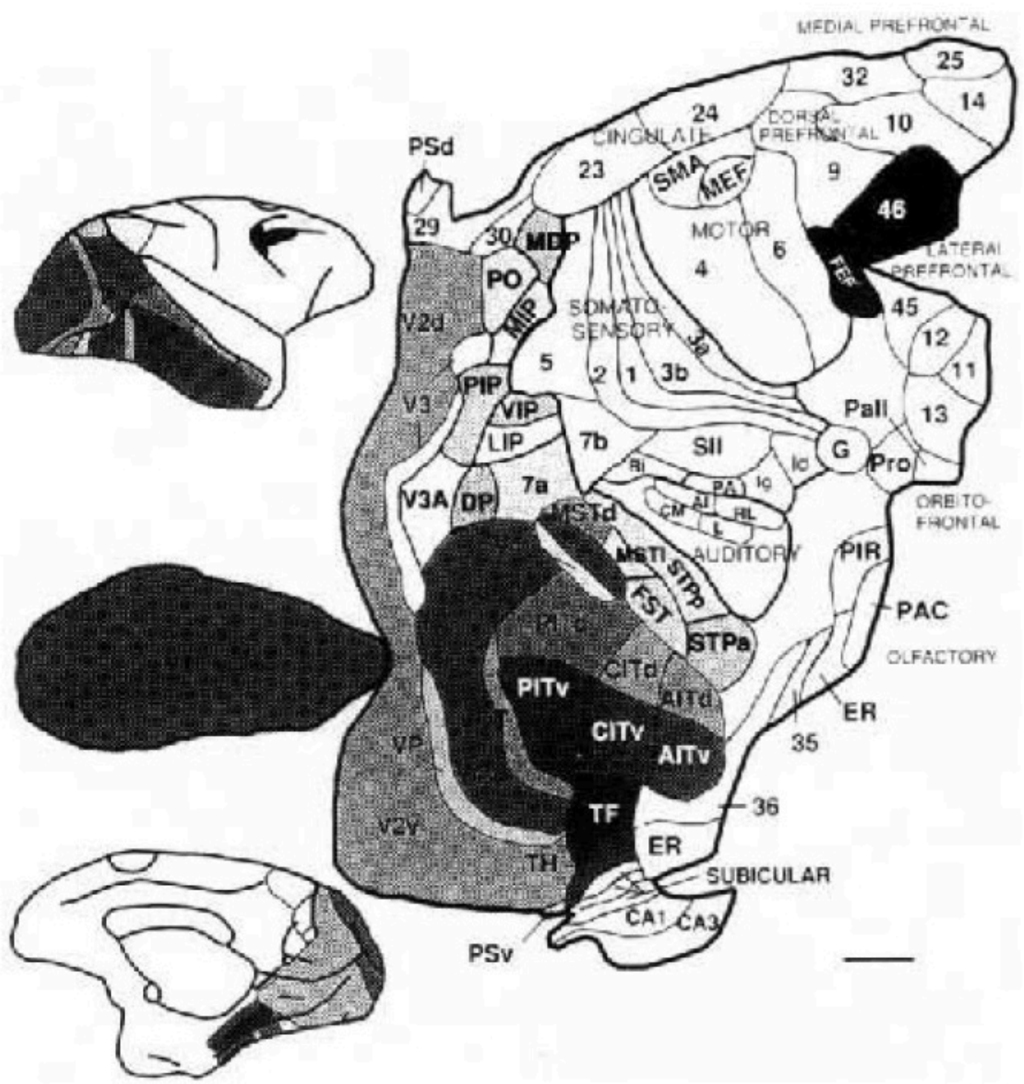

Connectional map of visual area

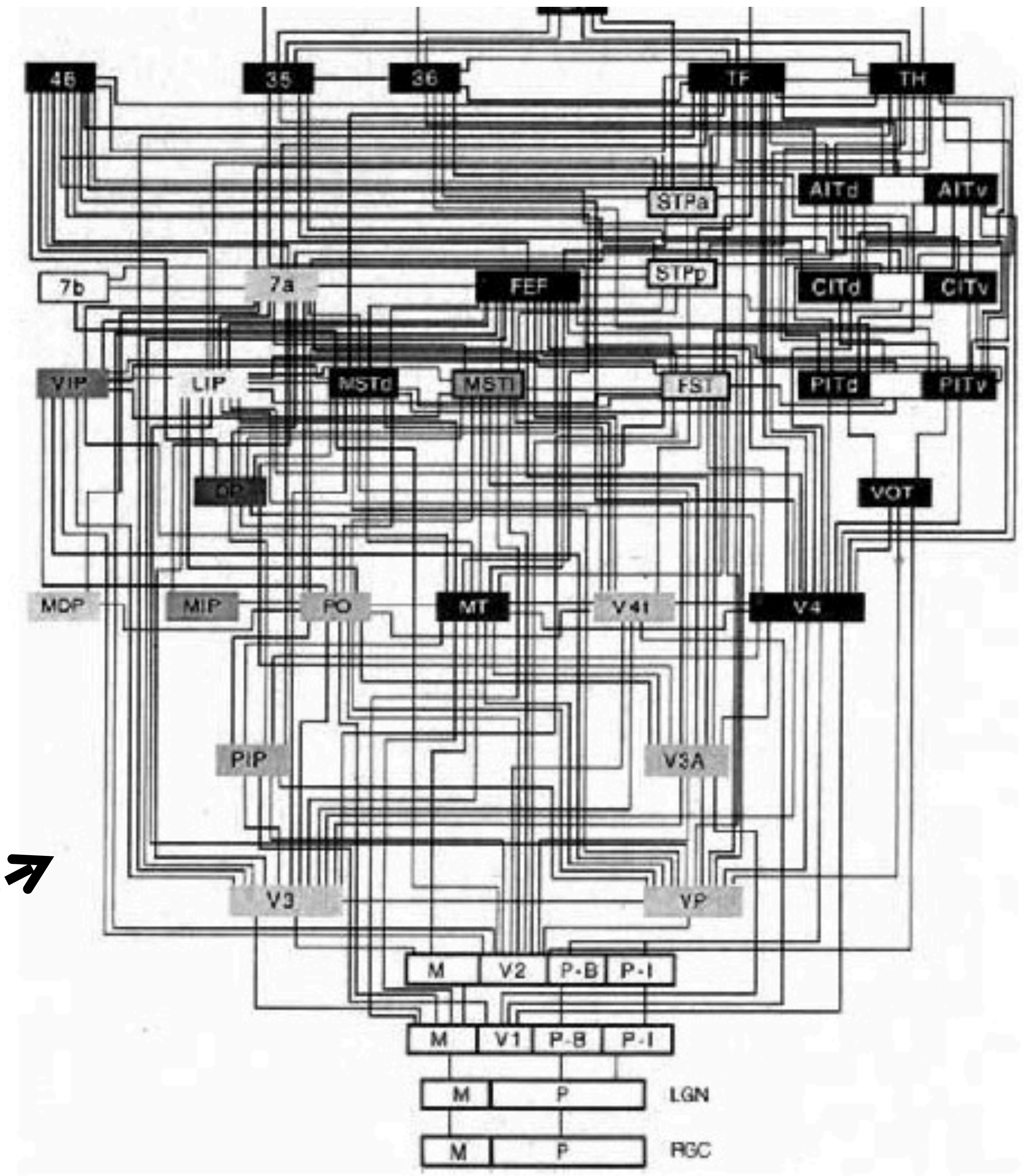

What we can say about the neuroanatomy of the human brain?

Outdated technique

Another new method that at last permits the tracing of connections in fixed postmortem material is the use of lipid stains such as the carbocyanine dye diI[10] or one of its relatives. This spreads along axons by a diffusion process so that, in general, it is a slow method: to go 10 times as far takes 100 times as long. It could take many months to spread through the full extent of a long pathway, so there are time limitations on using it to establish the longer connections. Nevertheless, the method is now

New technique

Diffusion Tensor Imaging (DTI)

Diffusion Tensor

Mori and van Zijl NMR Biomed 2002

isotropic diffusion

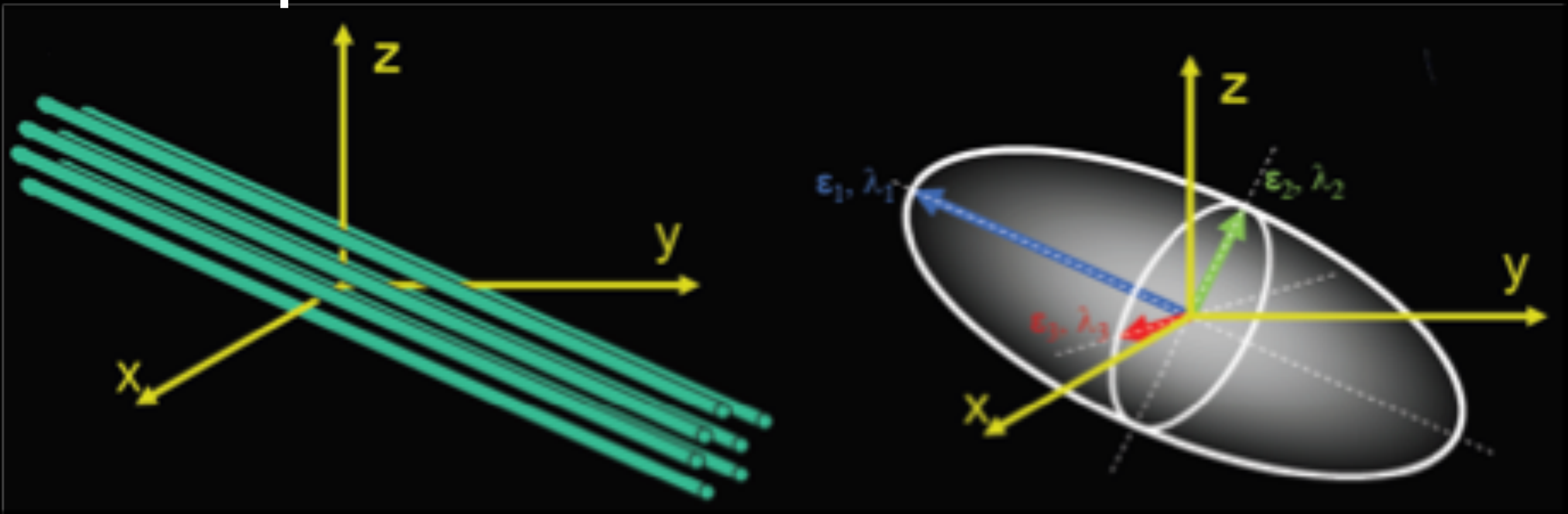

anisotropic diffusion

diffusion tensor

$$p(x \mid x_o, \tau) = \frac{1}{\sqrt{(4\pi\tau)^3 |\underline{D}|}} \exp\left(\frac{-(x - x_0)^T \underline{D}^{-1} (x - x_0)}{4\tau} \right)$$

transition probability from x_0 to x

Diffusion Tensor/ diffusion coefficients

$$\mathbf{D} = \begin{pmatrix} D_{xx} & D_{xy} & D_{xz} \\ D_{yx} & D_{yy} & D_{yz} \\ D_{zx} & D_{zy} & D_{zz} \end{pmatrix} = \mathbf{E} \begin{pmatrix} \lambda_1 & 0 & 0 \\ 0 & \lambda_2 & 0 \\ 0 & 0 & \lambda_3 \end{pmatrix} \mathbf{E}$$

Diffusion Tensor

Eigenvalues

Matrix of 3 eigenvectors

$$\mathbf{D} = \begin{pmatrix} D_{xx} & D_{xy} & D_{xz} \\ D_{yx} & D_{yy} & D_{yz} \\ D_{zx} & D_{zy} & D_{zz} \end{pmatrix} =$$

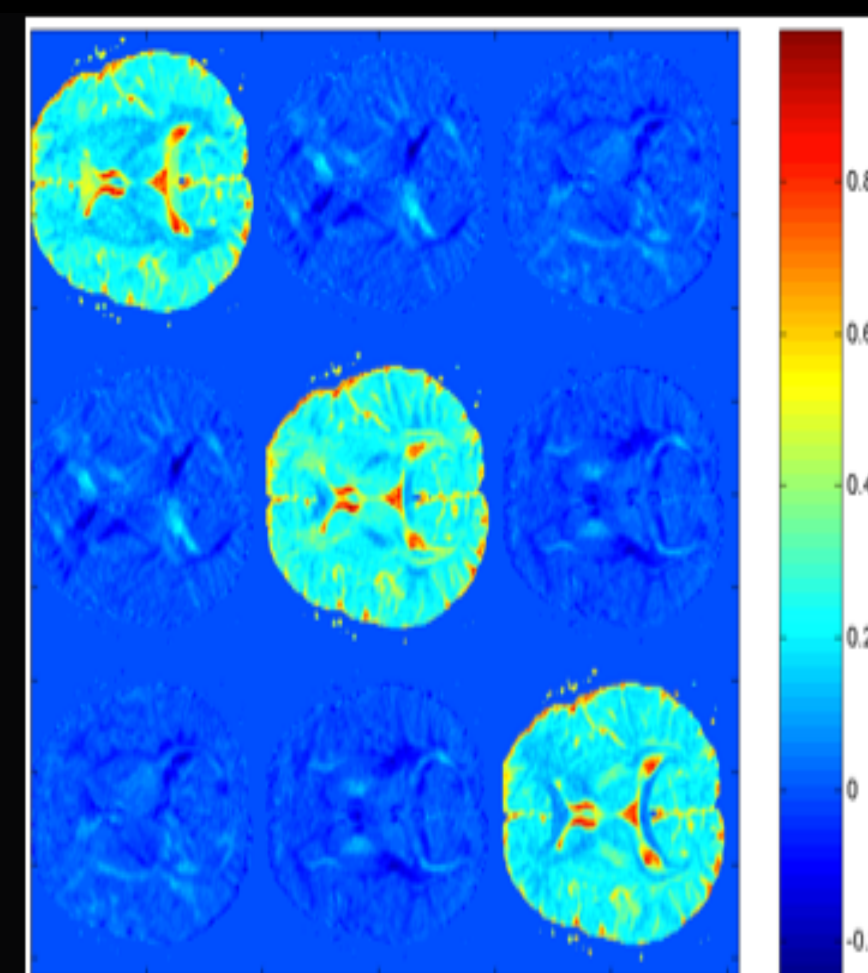

$$D_{xx}, D_{yy}, D_{zz} > 0 \qquad D_{xy} = D_{yx}; D_{xz} = D_{zx}; D_{yz} = D_{zy}$$

DTI data

6 diffusion coefficient matrix D_xx, D_xy, D_xz, D_yy, D_yz, D_zz

$$D = (d_{ij})$$

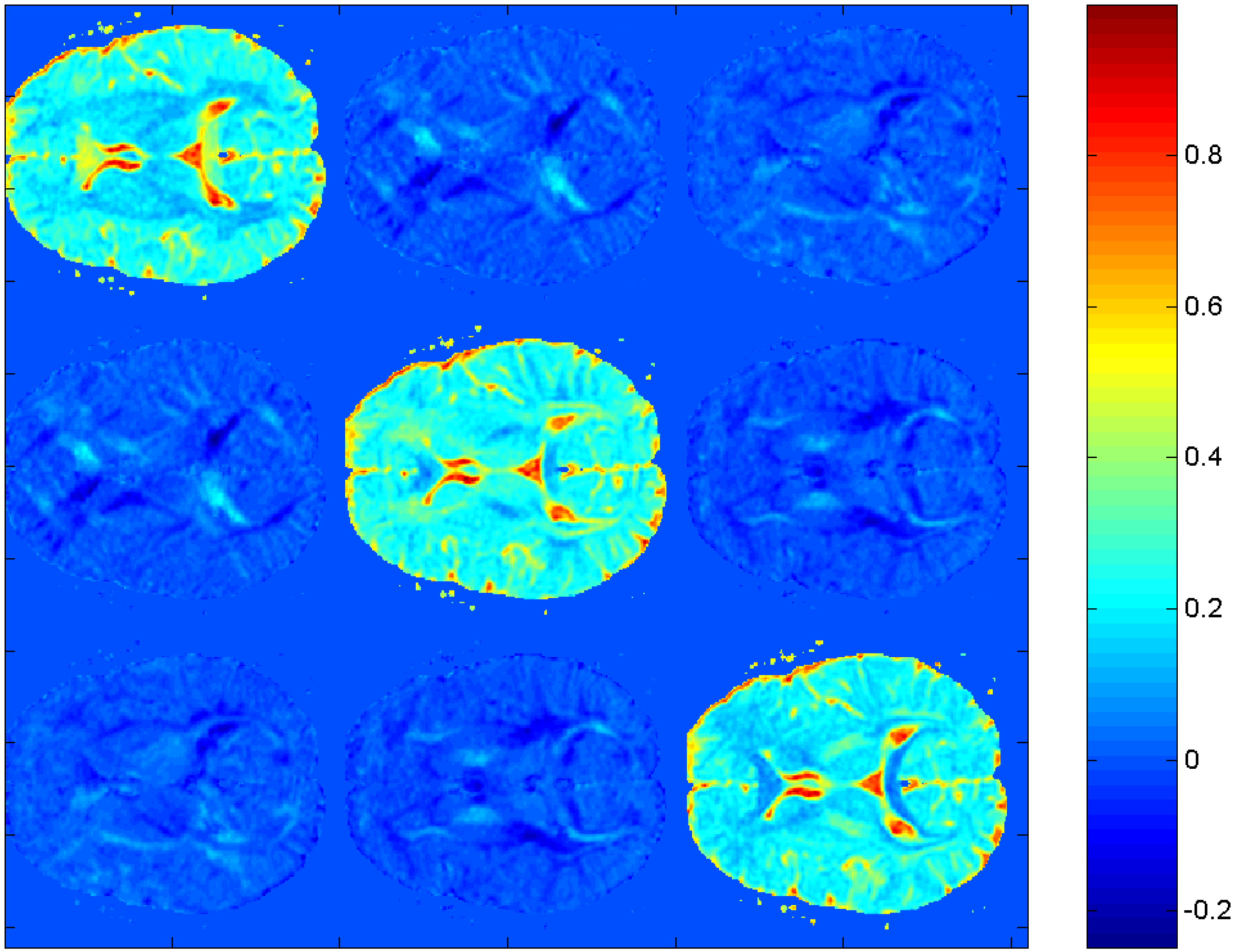

- Diffusion coefficient measures the diffusion of water molecules.
- The principal eigenvector = direction of water molecules.
- This gives indirect information about white matter fibers.

Direction of principal eigenvectors are color coded

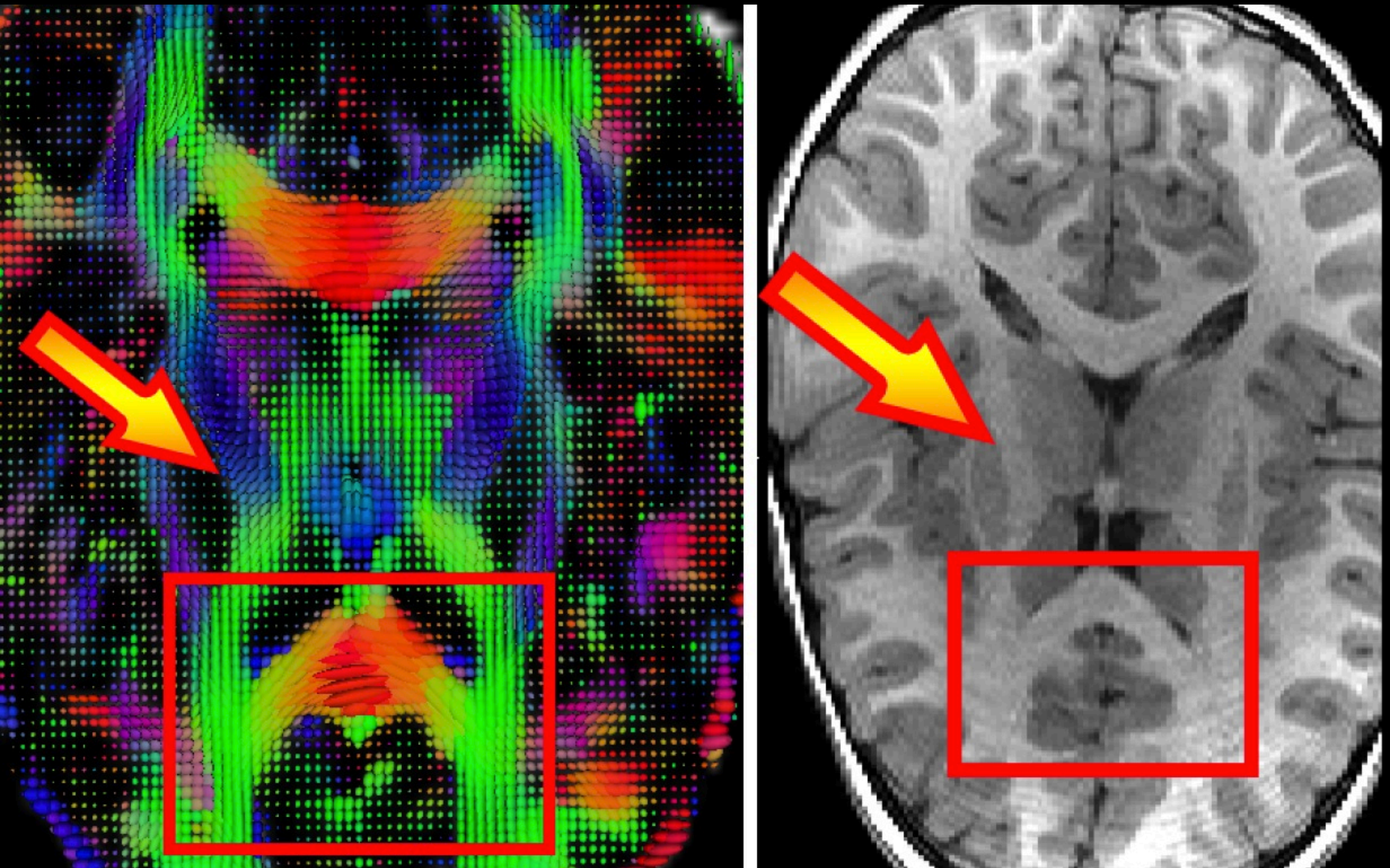

Nagesh Aldur, Univ. of Wisconsin

Simple DTI manipulation MATLAB demo

DTI processing tools

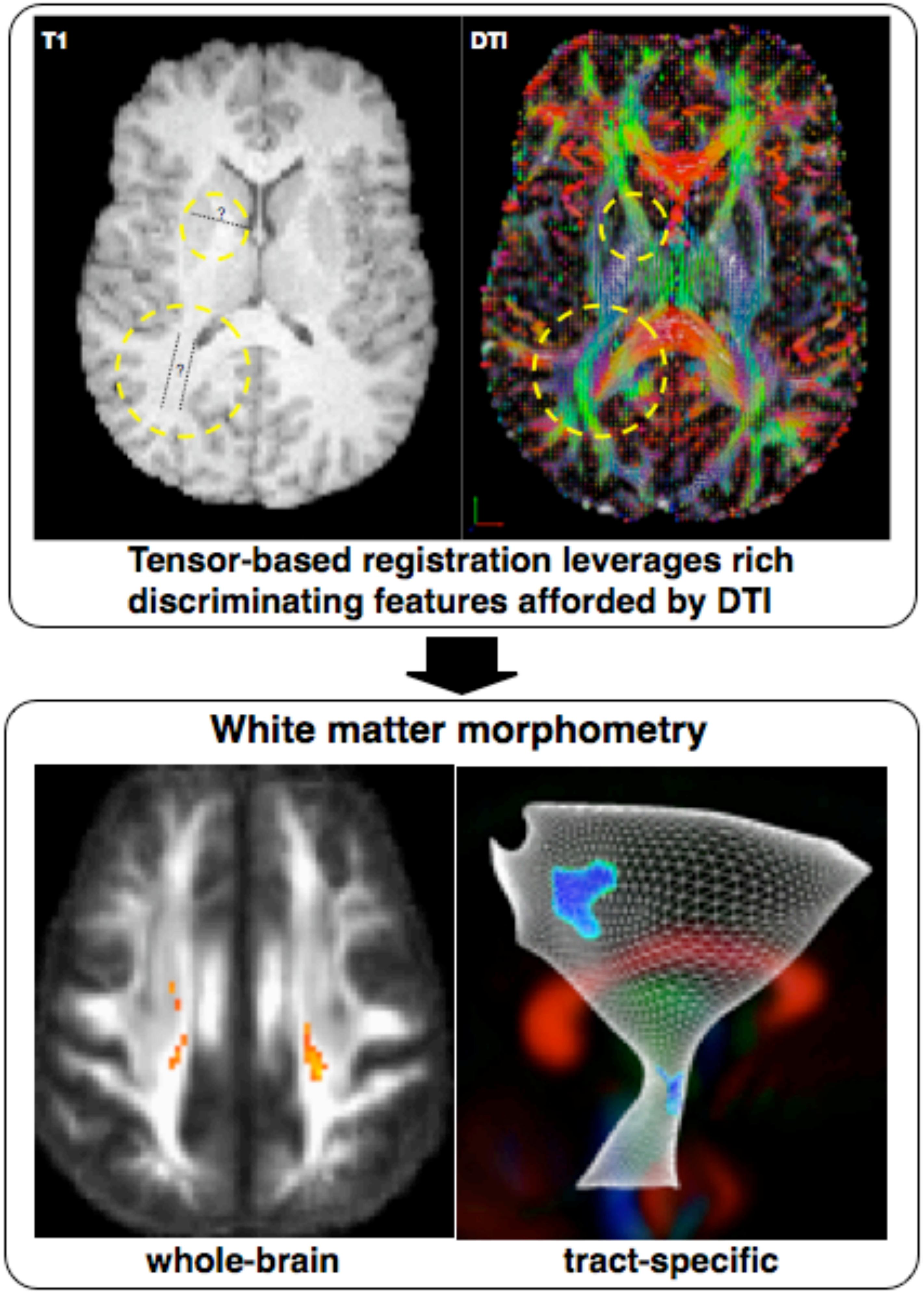

DTI-TK is a spatial normalization & atlas construction toolkit, designed from ground up to support the manipulation of diffusion-tensor images (DTI).

State-of-the-art registration algorithm that drives the alignment of white matter (WM) tracts by matching the orientation of the underlying fiber bundle at each voxel.

Tools: resampling, smoothing, warping, registration & visualization

Camino (reconstruction and tractography)

http://en.wikipedia.org/wiki/Camino

Reconstruction:
Fitting the Diffusion Tensor (DT) to diffusion-weighted MRI data.
Standard scalar measures, such as FA and Tr(D).
Fitting 2 and 3-tensor models.
Advanced reconstruction algorithms including RESTORE,
q-ball, and maximum-entropy spherical deconvolution (including PAS-MRI).

Data synthesis:
Generate synthetic data from standard diffusion tensors, full diffusion tensor images.
other models of diffusion within restricting media, Monte-Carlo simulation

Deterministic and probabilistic tractography (PICo):
Tractography and connectivity mapping with single and multiple tensor models.
Waypoints and multiple-ROI processing.

DT image warping
Preservation of principal directions (PPD)
Finite strain approximation

Simulating DTI

Property of positive definite symmetric matrix

Symmetric positive definite matrix:

$$D = (d_{ij})$$

Symmetry: $D = D'$

Positive definiteness:

For any x, $x' D x > 0$

Cholesky factorization:

$$D = R' R$$

$R = (r_{ij})$ ← upper triangle

Cholesky factorization in MATLAB

```
>> D=[4 2
      2 4]
>> chol(D)
ans =
    2.0000    1.0000
         0    1.7321
```

Simulating positive definite symmetric matrices

Symmetric positive definite matrix:

$$D = (d_{ij})$$

Add Gaussian noise to diffusion tensor:

$$d_{ij} + e_{ij}$$

Add Gaussian noise to Chokesky factor:

$$D = R'R \qquad R = (r_{ij})$$

$$r_{ij} + e_{ij}$$

Smoothing in DTI

Lee, J.E., Chung, M.K. , Alexander, A.L. (2006). Evaluation of anisotropic filters for diffusion tensor imaging. IEEE International Symposium on Biomedical Imaging (ISBI), 1241.

http://www.stat.wisc.edu/~mchung/papers/BMI2006/ISBI.1241.2006.pdf

Implementation:

function [dwData,xform,X,brainMask] = dtiRawSmooth(dwRaw, bvecs, bvals, iter, pmDeltaT)

https://white.stanford.edu/repos/vistasoft/trunk/mrDiffusion/preprocess/dtiRawSmooth.m

Diffusion tensors are noisy.
Need to filter out high frequency noise

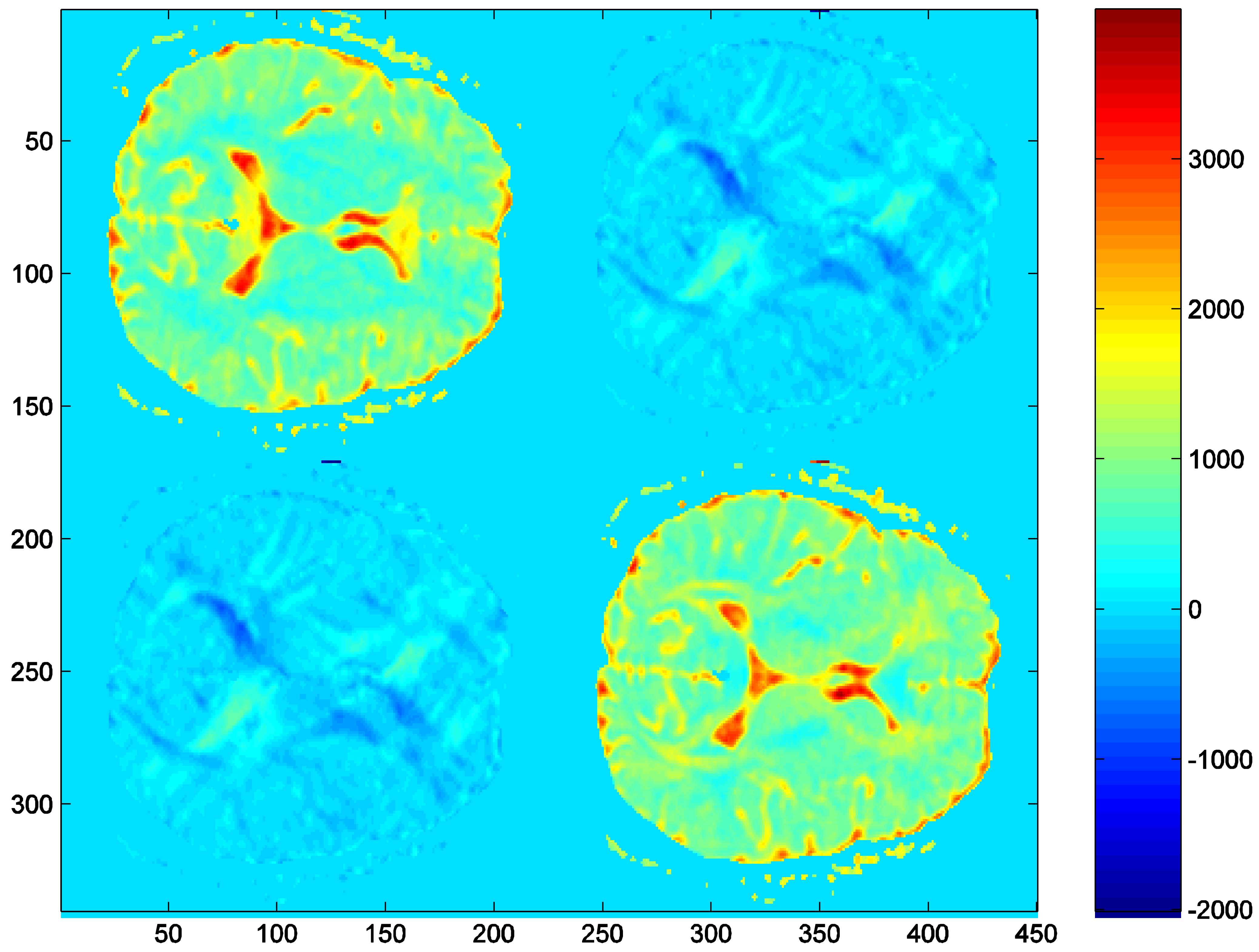

Smoothing DTI via Cholesky factorization

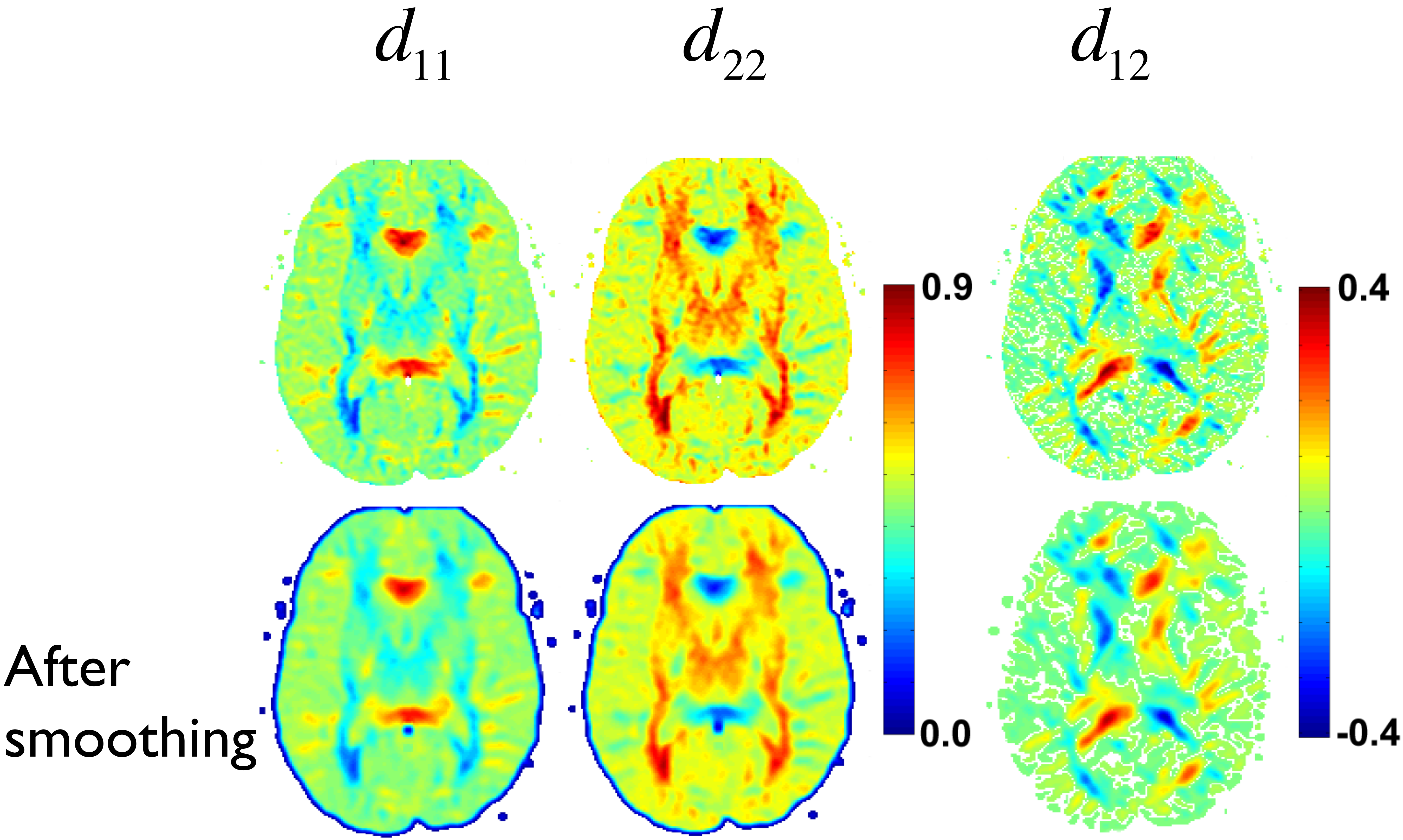

Inverting DTI via smoothing on Cholesky factor

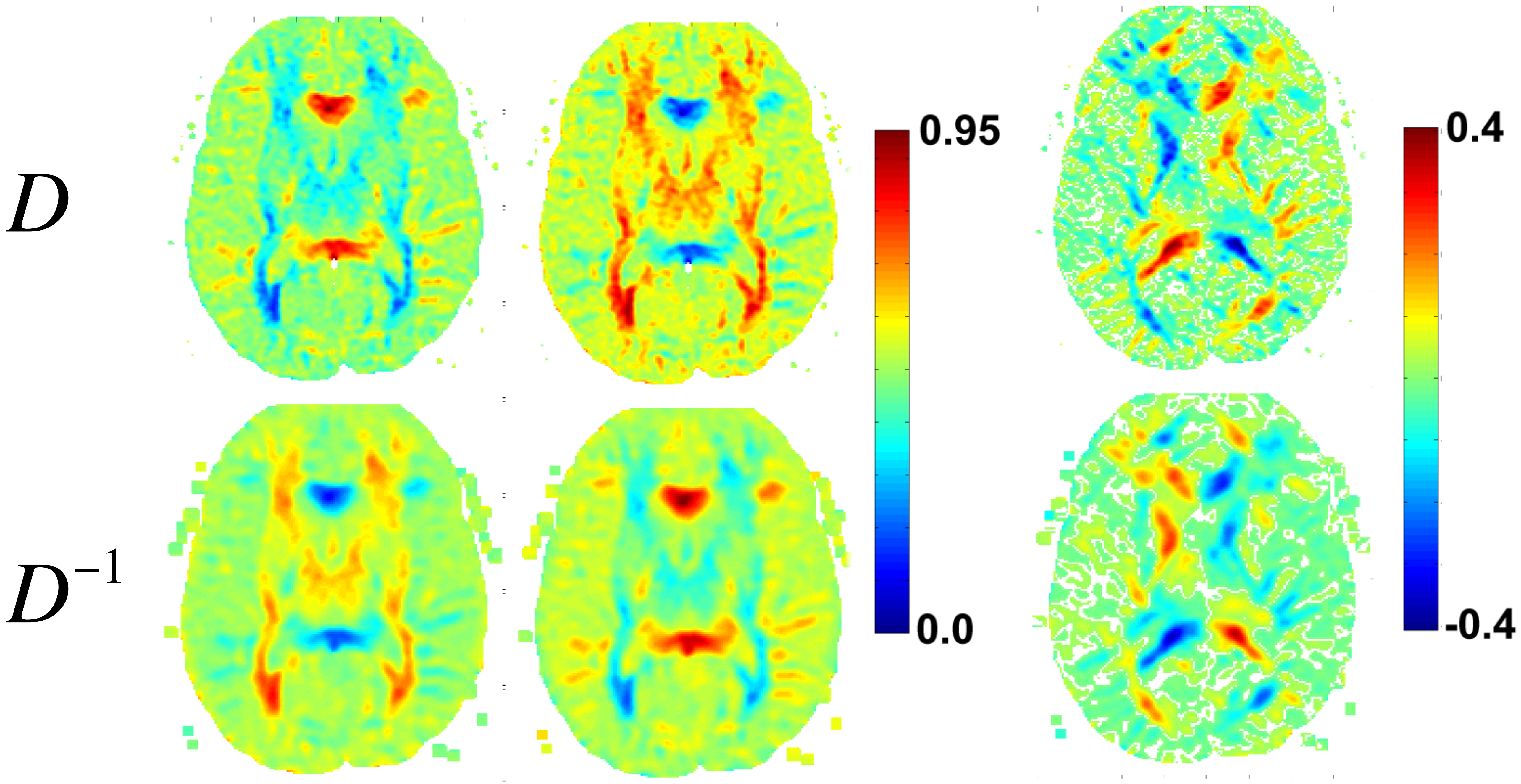

Spatially adaptive kernel smoothing on DTI

Principal eigenvalues

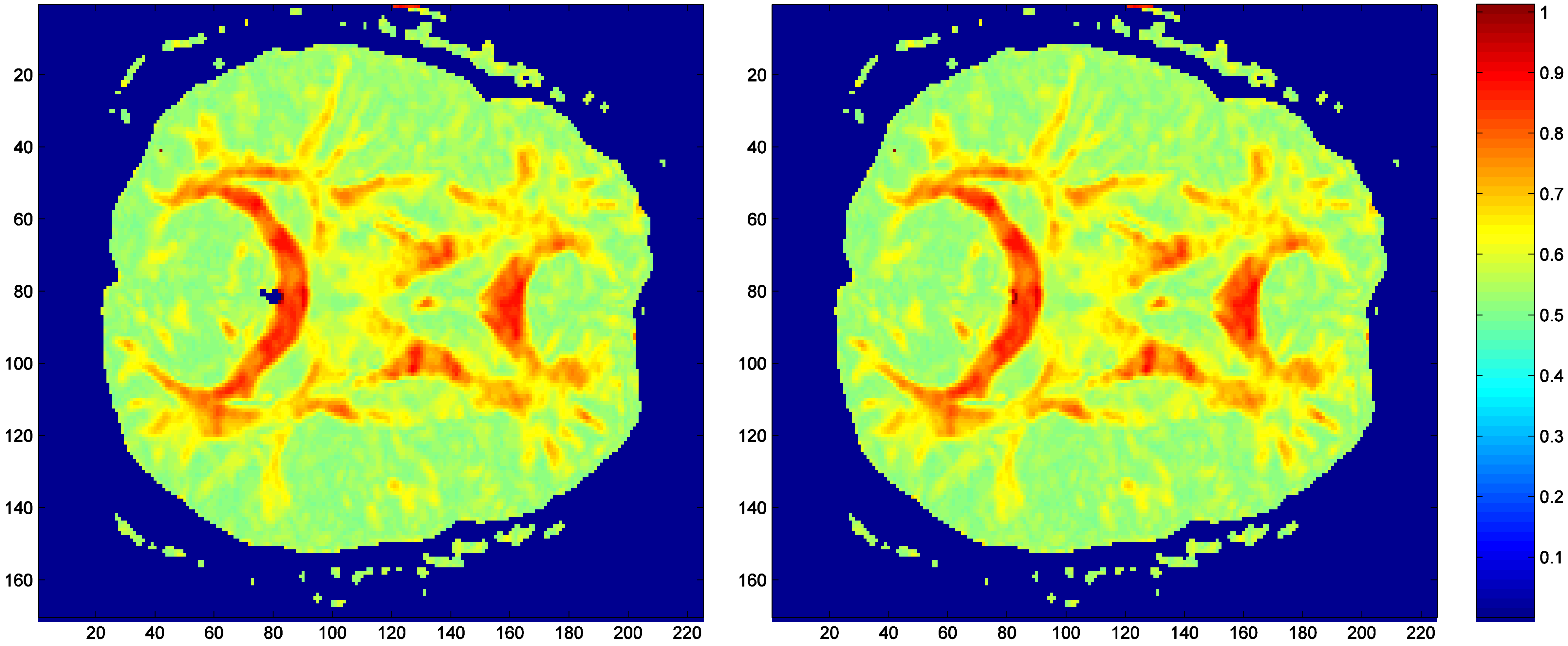

Problem:
Smooth DTI signal along principal eigenvectors

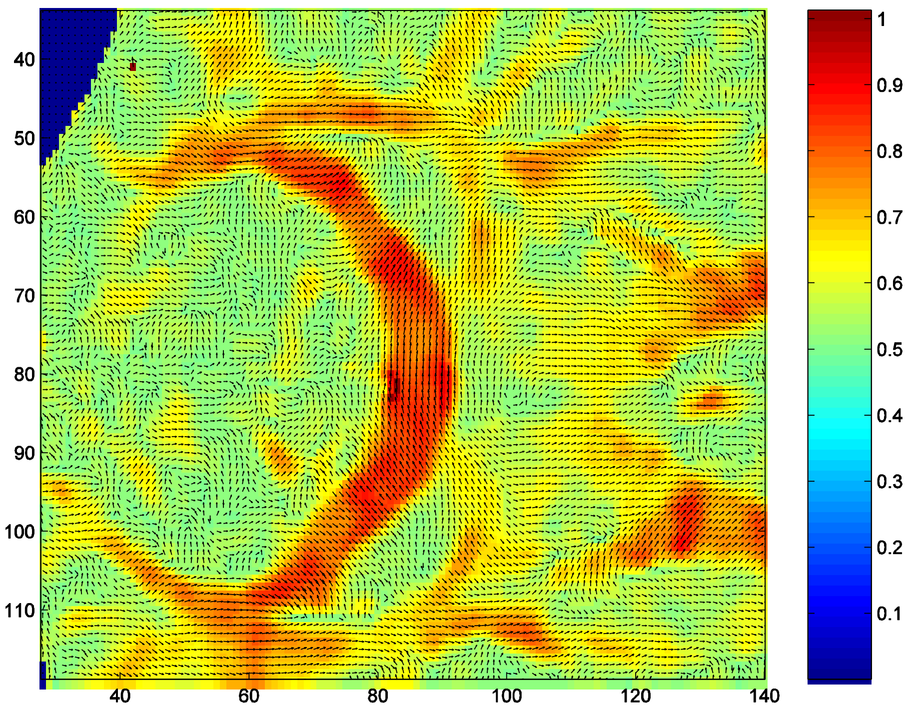

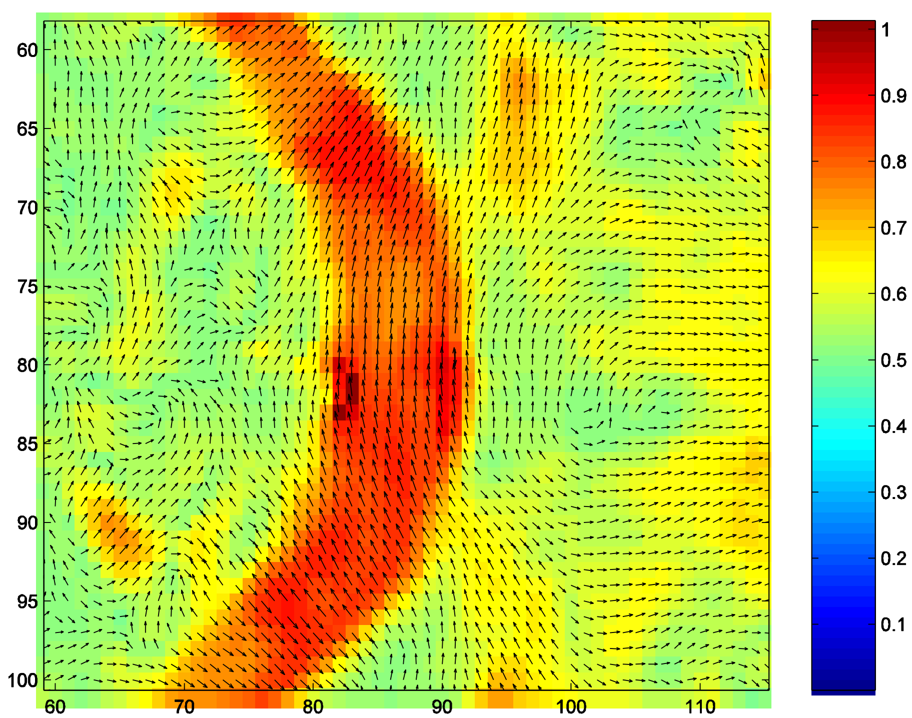

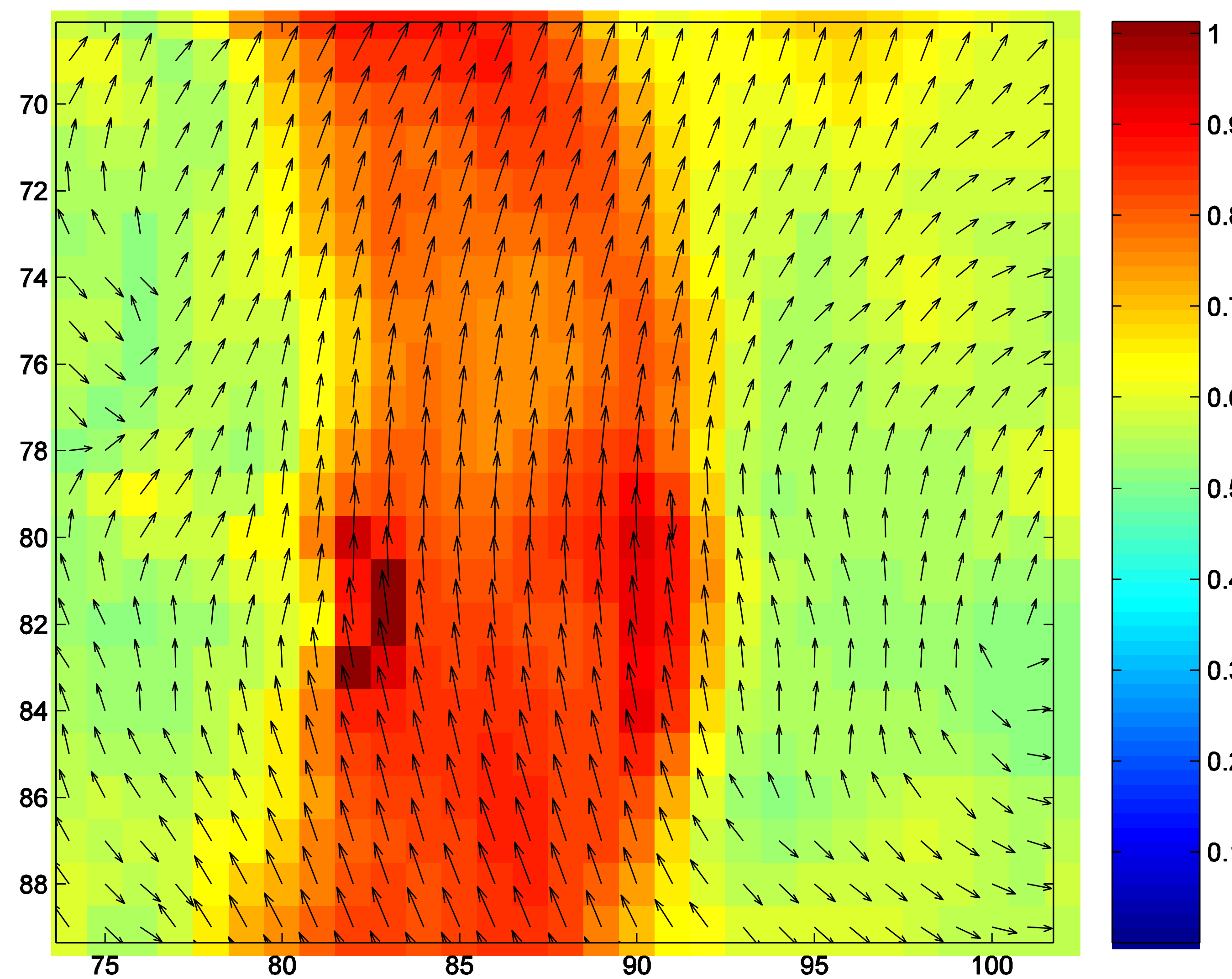

Spatially adaptive smoothing

Diffusion tensor imaging (DTI): Smoothing along vector or tensor fields

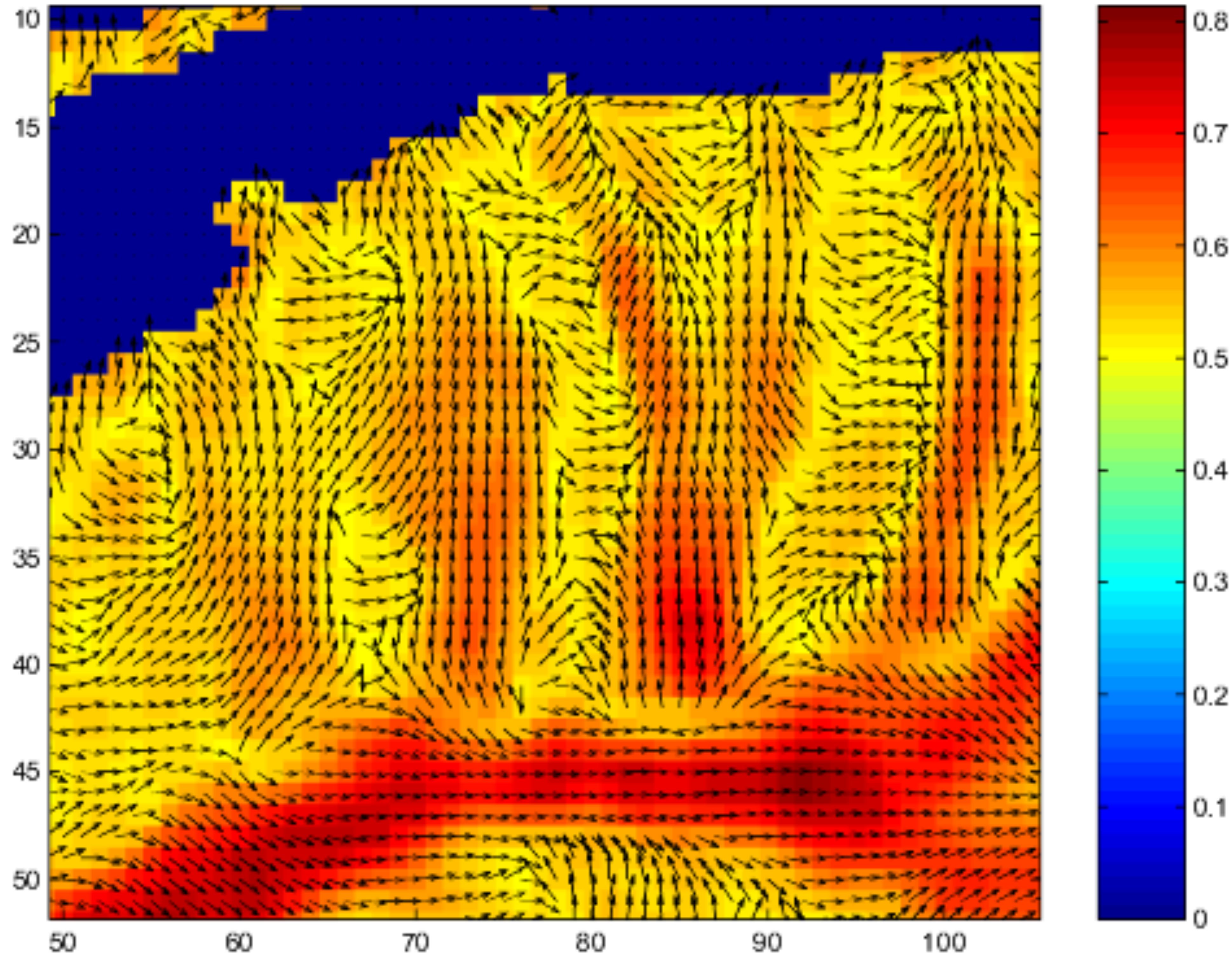

Arrows = Principal eigenvectors
Colors = Principal eigenvalues

of diffusion coefficient matrix.

Motivation for spatially adaptive smoothing

NOISY IMAGE DENOISED IMAGE

Figure 10. Image denoising using Beltrami flow [Kimmel et al].

Boundary preserving smoothing

Smoothing along tensor fields

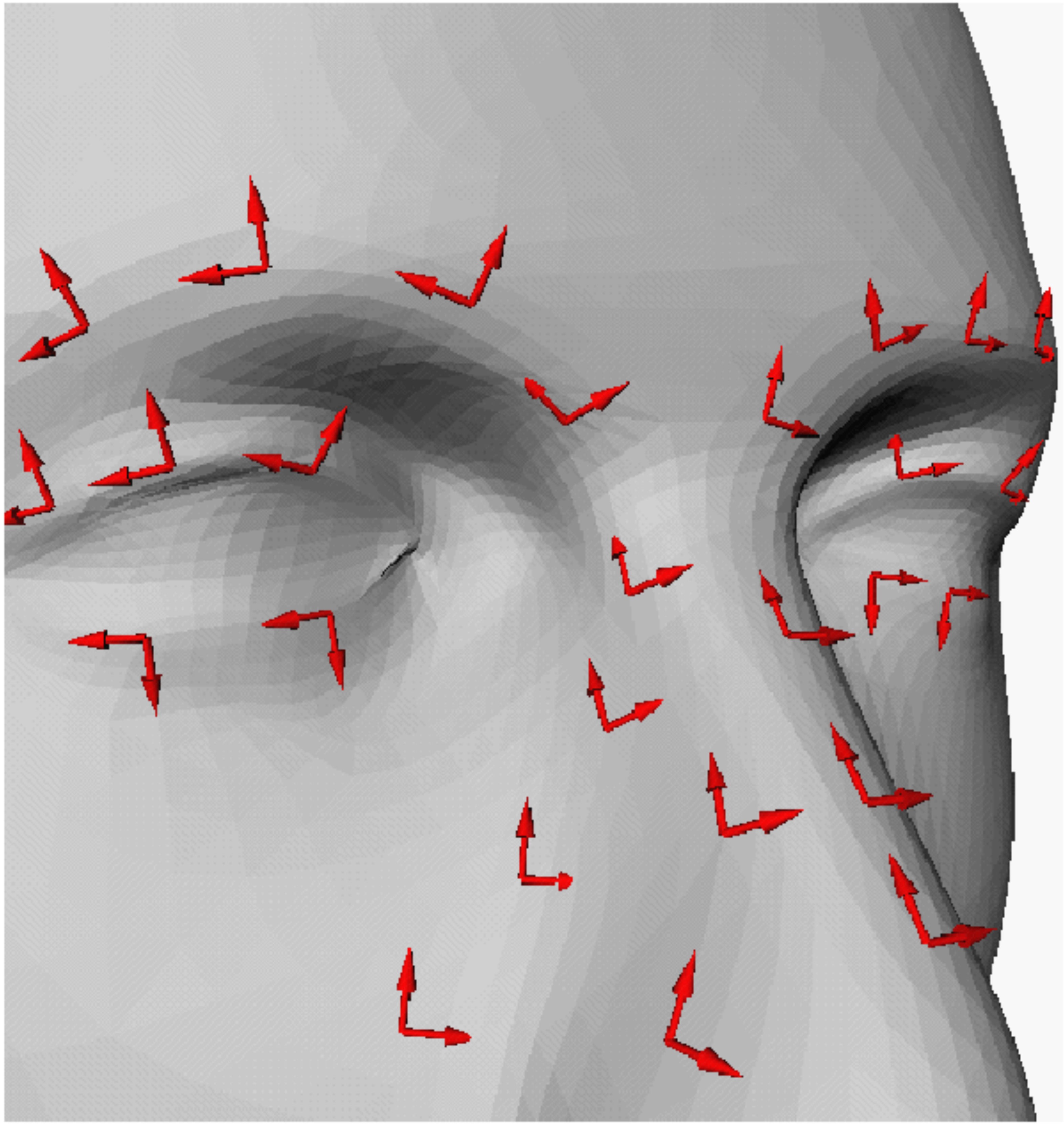

Principal curvature direction
Meyer *et al.*

Anisotropic diffusion smoothing

The concentration of water molecules follows the following anisotropic diffusion equation:

$$\frac{\partial C}{\partial t} = \nabla \cdot (D \nabla C)$$

We can use this idea for edge preserving image smoothing by taking D to be related to image gradient such that D obtains high value (more smoothing) in the interior and low value (less smoothing) near edges

(Perona and malik, 1986).

Riemannian metric tensor formulation/interpretation

Isotropic smoothing in some other space

Anisotropic smoothing in image space

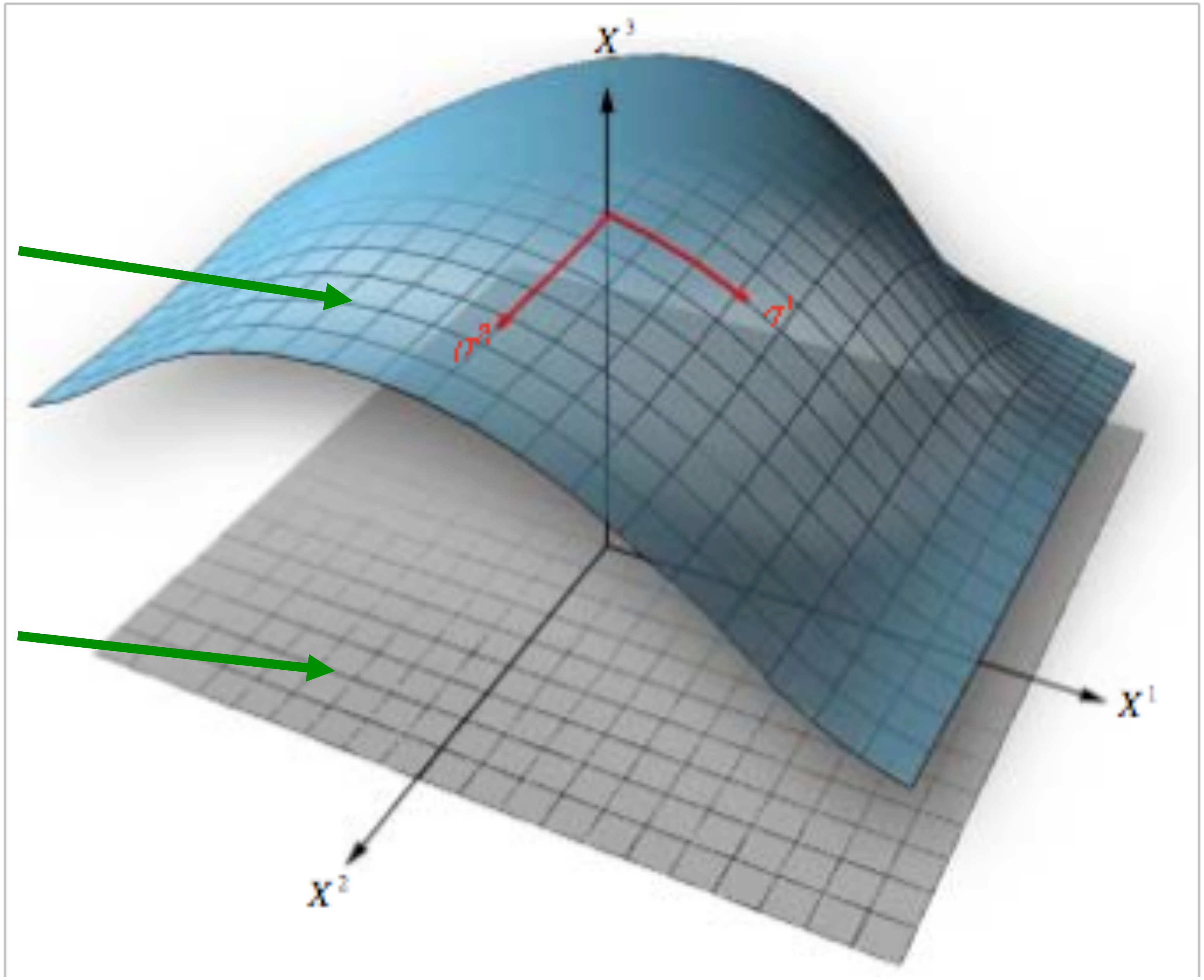

Anisotropic Gaussian kernel

3D Gaussian kernel

$$K_t(\mathbf{x}) = \exp(-\mathbf{x}' D^{-1}\mathbf{x}/4t)/(4\pi t \det D)^{3/2}$$

2D Gaussian kernel

$$K_t(\mathbf{x}) = \exp(-\mathbf{x}' D^{-1}\mathbf{x}/4t)/(4\pi t \det D^{1/2})$$

Gaussian kernel shapes

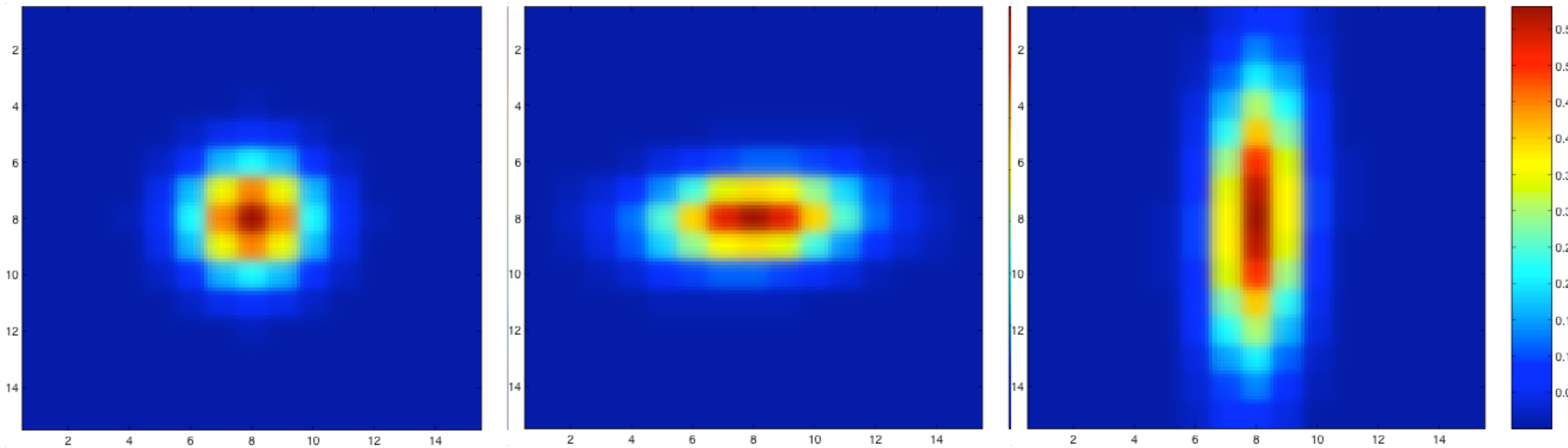

Isotropic kernel

Anisotropic kernels

$$D = I$$

$$D \neq I$$

The direction of kernel shape can be matched to follow the direction of white matter fiber tracts.

Tensor field visualization

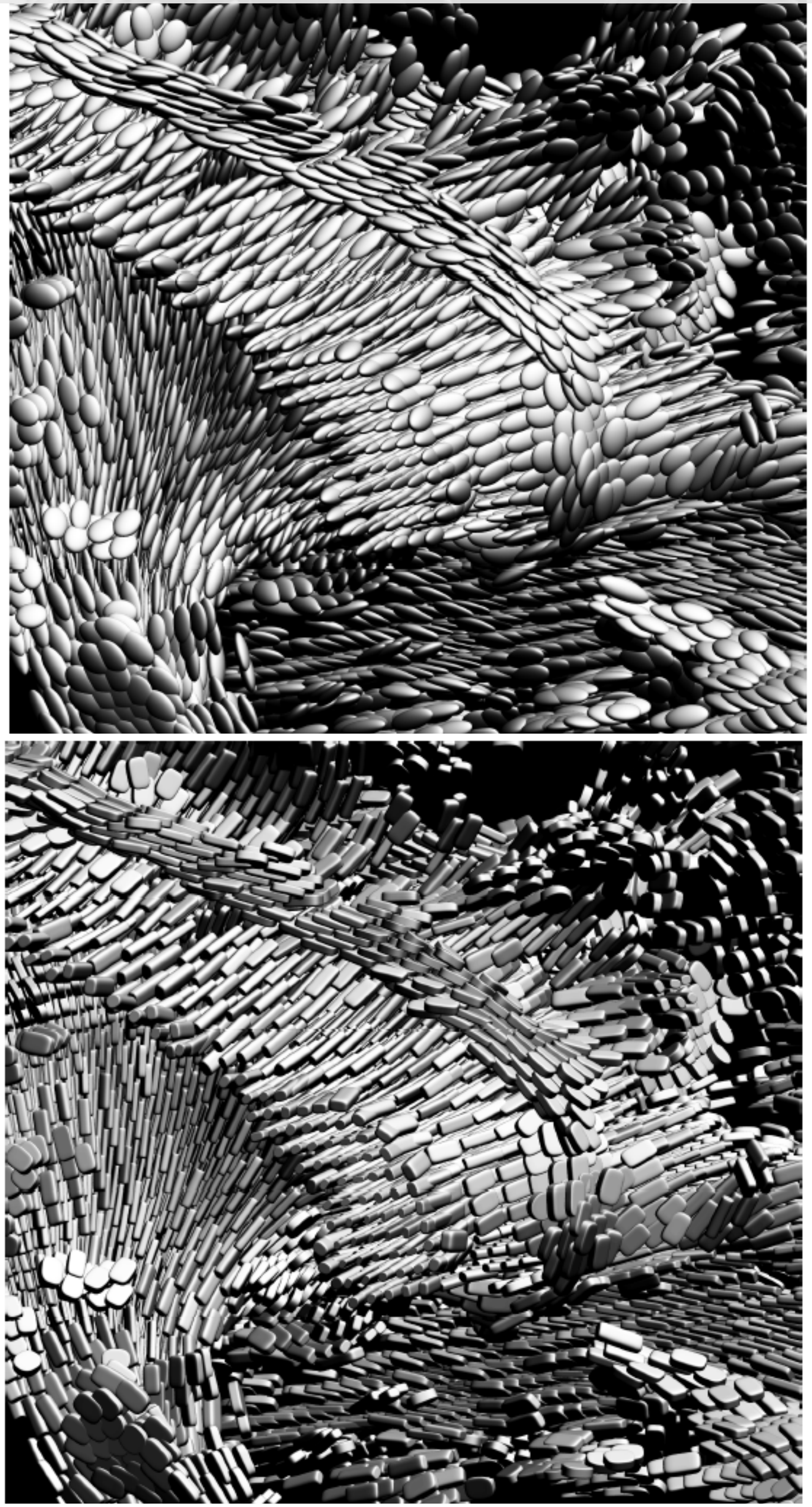

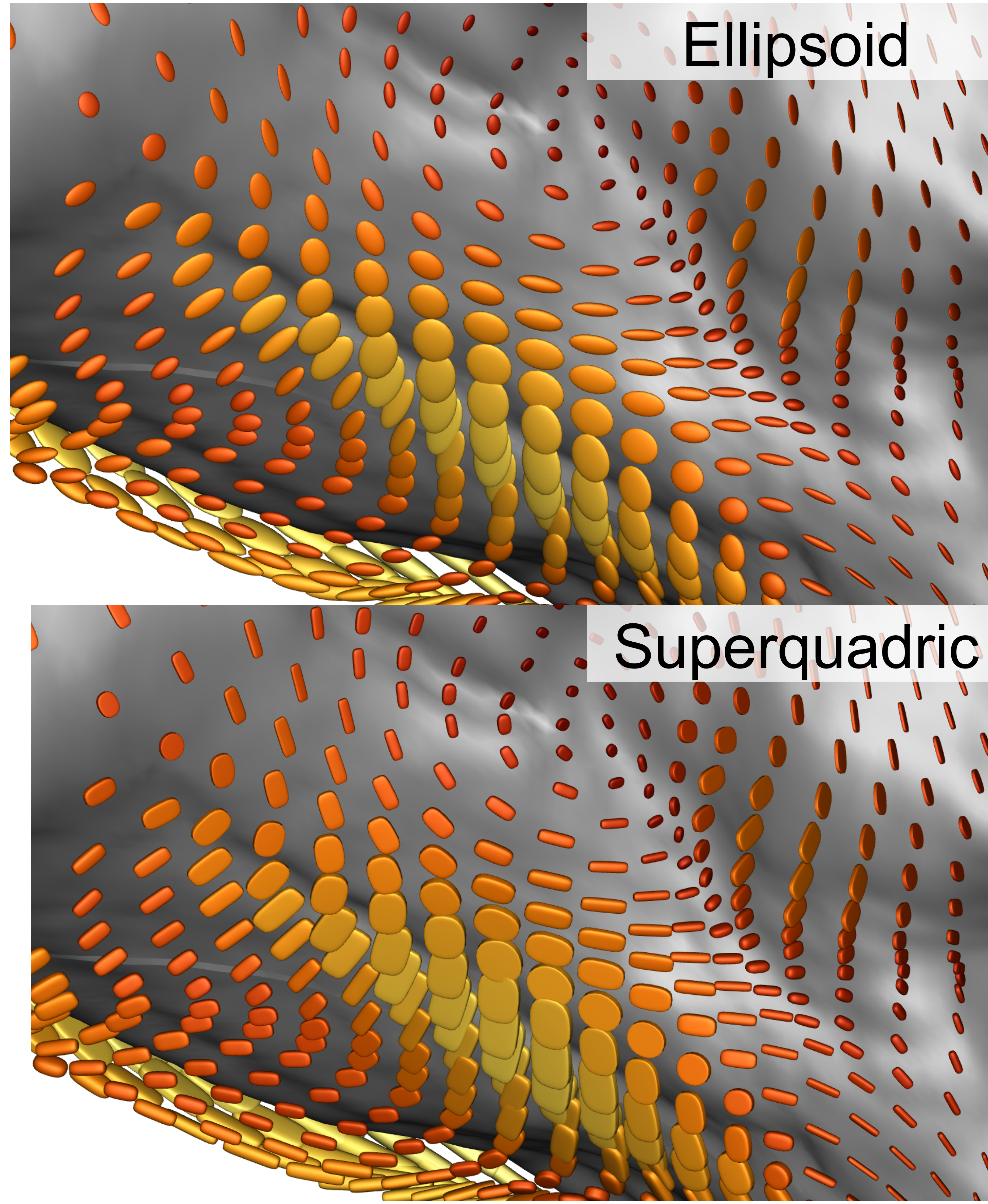

Kindlmann, “Superquadric Tensor Glyphs”, Joint Eurographics , IEEE TCVG Symposium on Visualization 2004

Anisotropic Gaussian kernel smoothing

$$F(\mathbf{x}, t) = \int_{\mathbb{R}^n} K_t(\mathbf{x} - \mathbf{y}) f(\mathbf{y})\, dy$$

$$F(\mathbf{x}, t) \doteq \frac{\int_{B_\mathbf{x}} K_t(\mathbf{x} - \mathbf{y}) f(\mathbf{y})\, d\mathbf{x}}{\int_{B_\mathbf{x}} K_t(\mathbf{x} - \mathbf{y})\, d\mathbf{y}}$$

$$F(\mathbf{x}, t) \doteq \sum_{x_j \in B_\mathbf{x}} w_j(\mathbf{x}) f(\mathbf{x}_j)$$

Full width at half maximum (FWHM)

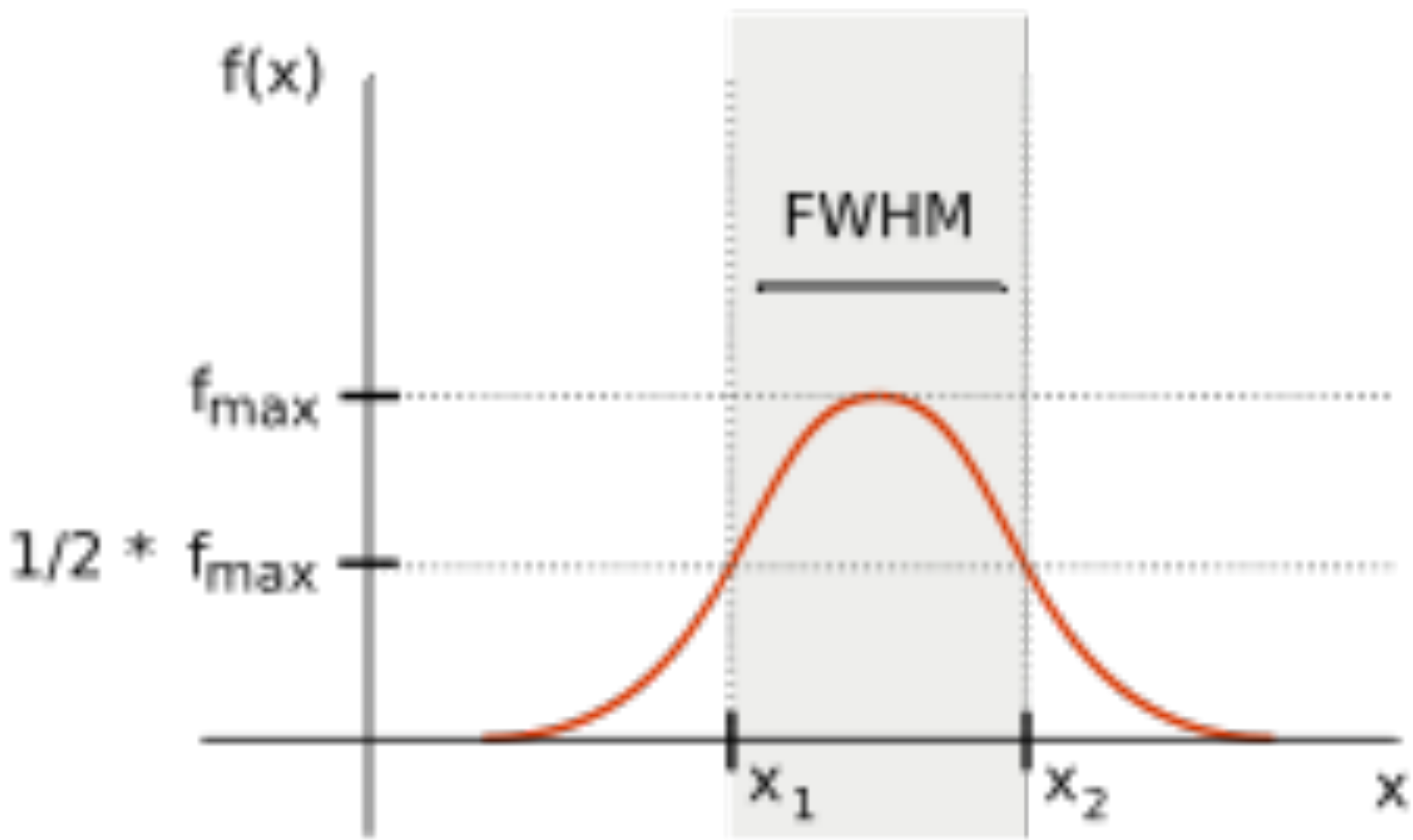

Isotropic Gaussian kernel smoothing (*D*= *I*)

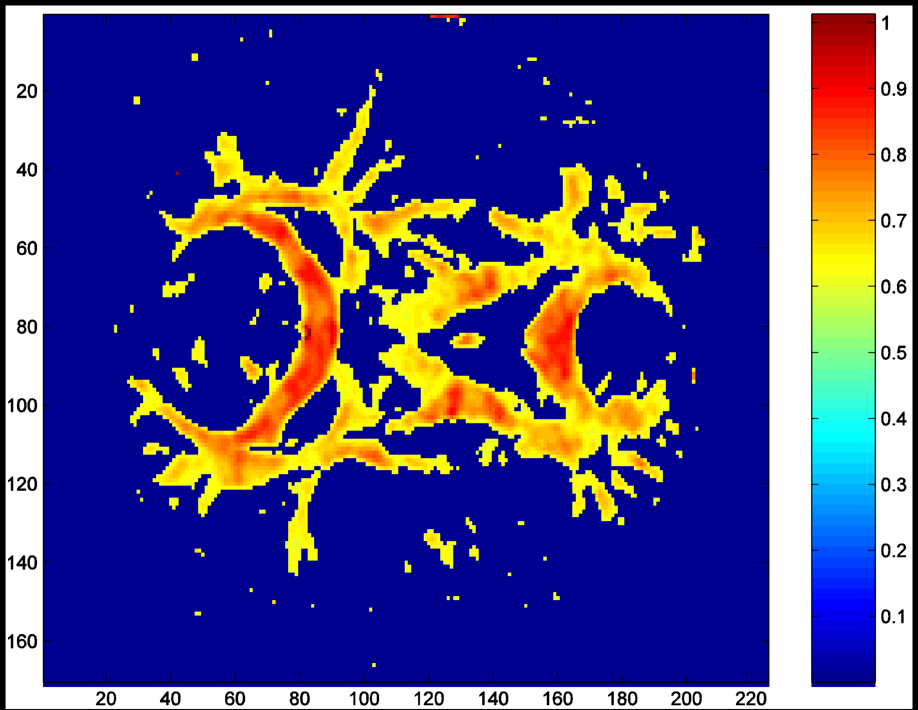

Principal eigenvalues > 0.6

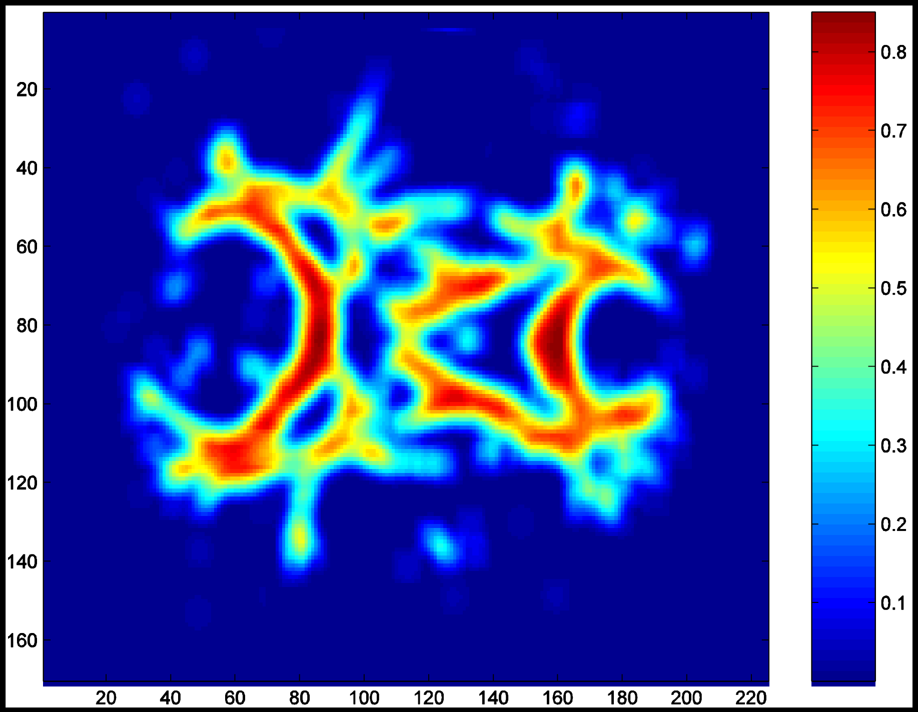

10mm FWHM

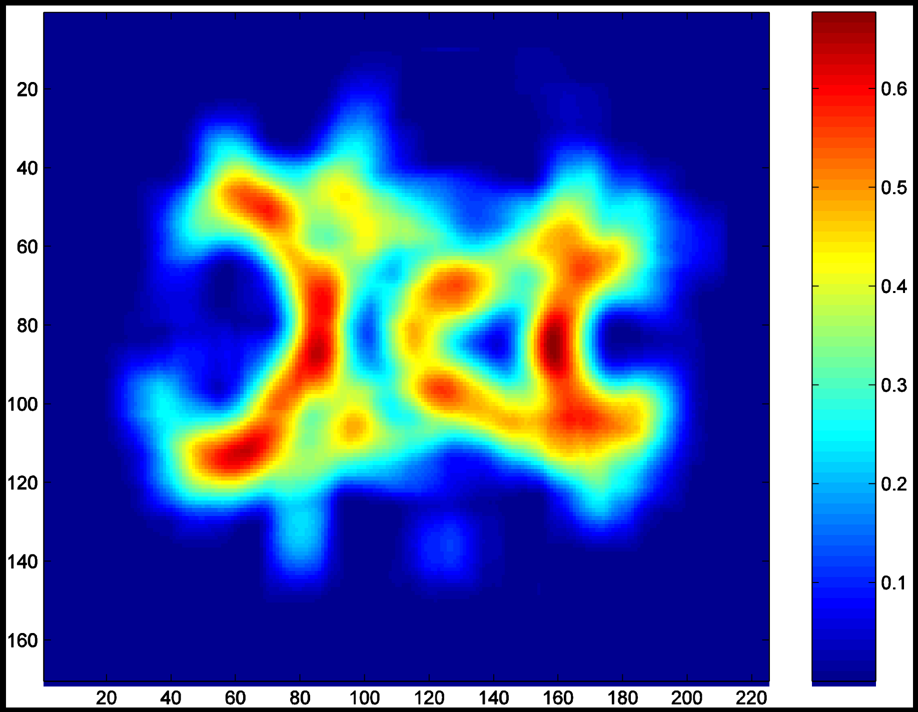

20mm FWHM

Iterative kernel smoothing

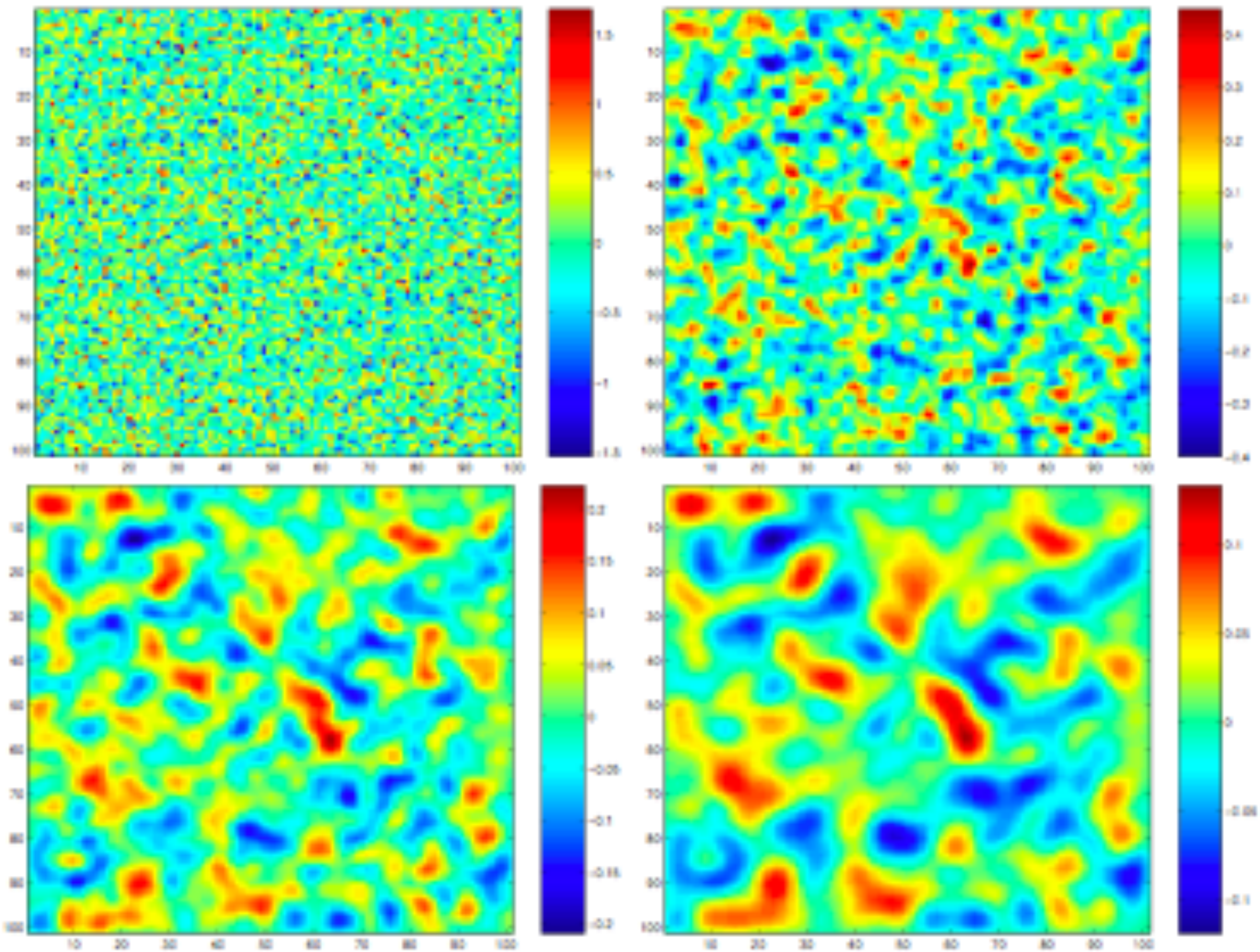

N(0, 0.4^2) Gaussian white noise
Iterative kernel smoothing with sigma=0.4 and 1,4, 9 iterations

Anisotropic Gaussian kernel weights

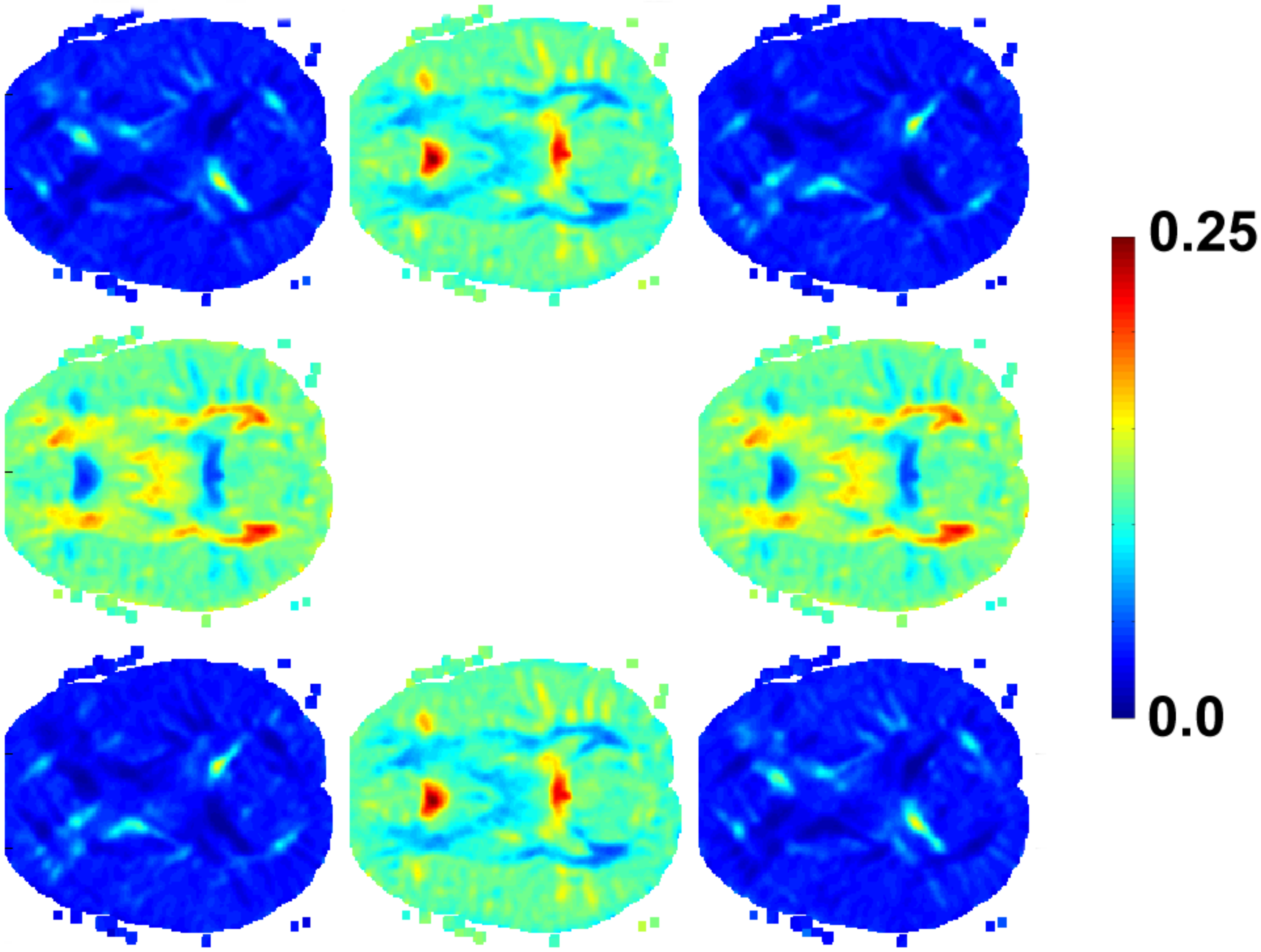

Isotropic vs. anisotropic kernel smoothing

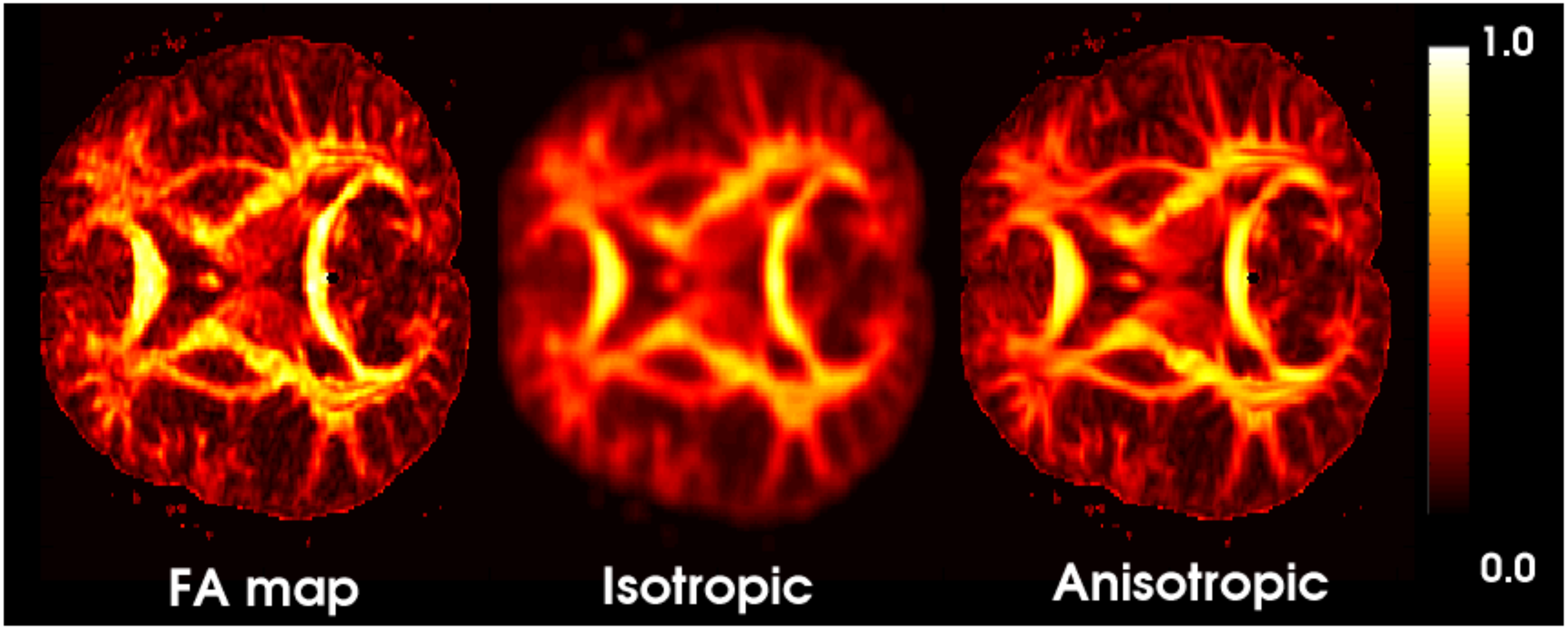

Anisotropic kernel construction using image intensity gradient

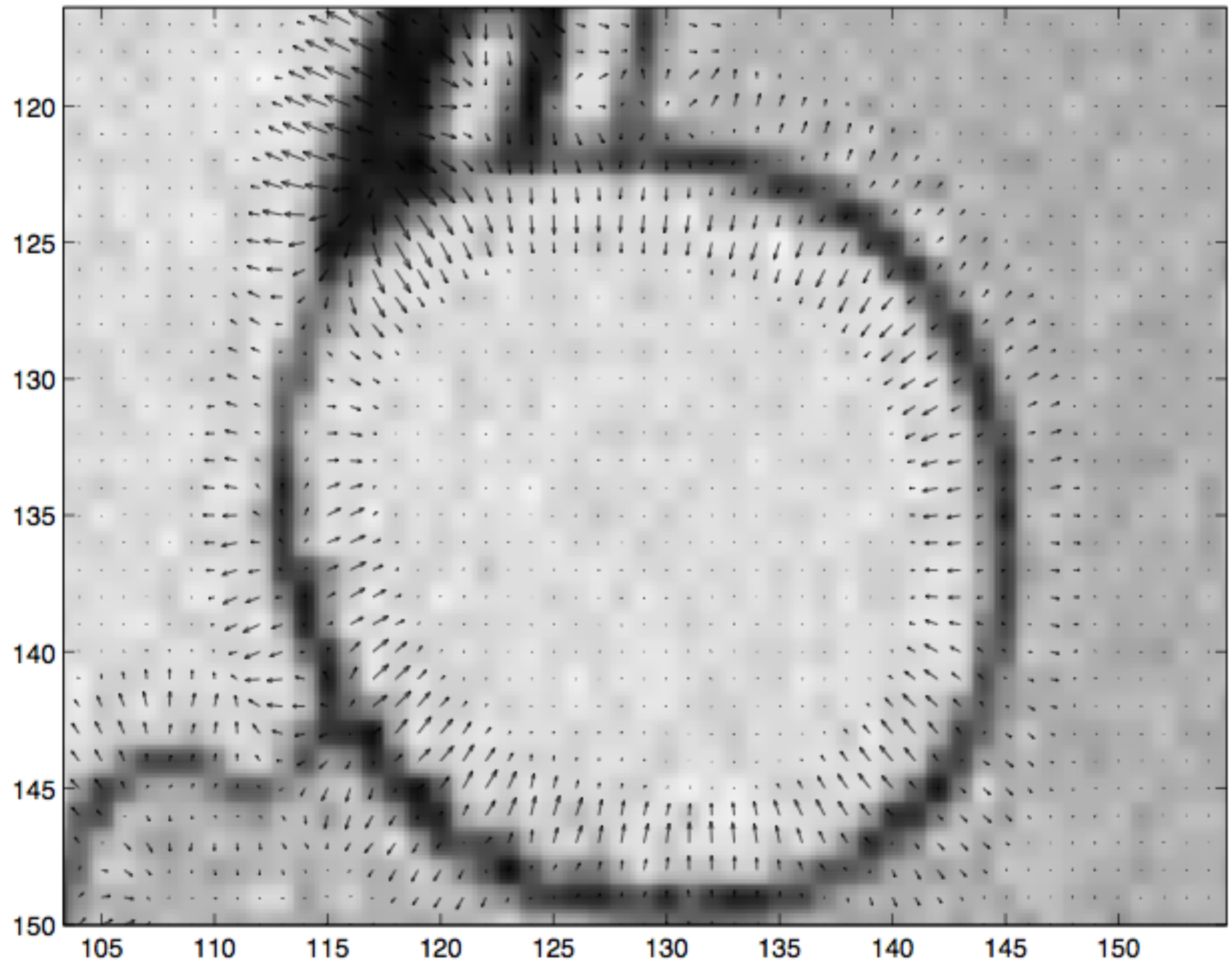

$$\frac{\partial}{\partial x}(K_\sigma * I) \qquad \frac{\partial}{\partial y}(K_\sigma * I)$$

Image gradient change

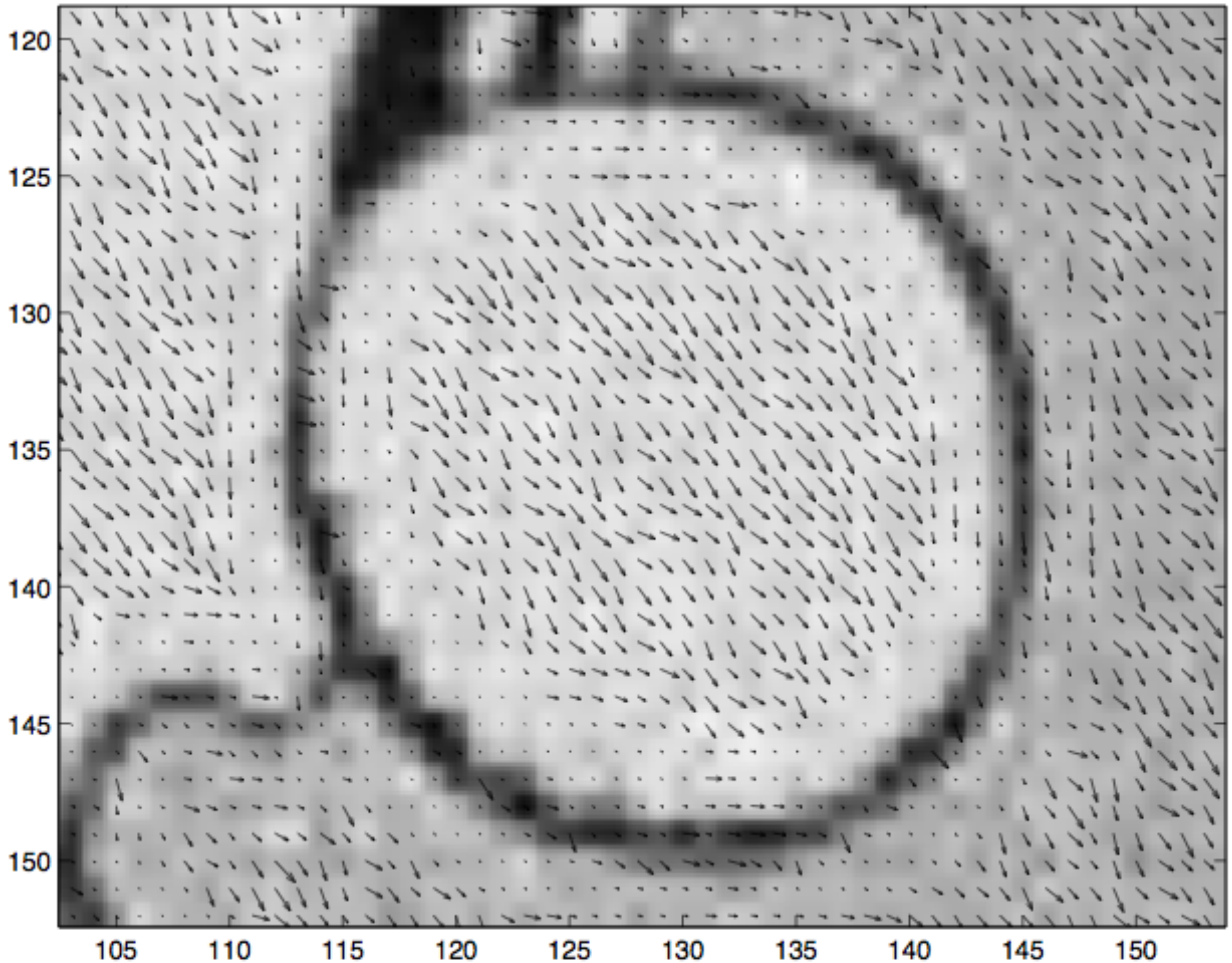

$$\frac{1}{1+\frac{\partial}{\partial x}(K_\sigma * I)} \qquad \frac{1}{1+\frac{\partial}{\partial y}(K_\sigma * I)}$$

Anisotropic smoothing

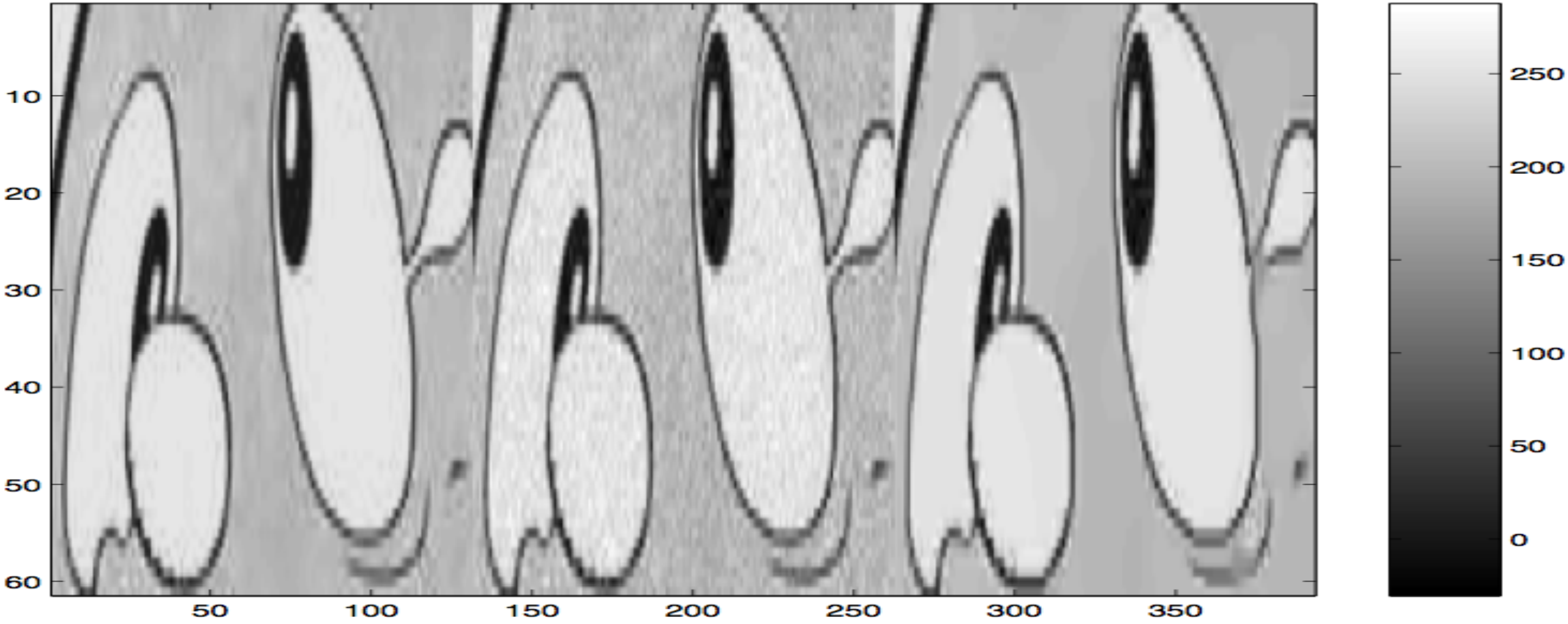

$$D = \begin{pmatrix} \dfrac{1}{1 + \dfrac{\partial}{\partial x}(K_\sigma * I)} & 0 \\ 0 & \dfrac{1}{1 + \dfrac{\partial}{\partial y}(K_\sigma * I)} \end{pmatrix}$$

Diffusion coefficients can be used in solving either diffusion equation or kernel smoothing

Probabilistic connectivity

Press Release • July 16, 2009

NIH Launches the Human Connectome Project to Unravel the Brain's Connections

The National Institutes of Health Blueprint for Neuroscience Research is launching a $30 million project that will use cutting-edge brain imaging technologies to map the circuitry of the healthy adult human brain. By systematically collecting brain imaging data from hundreds of subjects, the Human Connectome Project (HCP) will yield insight into how brain connections underlie brain function, and will open up new lines of inquiry for human neuroscience.

www.humanconnectomeproject.org

The NIH Human Connectome Project | Harvard/MGH-UCLA Consortium | WU-Minn Consortium | Neuroscience Blueprint

Human Connectome Project

Enter search keyword

Home | Overview | Collaborators | Publications | Data | Links | Contact

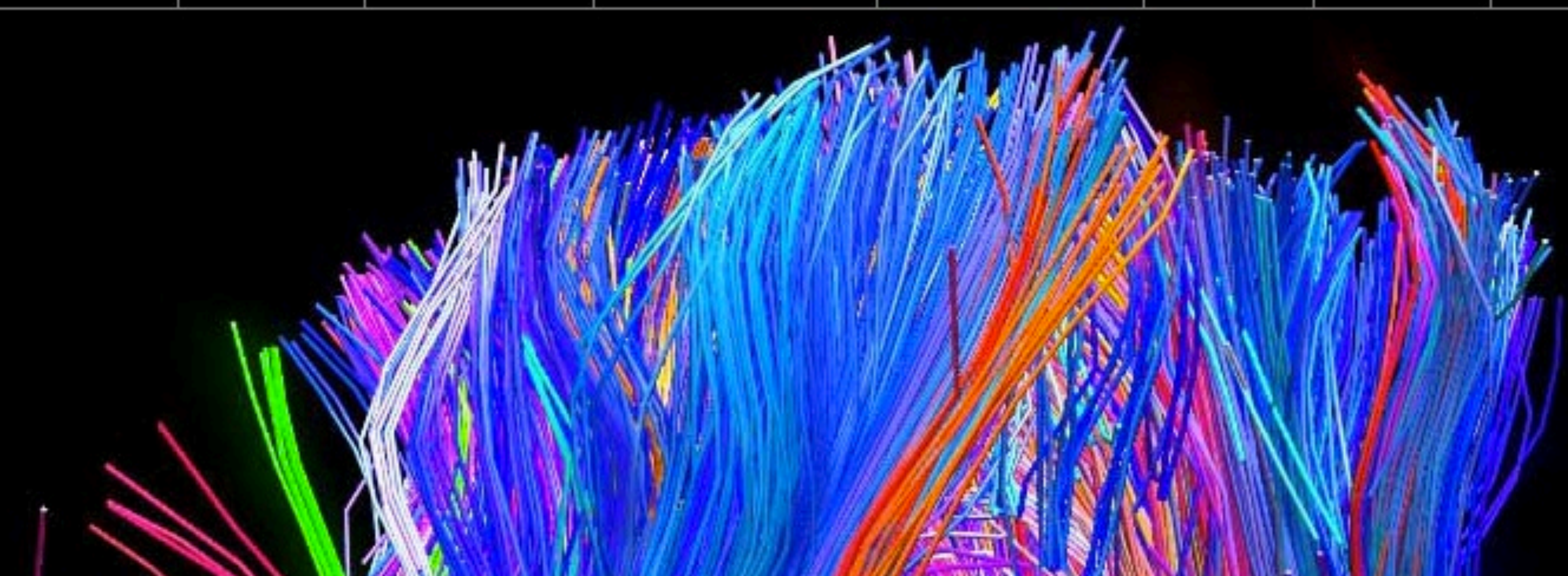

The Human Connectome Project

Navigate the brain in a way that was never before possible; fly through major brain pathways, compare essential circuits, zoom into a region to explore the cells that comprise it, and the functions that depend on it.

The Human Connectome Project aims to provide an unparalleled compilation of neural data, an interface to graphically navigate this data and the opportunity to

Previous probabilistic methods

Heat equation Batchelor *et al.* Lecture notes in computer sicnece. 2002.

$$\partial_t f = \nabla \cdot (D \nabla f)$$

$$f(\mathrm{x}, 0) = \delta(\mathrm{x}_0), \text{ Dirac-delta}$$

$\nabla = (\partial_{x_1}, \cdots, \partial_{x_n})'$. The solutation $f(\mathrm{x}, t)$ to PDE gives the probability of connectivity from x_0 to x.

Monte-Carlo ranom walk Koch *et al.* NeuroImage. 2002. Transition probability of random walk is based on Einstein's equation (Einstein, 1905). The random walk is constrained to give a very smooth path.

1D Brownian motion

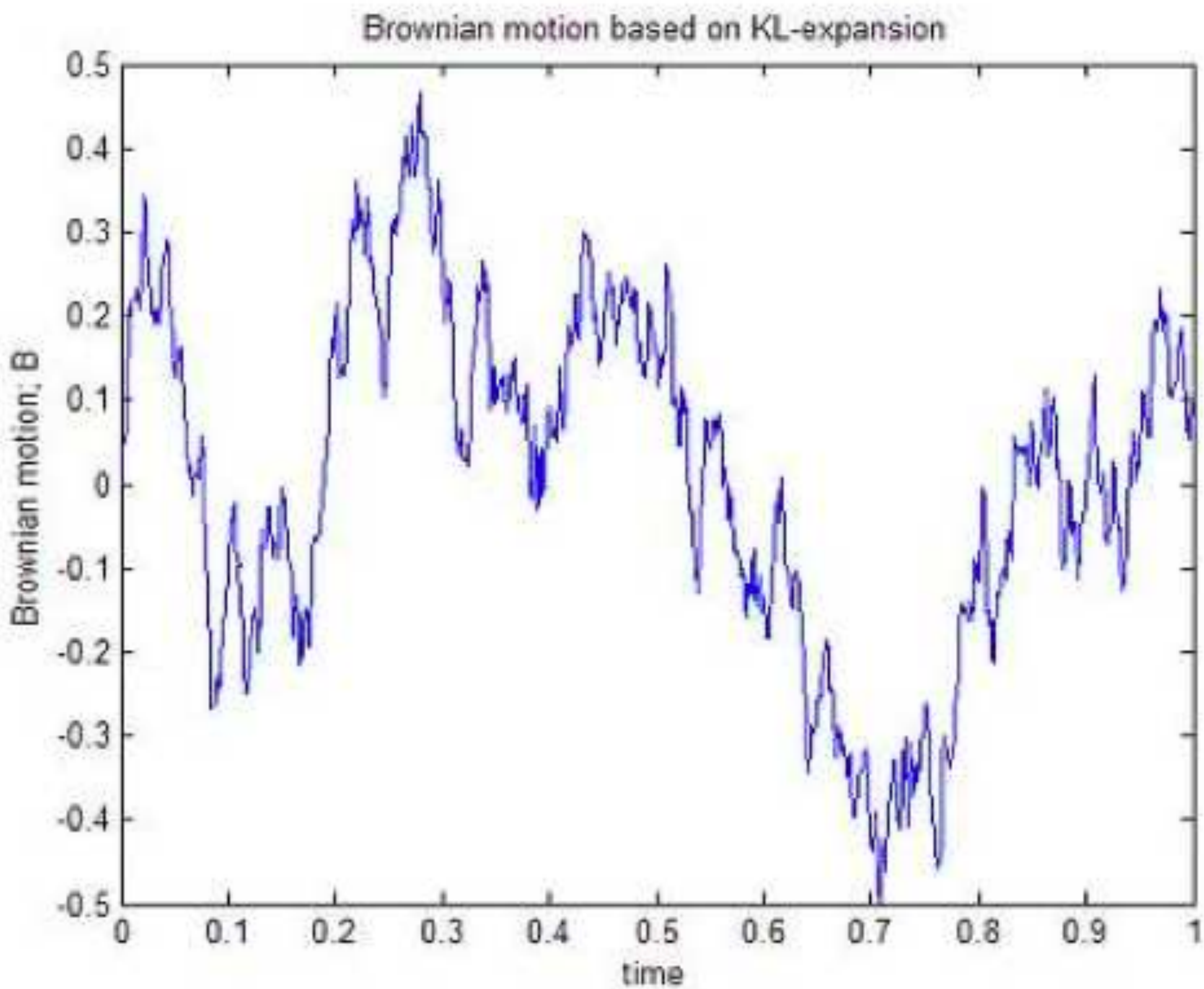

Brownian motion simulation

$$\text{Probability} = \frac{\#\ \text{random walk hitting a target voxel}}{\#\ \text{total random walk}}$$

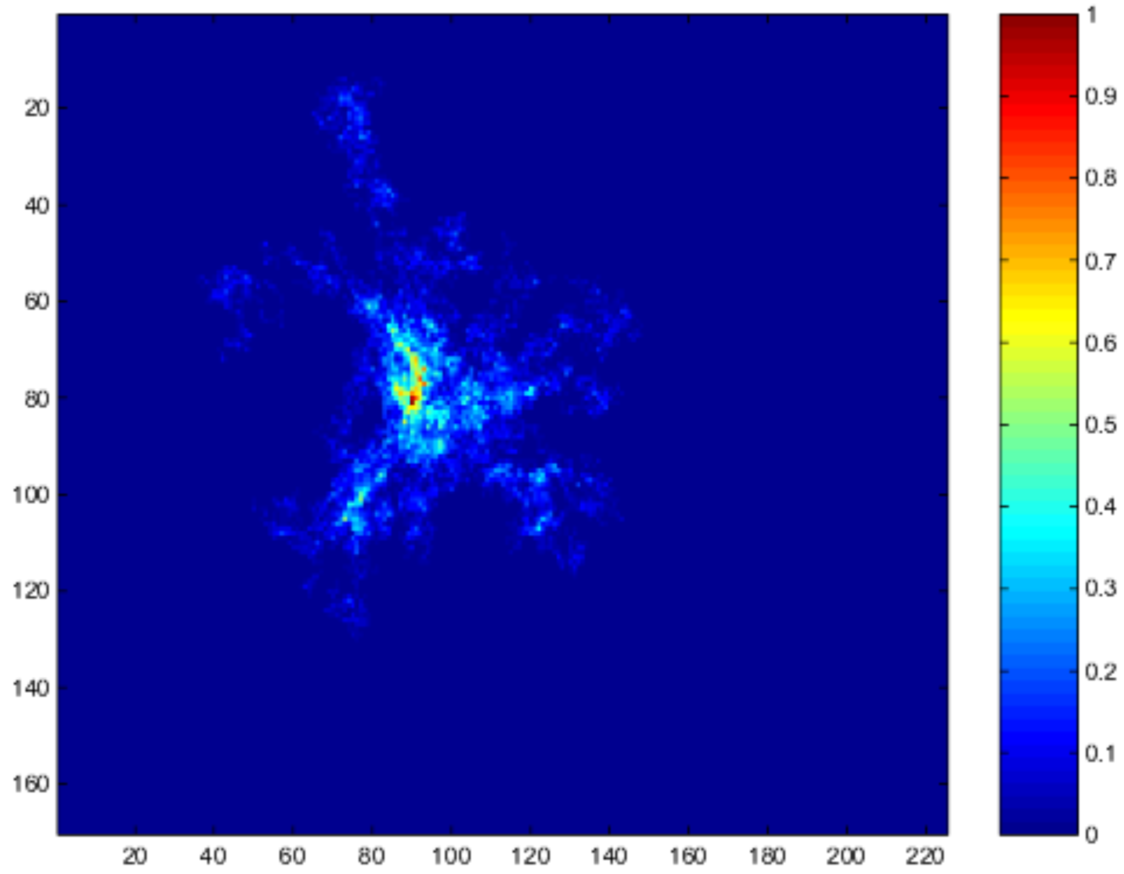

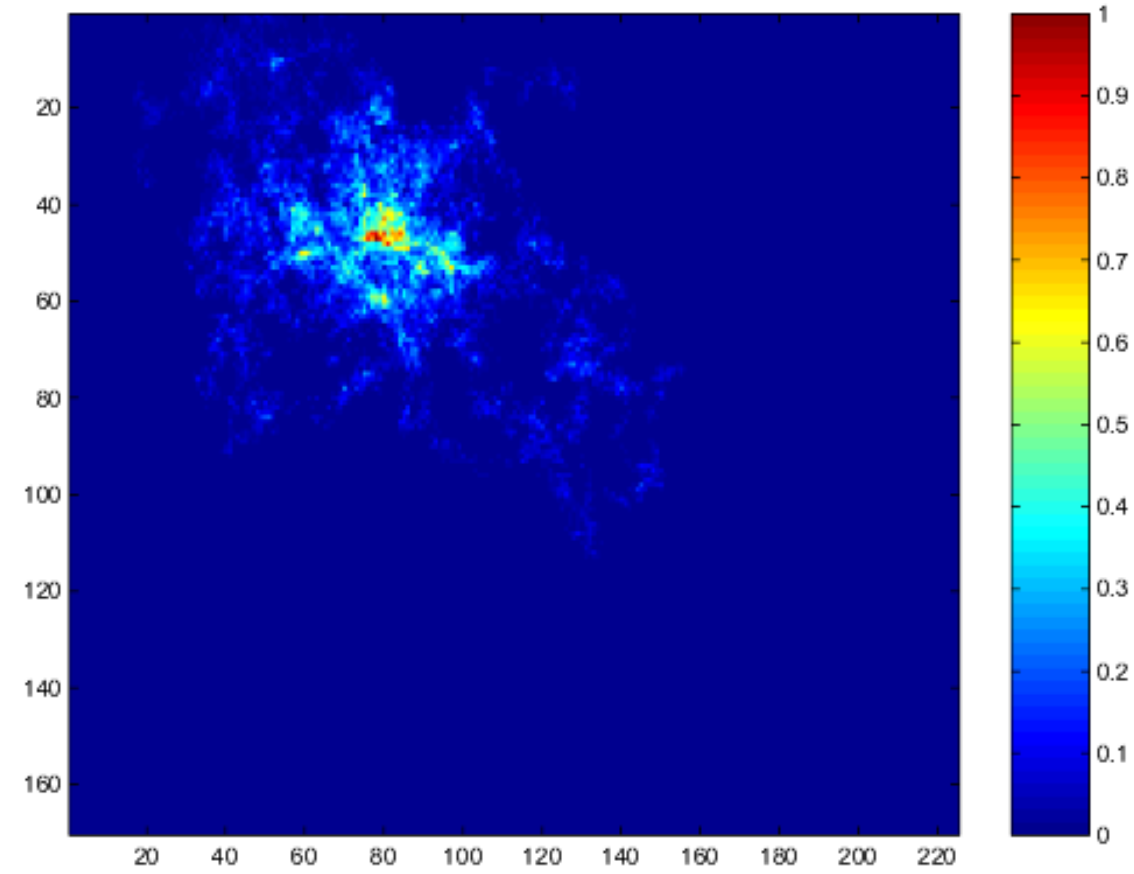

Transition probability

Let $P_t(\mathbf{p}, \mathbf{q})$ be the *transition probability density* of a particle going from $\mathbf{p}$ to $\mathbf{q}$ under diffusion process. This is the conditional probability density of the particle hitting $\mathbf{q}$ at time t when the particle is at $\mathbf{p}$ at time 0.

Property 1. $\int_{\mathbb{R}^n} P_t(\mathbf{p}, \mathbf{x})\, d\mathbf{x} = 1.$

Property 2. If D is constant in $\mathbb{R}^n$,

$$P_t(\mathbf{p}, \mathbf{q}) = K_t(\mathbf{q} - \mathbf{p}).$$

So if $\mathbf{q} \in B_{\mathbf{p}}$ for small t,

$$P_t(\mathbf{p}, \mathbf{q}) \approx K_t(\mathbf{q} - \mathbf{p}).$$

Transition probability from the center voxel

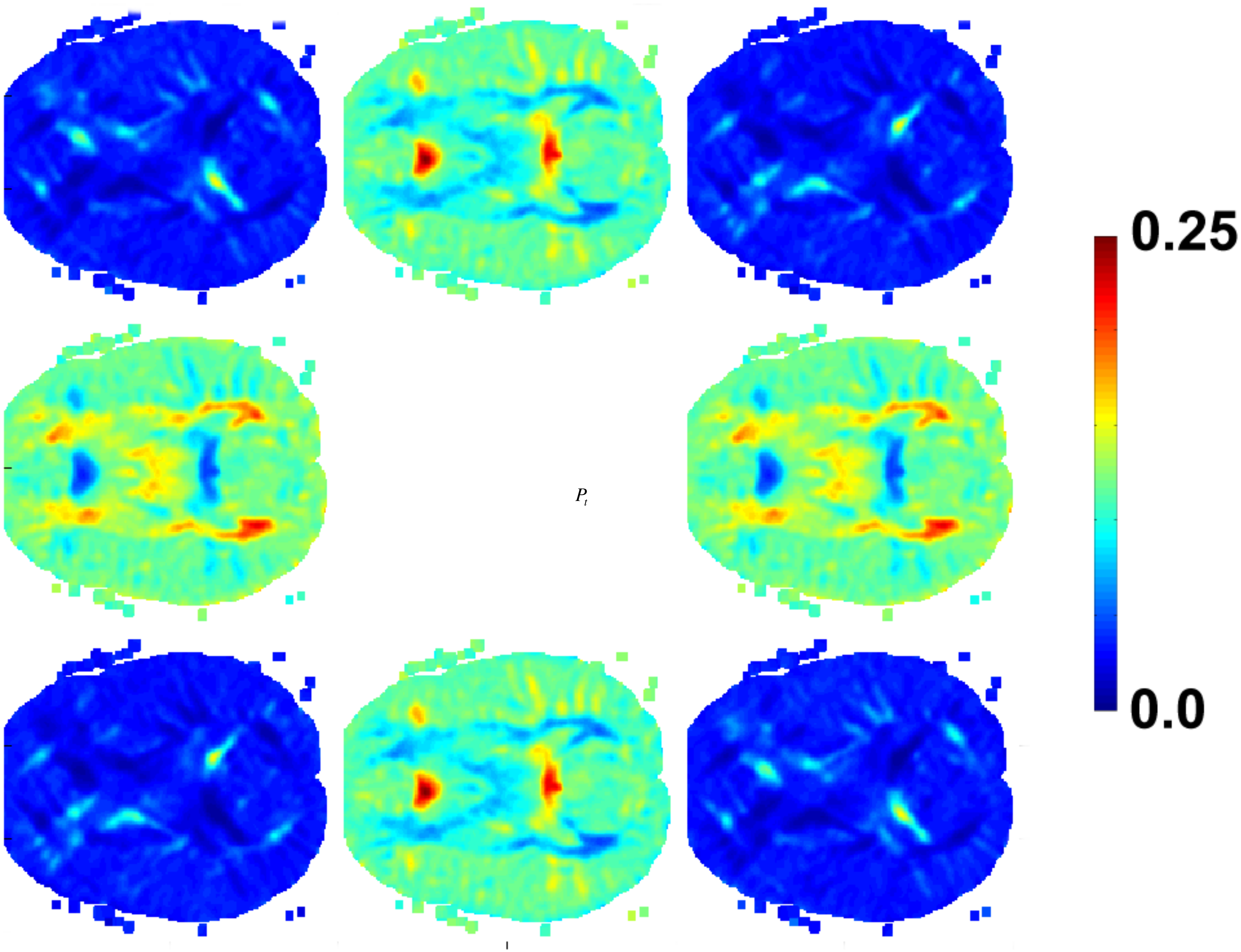

Transition probability can be used in isotropic kernel smoothing

Chapman-Kolmogorov equation

$$P_t(p,q) = \int_{R^n} P_s(p,x) P_{t-s}(x,q)\,dx$$

The probability of going from *p* to *q* is the total sum of probabilities going from *p* to *q* through all possible intermediate points *x*.

In Markov chains, this can be stated as matrix multiplication:

$$P_t = P_s P_{t-s}$$

Anisotropic kernel smoothing via Chapman-Kolmogorov equation

$$P_t(p,q) = \int_{R^n} P_s(p,x) P_{t-s}(x,q)\, dx$$

For sufficiently small s,

$$P_t(p,q) = \int_{R^n} K_s(p,x) P_{t-s}(x,q)\, dx$$

Log transition probability from a seed point in the corpus callosum

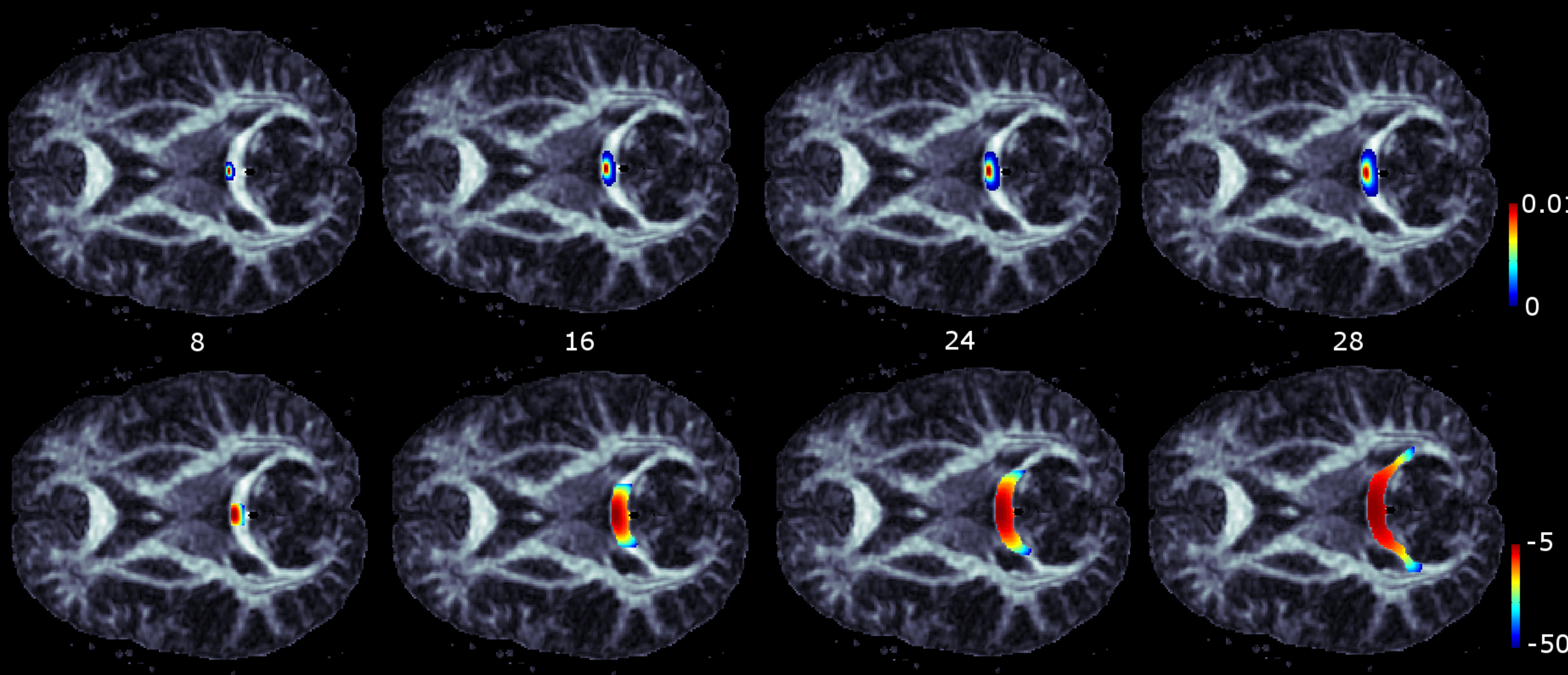

Tractography

Whole Brain Tractography

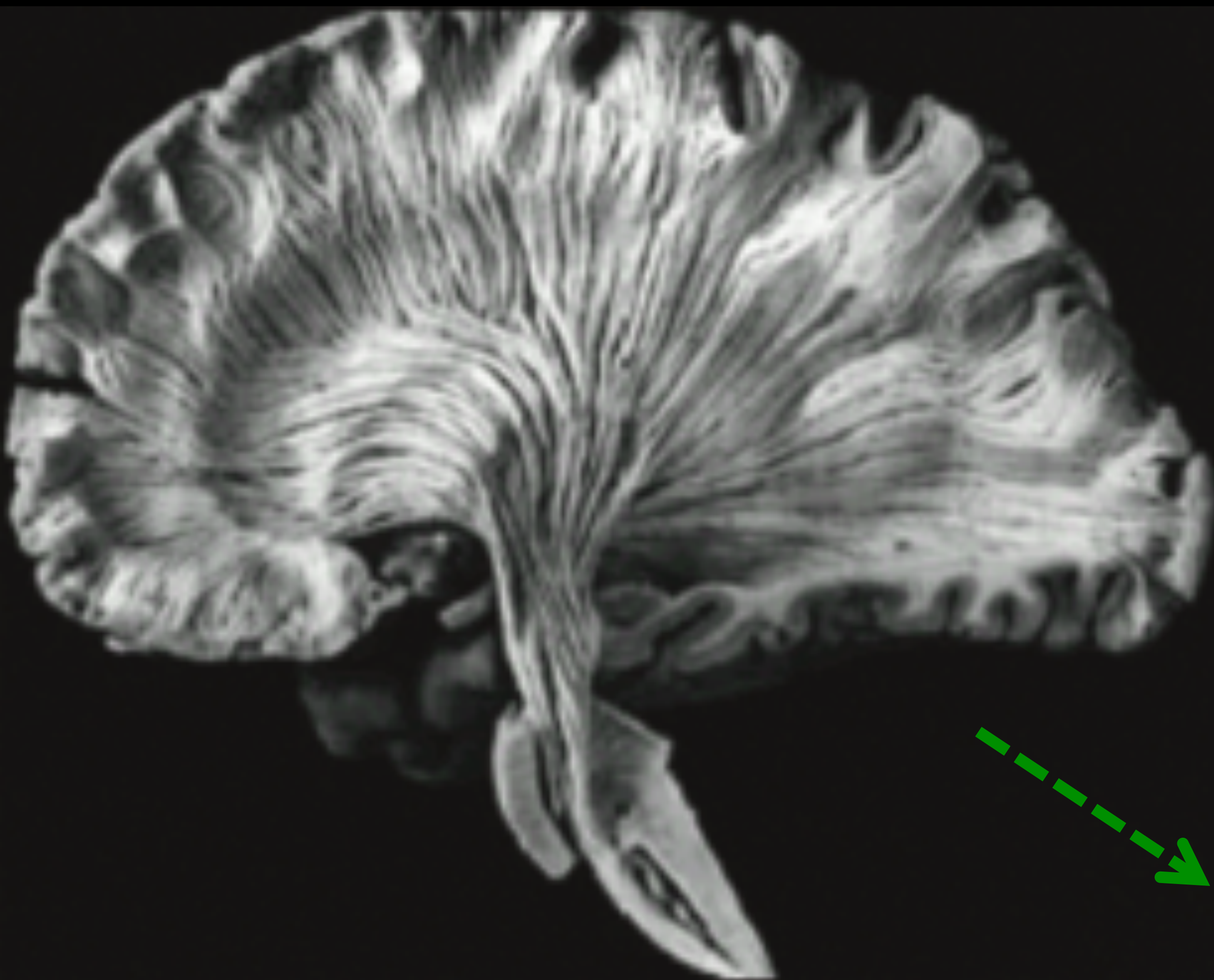

Postmortem

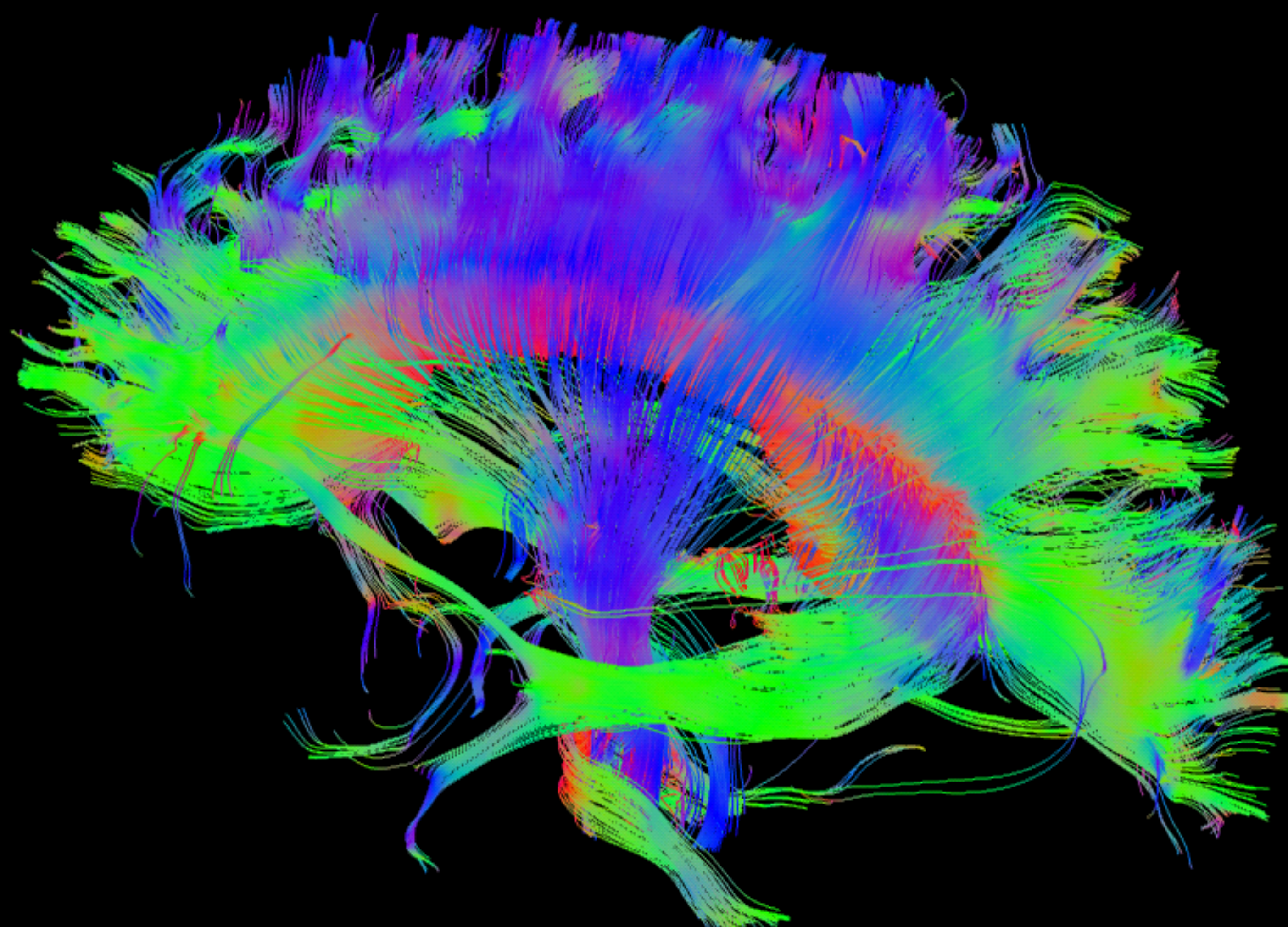

Reconstructed
0.5 million tracts

Tractography is done using the second order Runge-Kutta algorithm with TEND

Diffusion Tensor Imaging

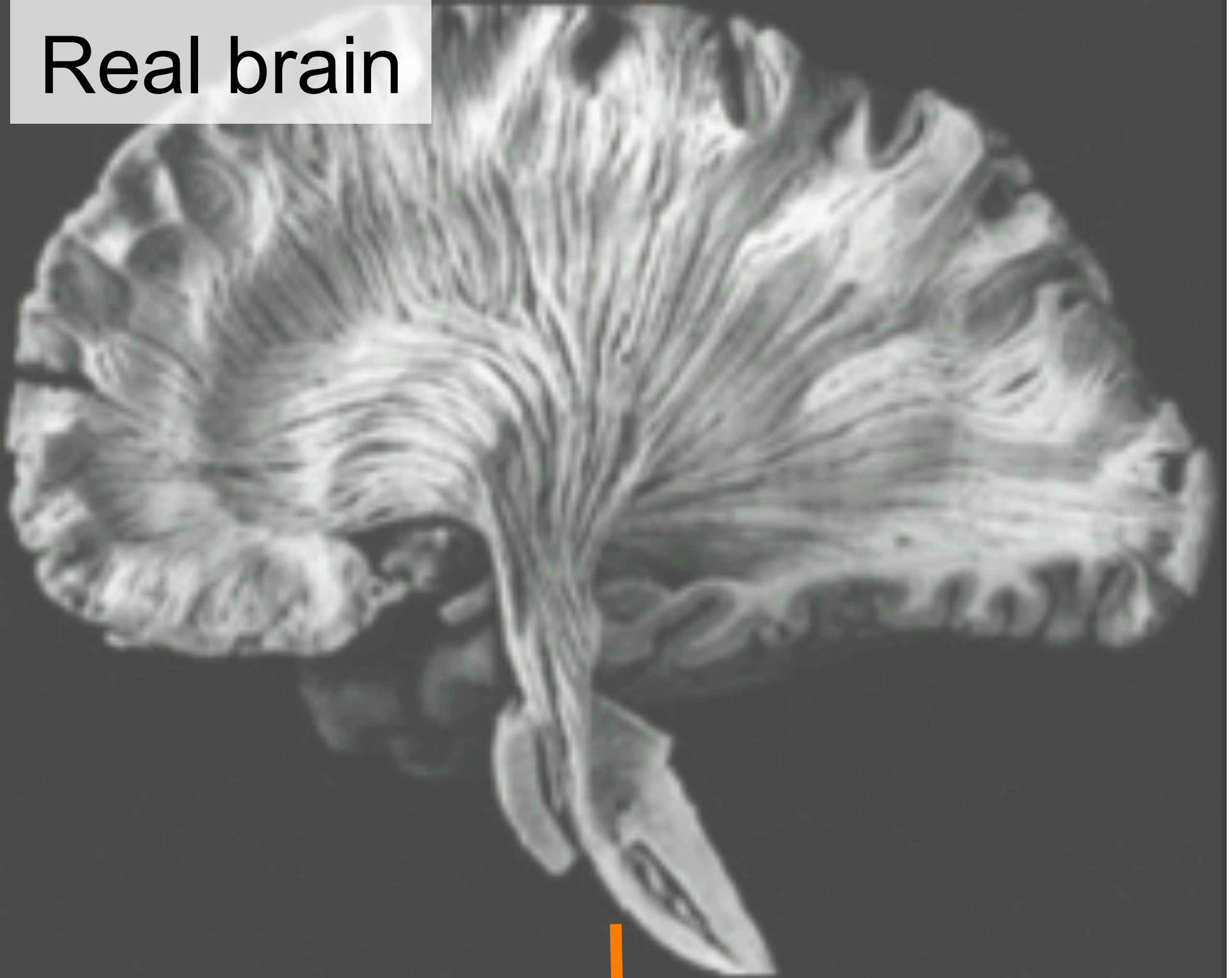

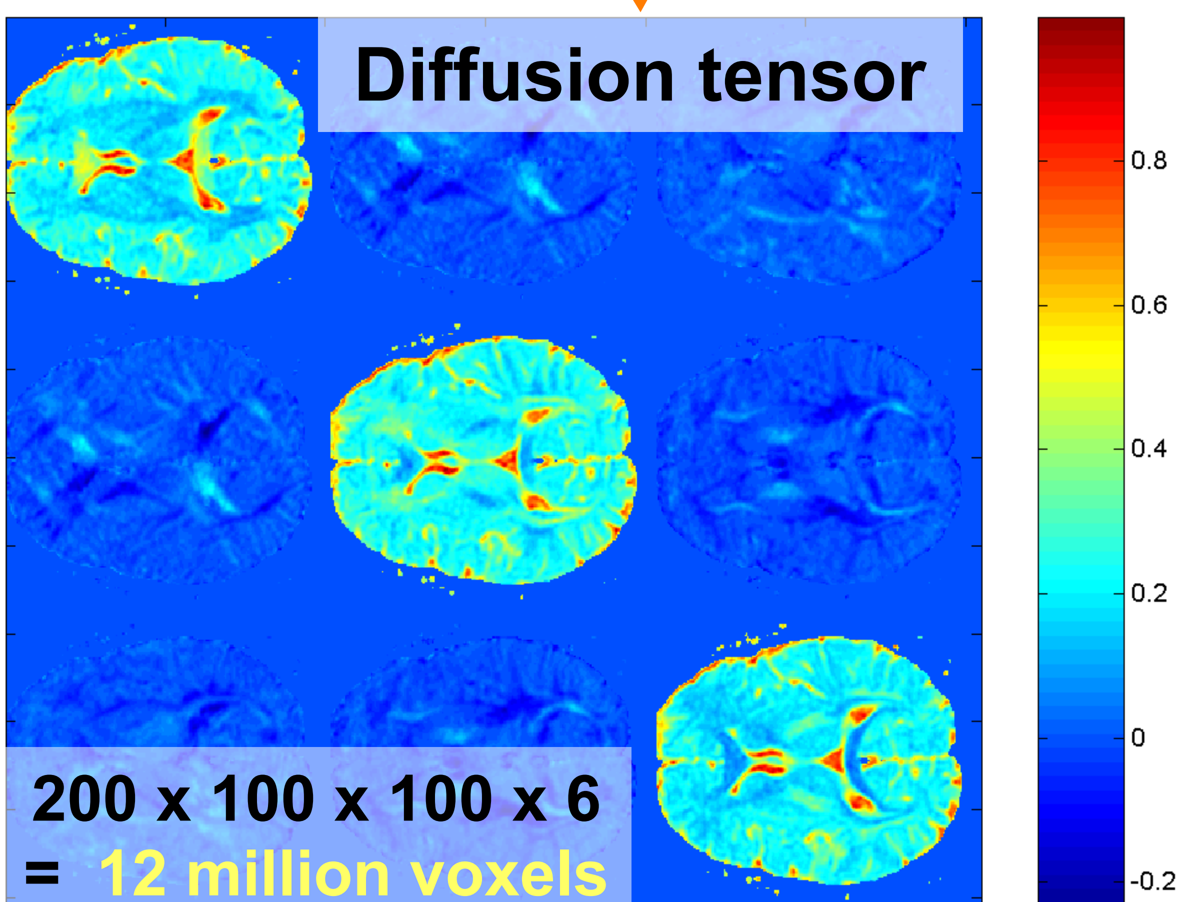

White matter fiber tractography

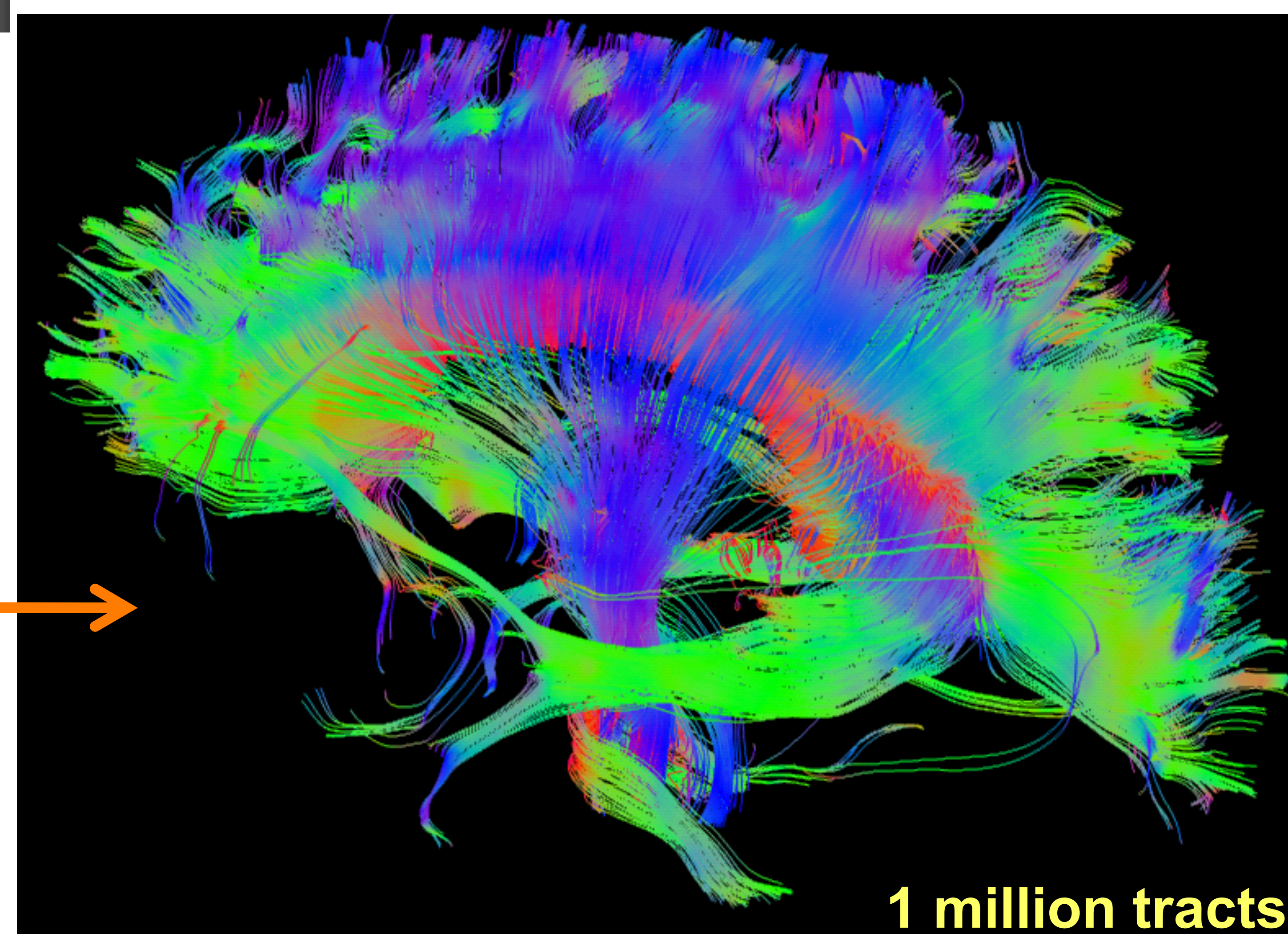

Streamline equation

Main direction of diffusion: principal eigenvector

$$Dv = \lambda v$$

Streamline equation

$$\frac{d\varphi(t)}{dt} = \lambda V \circ \varphi(t)$$

Solved by the second order Runge-Kutta algorithm with TEND (Lazar et al., HBM 2003).

For a given vector field there exists a family of curves whose tangent is given by the vector field.

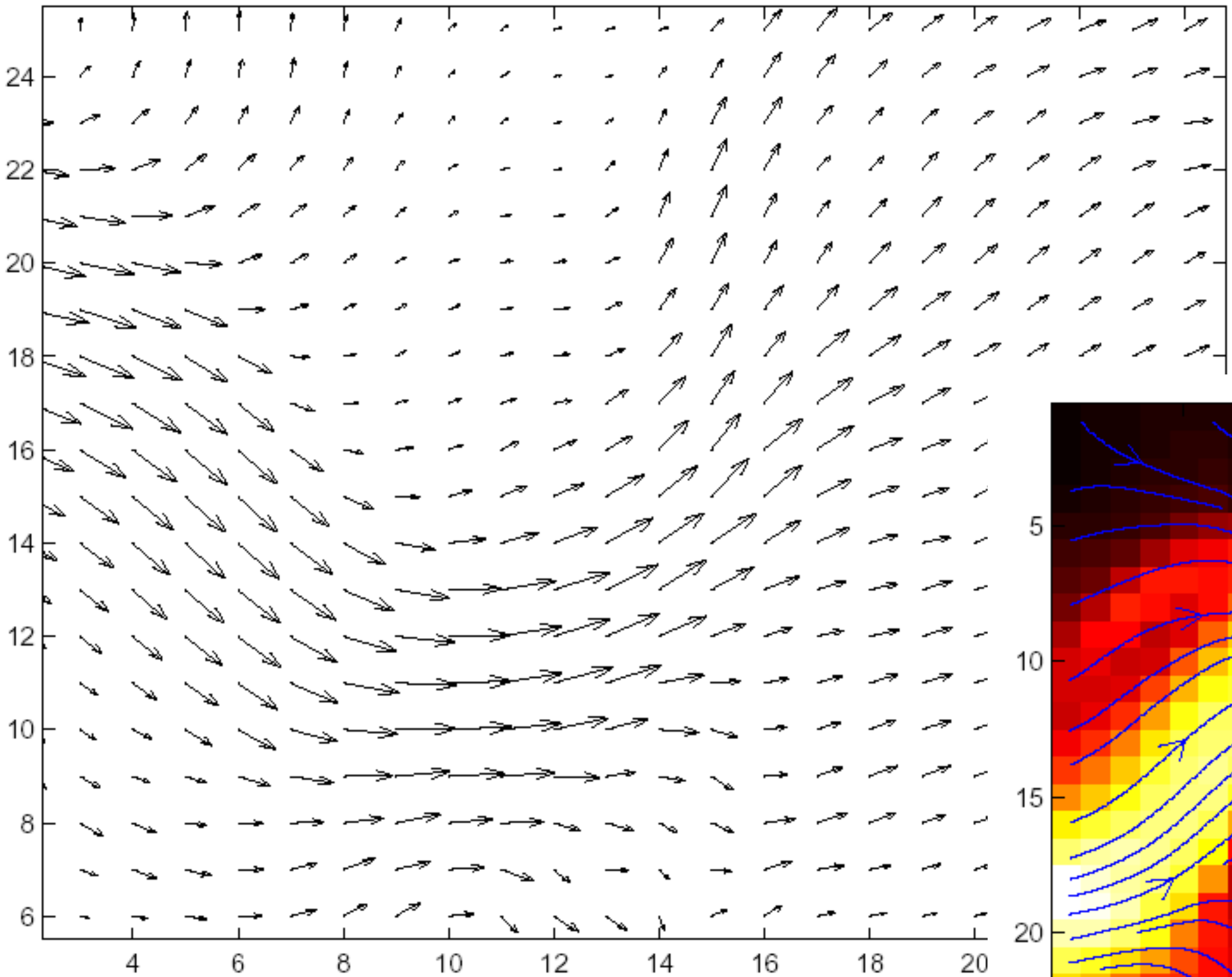

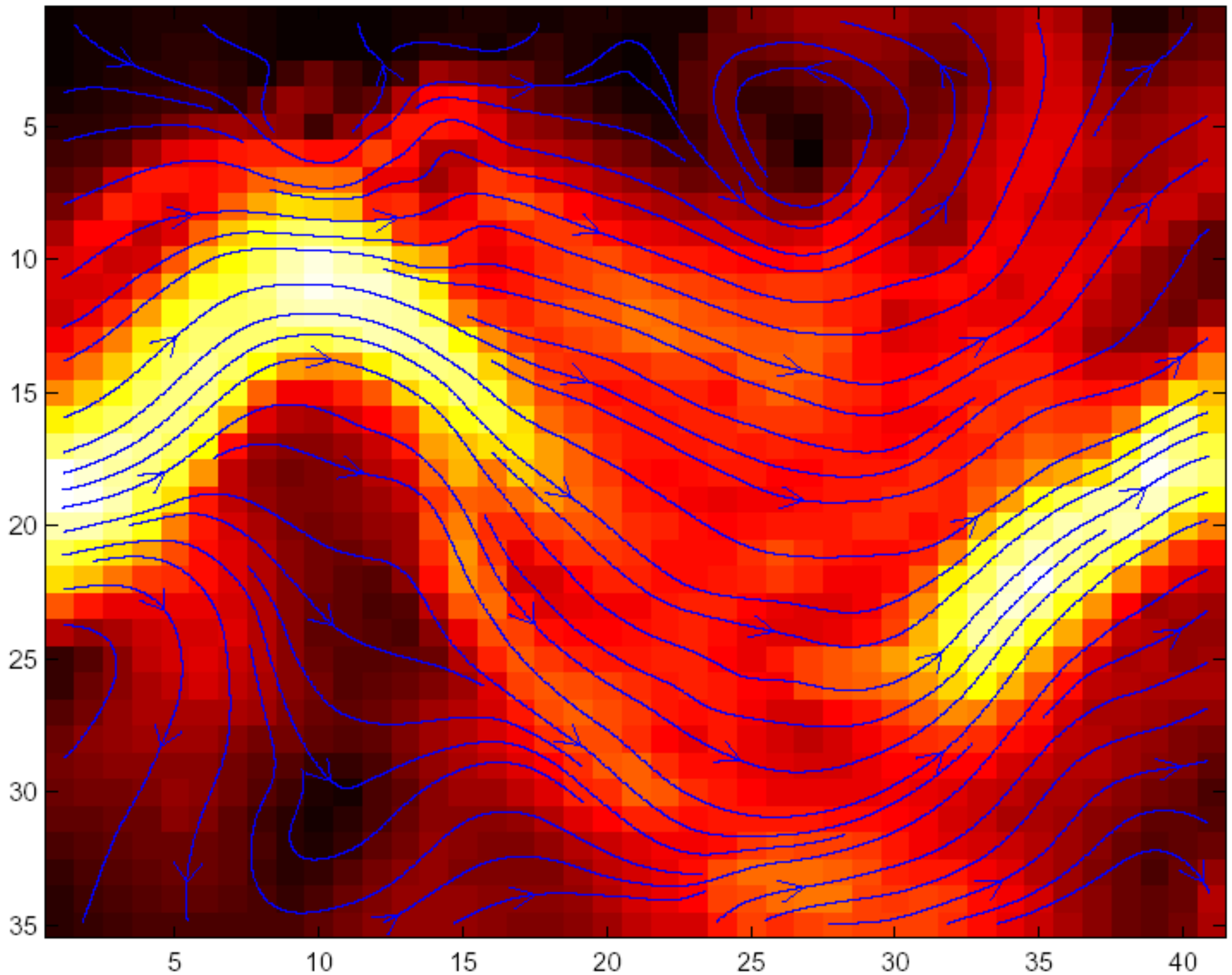

Stream lines generated
by the built-in MATLAB function

Tractography

Underlying Camino algorithm

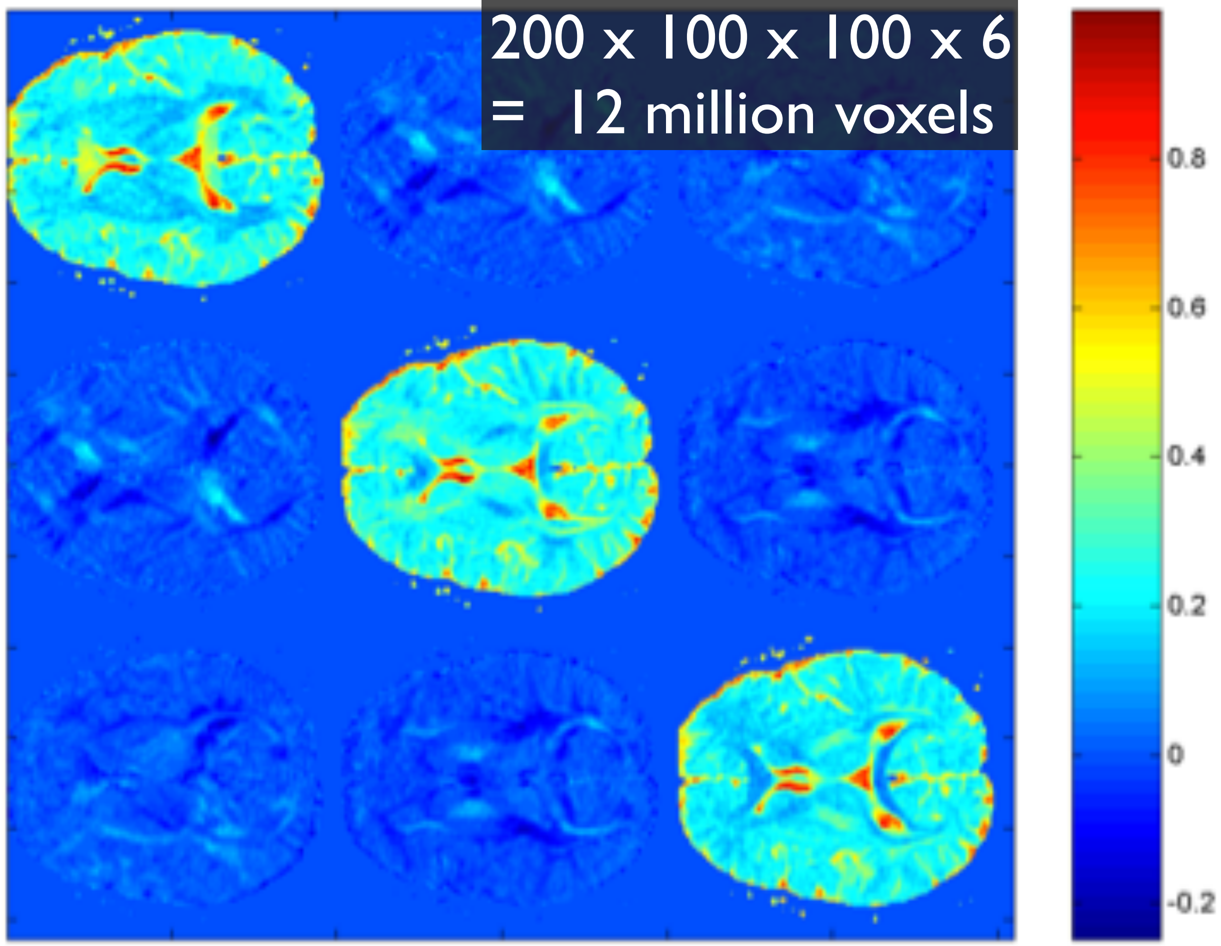

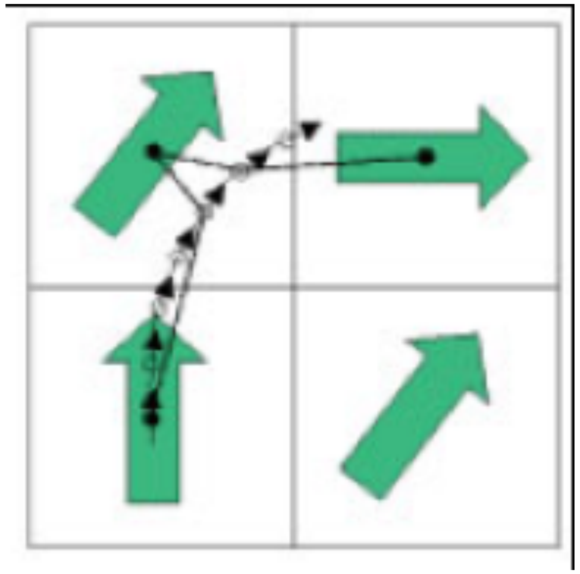

TENsor Deflection (TEND) algorithm

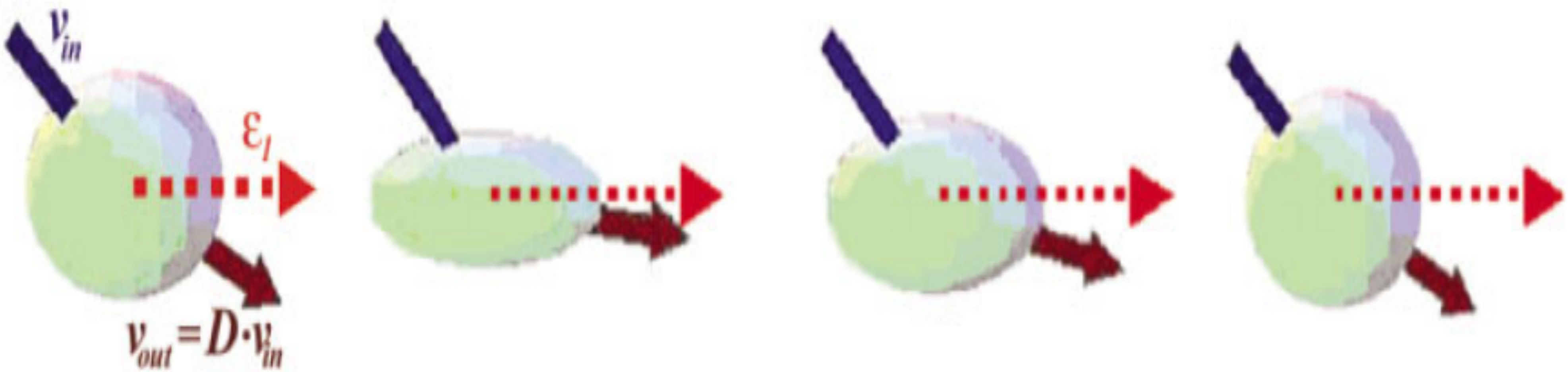

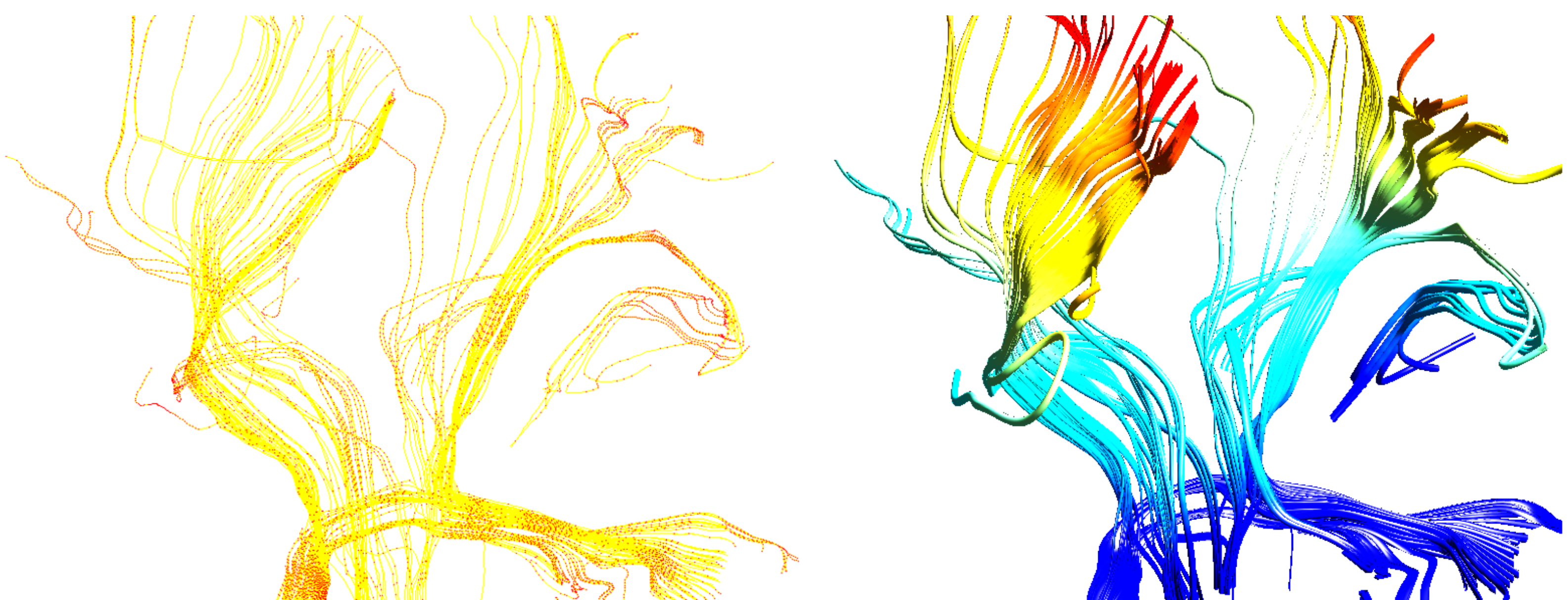

Second order Runge-Kutta algorithm with TEND

Lazar et al., HBM 2003

Tract Parametrization

Statistics and Its Interface Volume 3 (2010) 69–80

Cosine series representation of 3D curves and its application to white matter fiber bundles in diffusion tensor imaging

Moo K. Chung*, Nagesh Adluru, Jee Eun Lee, Mariana Lazar, Janet E. Lainhart and Andrew L. Alexander

Previous parametric model on white fiber tracts

Clayden et al. IEEE TMI 2007

Cubic B-spline is used to model and match tracts.

:computational nightmare

Batchelor et al. MRM 2006

Sine and cosine Fourier descriptors are used to extract global shape features for classification

: inefficient representation

Main contribution of Chung et al. (2010)

1. More efficient Fourier descriptor. It uses 1/2 number of basis than Batchelor et al. (2006).

2. Developed registration and averaging framework for 3D curves without numerically demanding optimization routines shown in Clayden et al. (2007).

Orthonormal basis in [0,1]

$$\Delta f + \lambda f = 0$$ Eigenfunctions form orthonormal basis

$$f(t) = f(-t)$$ Sine and cosine basis

$$f(t+2) = f(t)$$ Cosine basis: more compact representation

$$\lambda_l = -l^2\pi^2$$

$$\psi_0 = 1, \psi_l = \sqrt{2}\cos(l\pi t)$$

Fourier analysis in [0,1]

$$\sum_{l=0}^{k} f_l \psi_l(t) \to f$$

$$f_l = \langle f, \psi_l \rangle = \int_0^1 f(t)\psi_l(t)\, dt$$

This integral can be magically computed by matrix inversion

Least squares estimation

x, y, z coordinate vector → $$f(p_i) = \sum_{j=0}^{k} \beta_j \psi_j(p_i)$$

$$\mathbf{f} = (f(p_1), \cdots, f(p_n))' \quad \beta = (\beta_0, \cdots, \beta_k)'$$

$$\mathbf{Y} = \begin{bmatrix} \psi_0(p_1) & \cdots & \psi_k(p_1) \\ \vdots & \ddots & \vdots \\ \psi_0(p_n) & \cdots & \psi_k(p_n) \end{bmatrix}$$

$$\mathbf{f} = \mathbf{Y}\beta \quad \longrightarrow \quad \beta = (\mathbf{Y}'\mathbf{Y})^{-1}\mathbf{Y}'\mathbf{f}$$

White matter fiber tract model

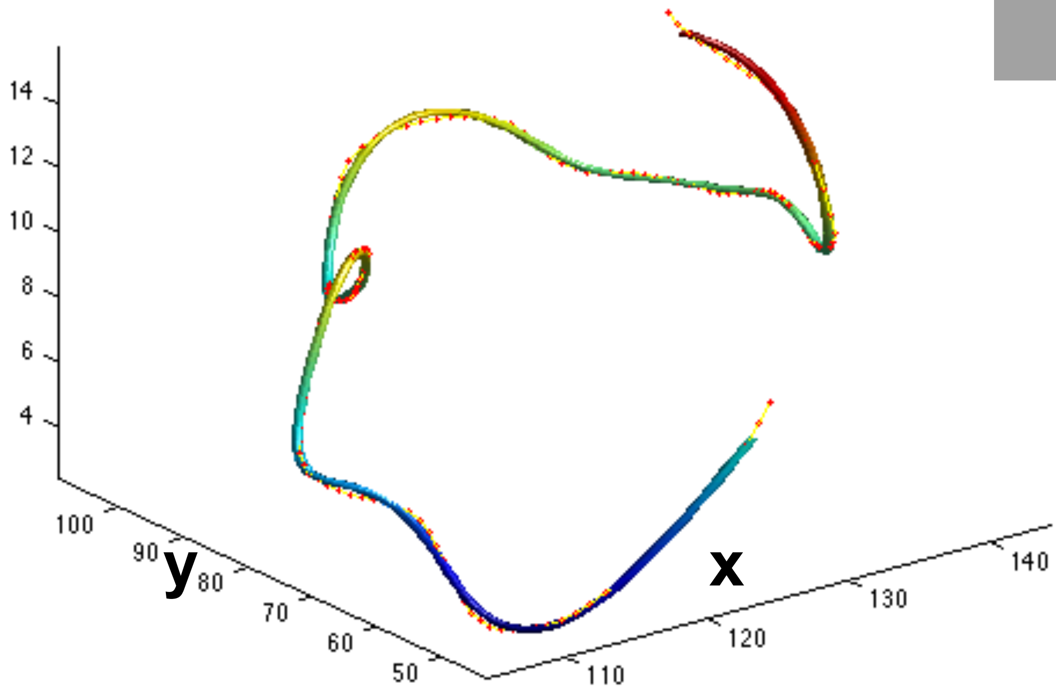

parameterization

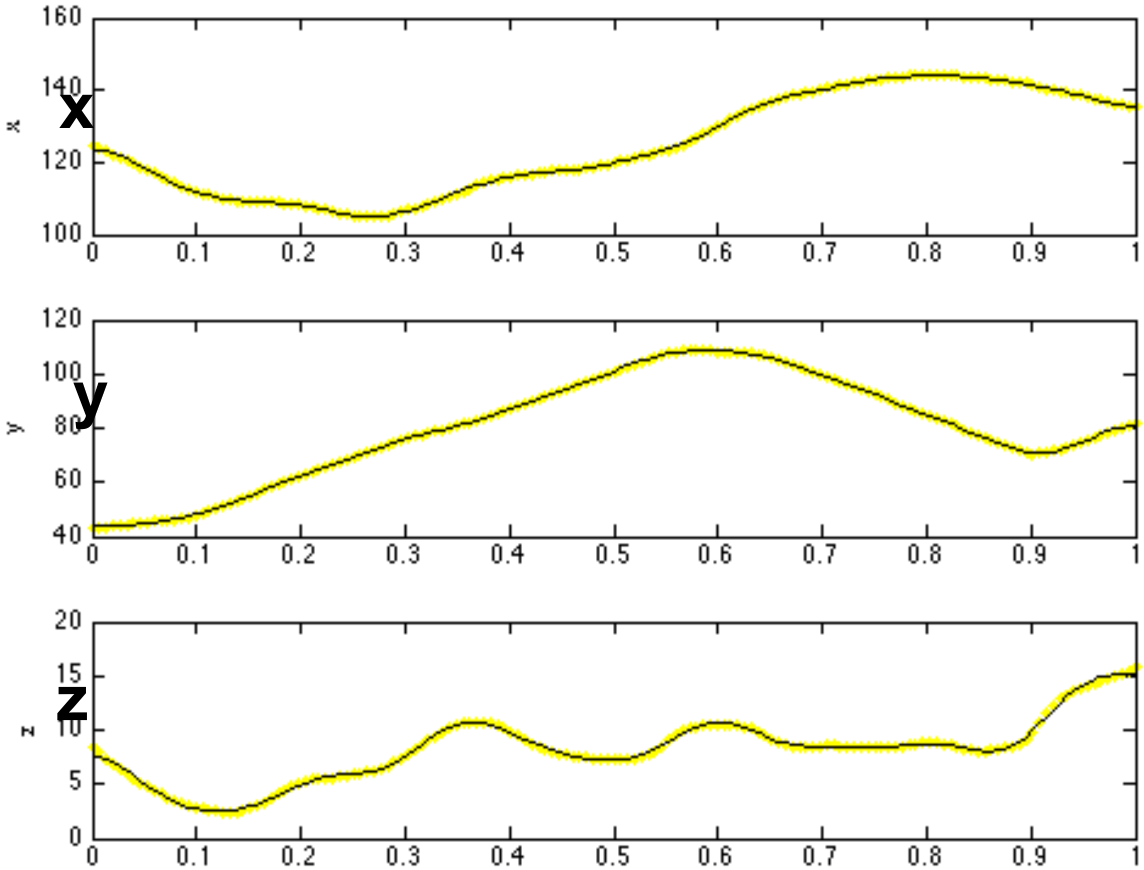

88.1799	56.6336	5.7367
-12.4775	-11.2552	-2.0791
2.4336	-15.4428	-0.4021
4.3956	2.2733	-0.9354
-0.0106	-0.0674	0.6999
2.1773	-2.4194	-0.1176
0.5808	0.8390	1.2942
0.0615	-0.1893	0.1188
-0.2629	0.7524	0.1089
0.7909	-0.7276	-0.1901
0.5458	0.6236	0.6939
0.4295	-0.4337	0.2185
0.2150	0.4157	0.0254
0.1584	-0.1973	0.0762
-0.1557	0.2466	-0.1086
0.0632	-0.0978	-0.0208
0.0389	-0.0143	-0.0284
-0.0014	-0.1193	0.1970
0.0004	0.0129	-0.0198
0.1342	0.0002	0.0260

Any tract can be compactly parameterized with only 60 coefficients.

basis expansion

$$(x, y, z)' = \sum_{l=0}^{19} \beta_l \cos(l\pi t)$$

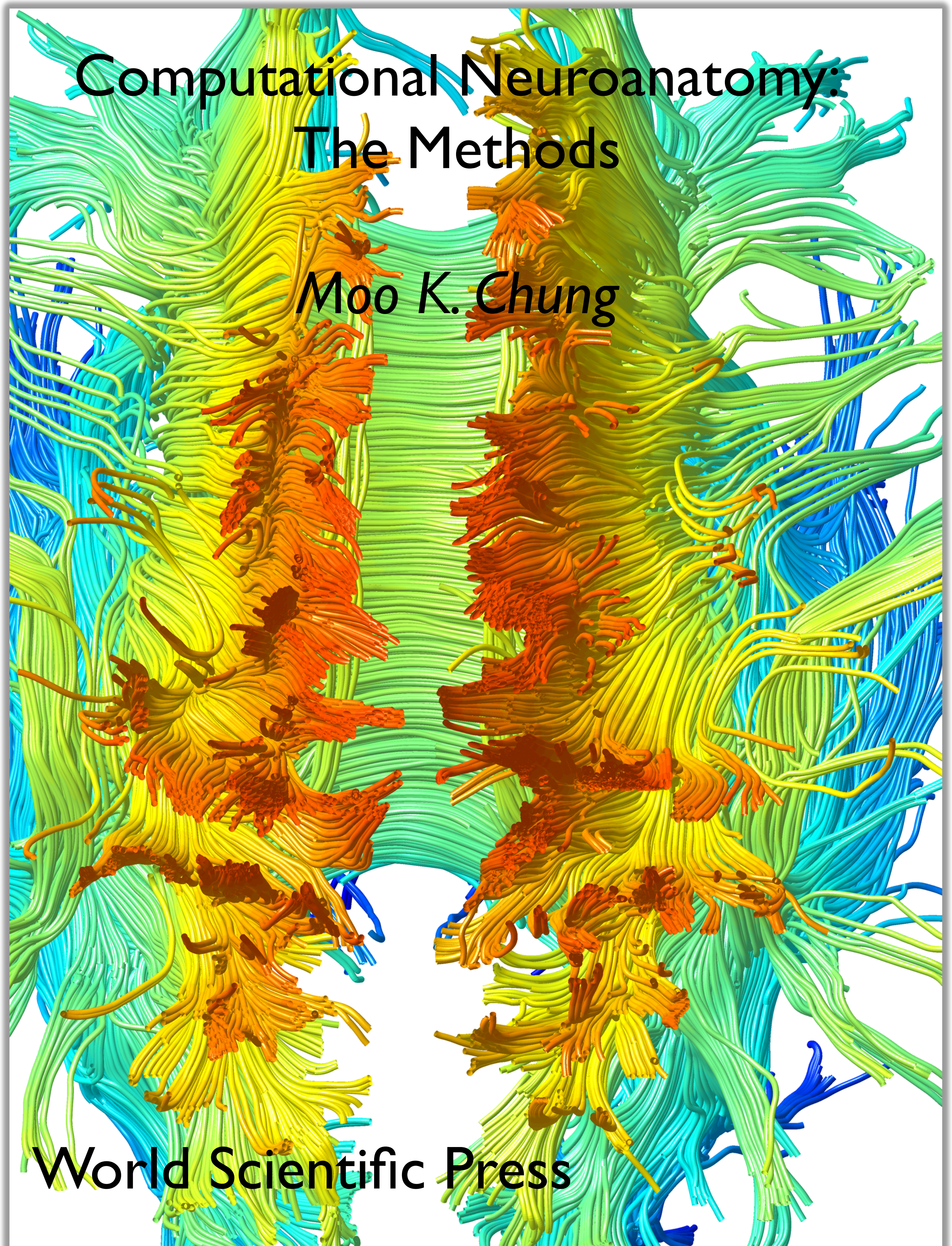

Cover art done using cosine series representation

409 page hardcover
50 color pages
available on Nov 30 2012 through www.amazon.com

Discrepancy measure: distance between tracts

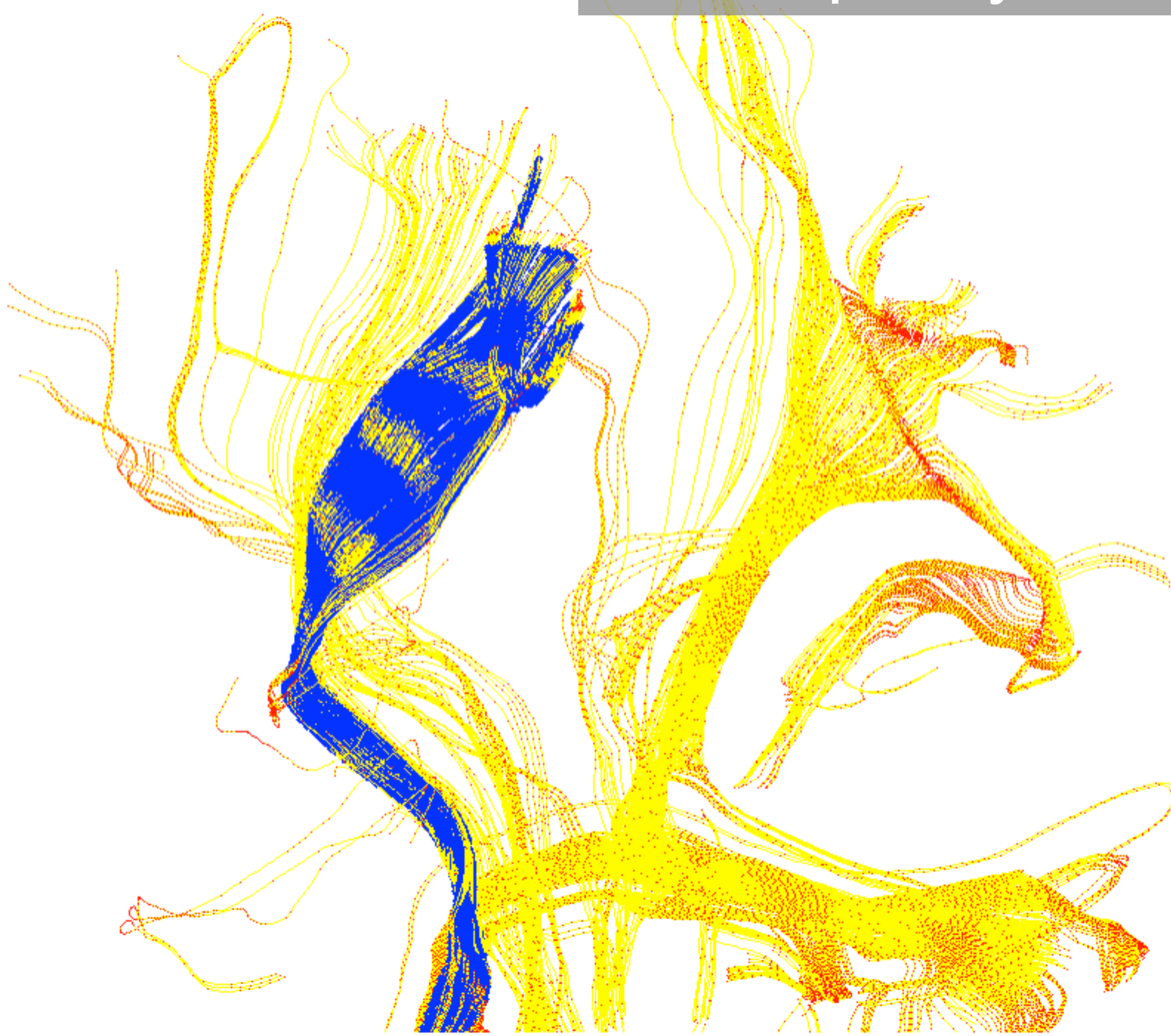

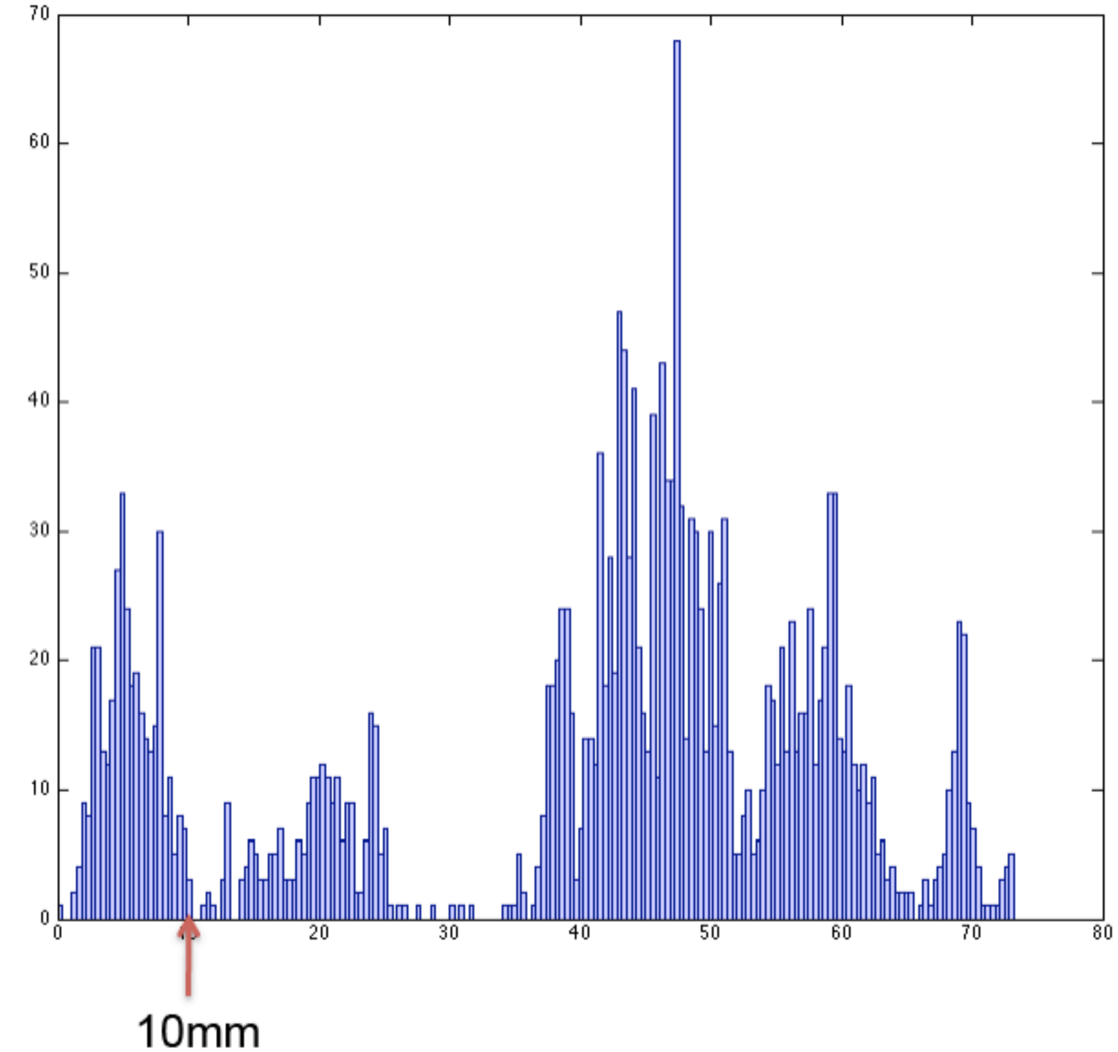

Histogram of discrepancy measure

$$\rho(\boldsymbol{\zeta}, \boldsymbol{\eta}) = \int_0^1 \|\boldsymbol{\zeta}(t) - \boldsymbol{\eta}(t)\|^2 \, dt$$

$$= \int_0^1 \sum_{j=1}^{3} \left[\sum_{l=0}^{k} (\zeta_{lj} - \eta_{lj}) \psi_l(t) \right]^2 dt = \sum_{j=1}^{3} \sum_{l=0}^{k} (\zeta_{lj} - \eta_{lj})^2$$

Define average tract

Given m cosine series representations $\zeta^1, \cdots, \zeta^m$

we define the average tract as

$$\overline{\zeta}(t) = \arg\min_{\zeta} \sum_{j=1}^{m} \rho(\zeta^j, \zeta)$$

$$= \sum_{l=0}^{k} \overline{\zeta}_l \psi_l(t)$$

The average tract is simply given by averaging coefficients.

Tract alignment

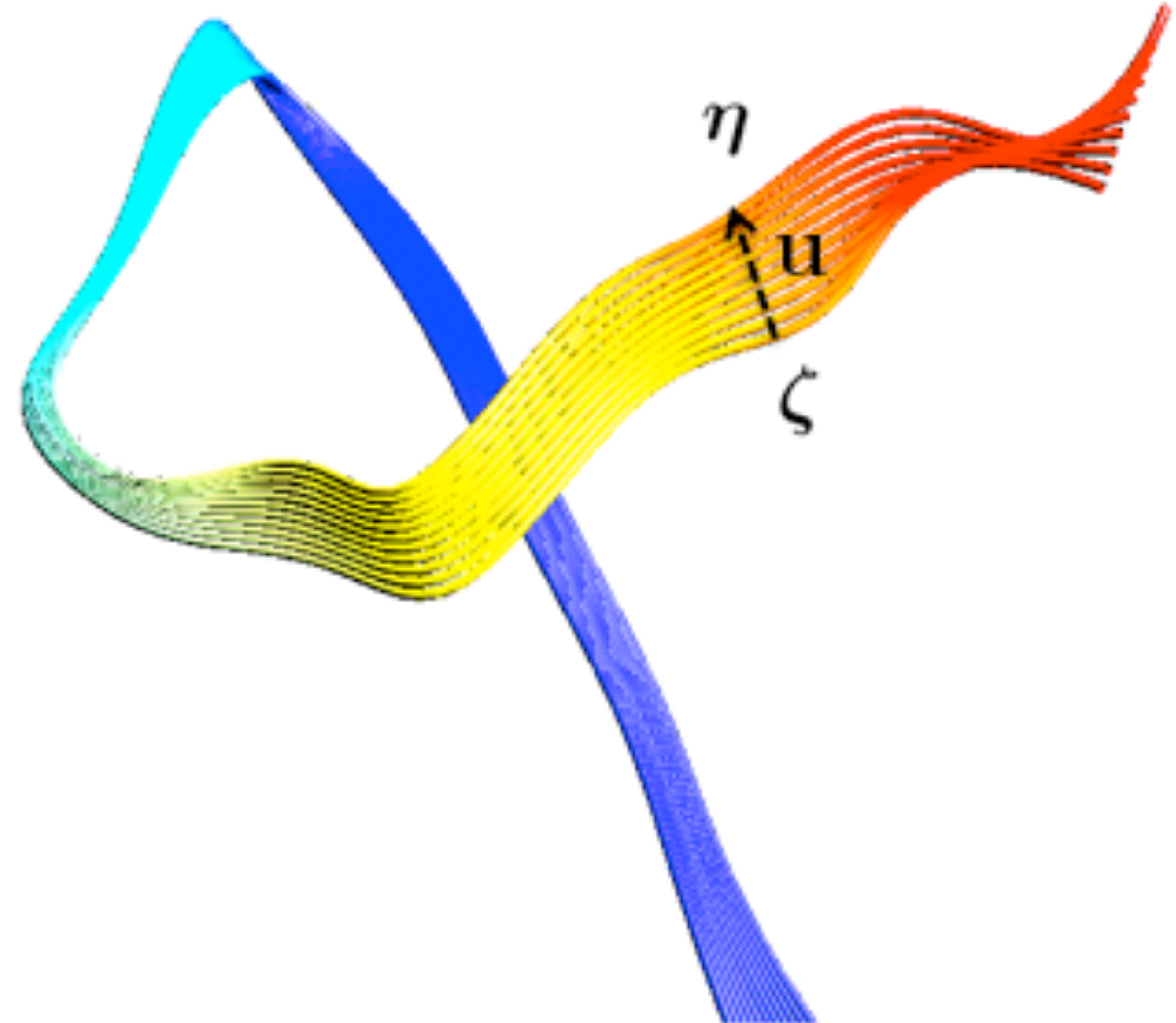

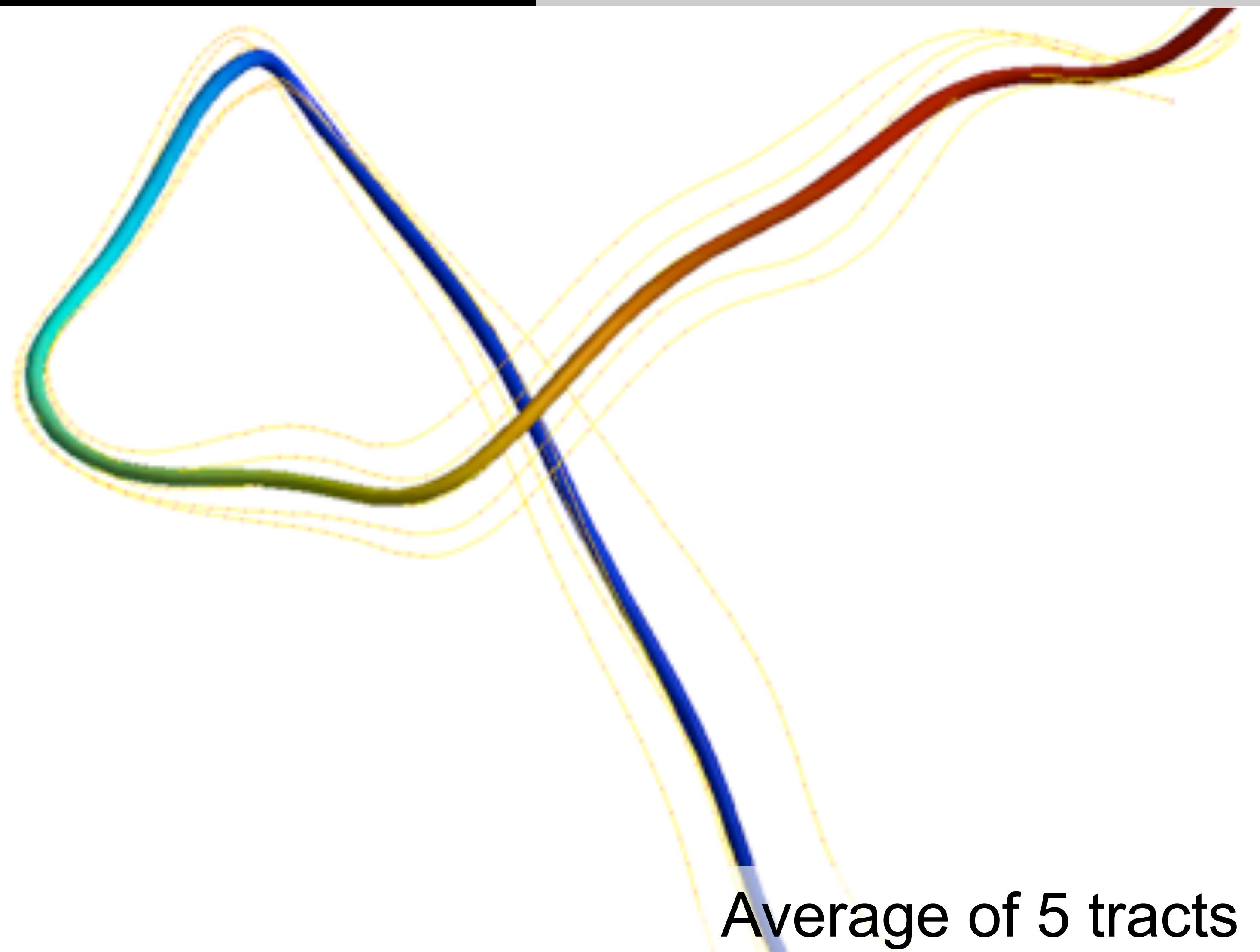

$$\boldsymbol{\eta}(t) = \sum_{l=0}^{k} \boldsymbol{\eta}_l \psi_l(t)$$

$$\boldsymbol{\zeta}(t) = \sum_{l=0}^{k} \boldsymbol{\zeta}_l \psi_l(t)$$

→

optimal displacement

$$\mathbf{u}^*(t) = \arg \min_{u_1, u_2, u_3} \rho(\boldsymbol{\zeta} + \mathbf{u}, \boldsymbol{\eta})$$

Minimum is taken over the subspace spanned by the basis functions.

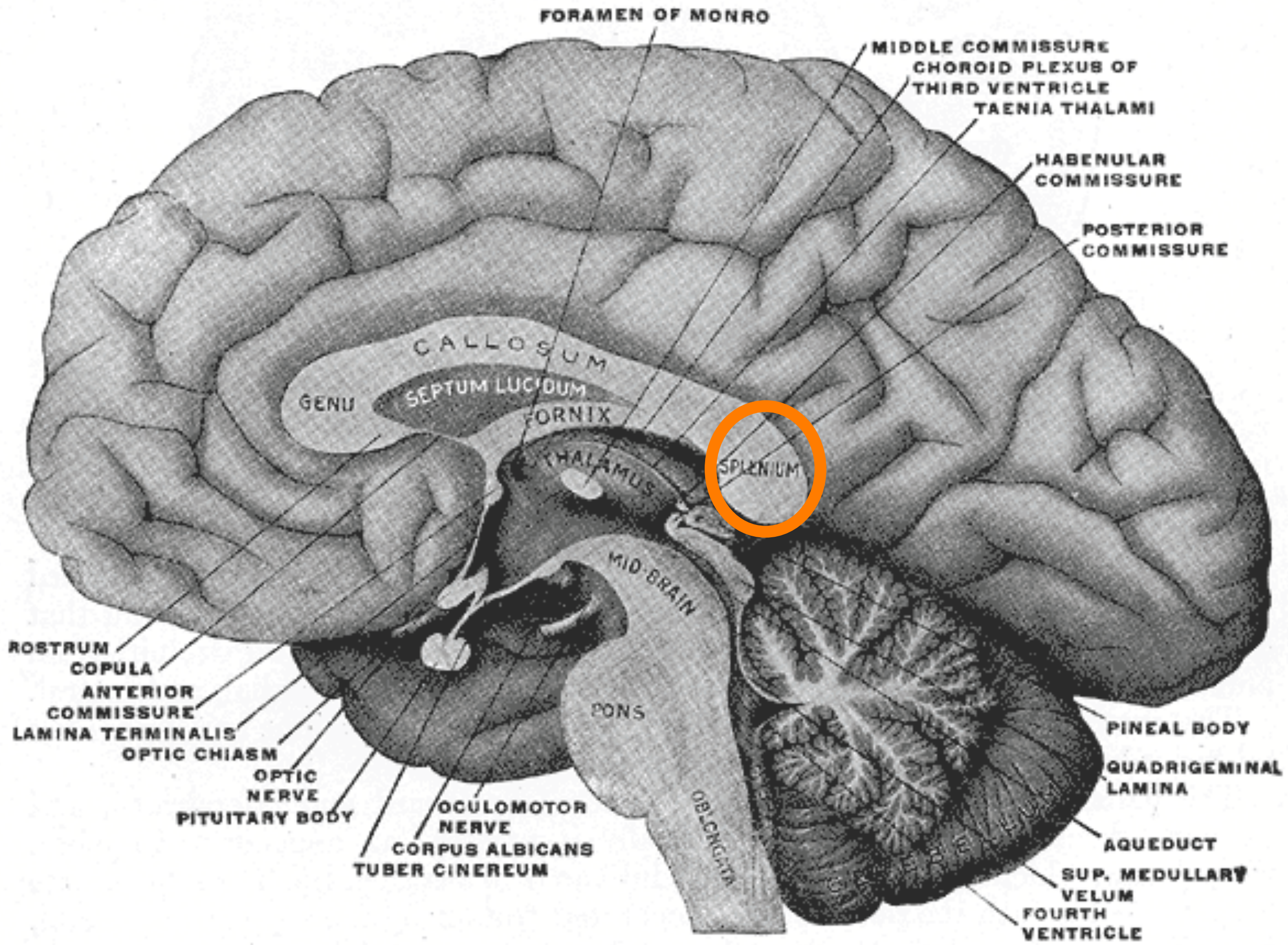

Average tracts passing through the splenium of the corpus callosum

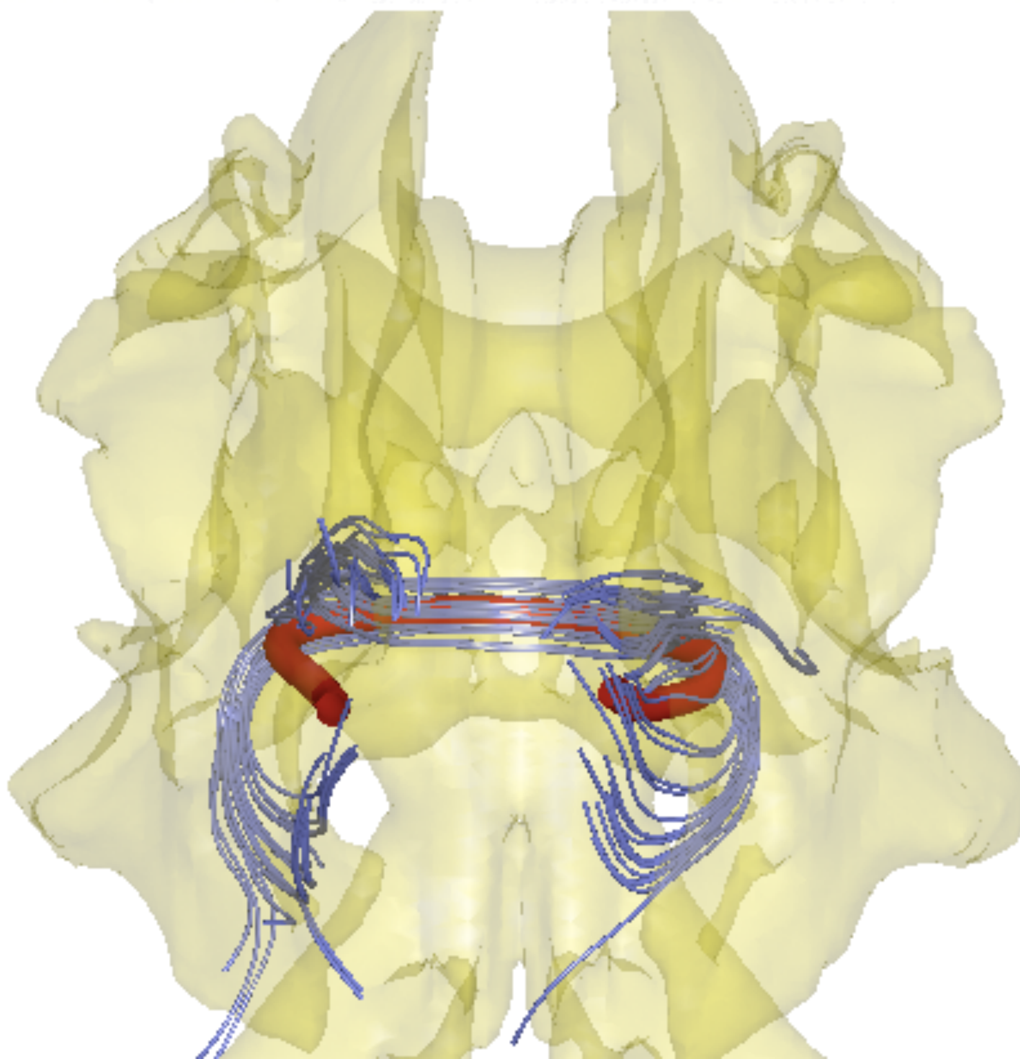

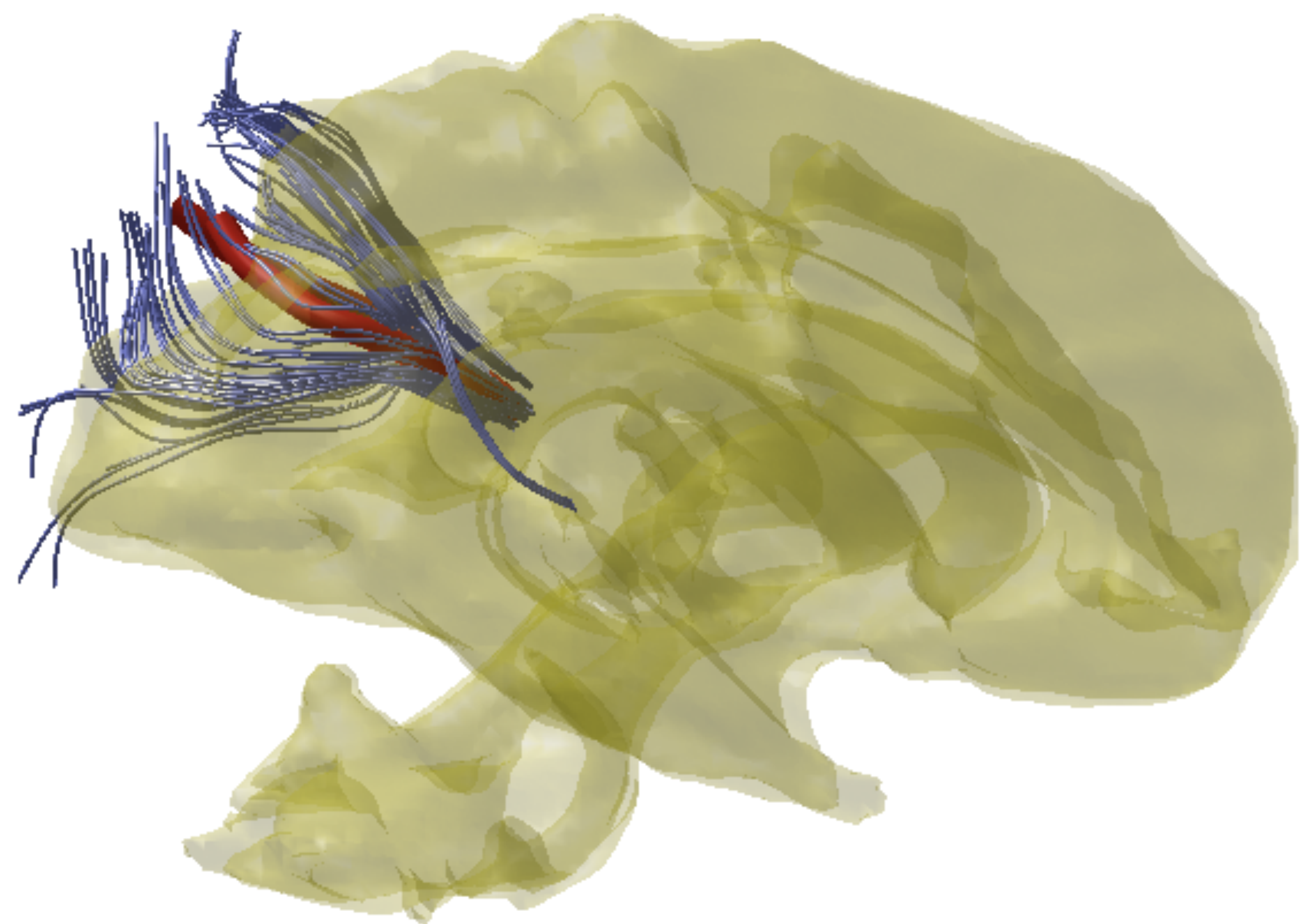

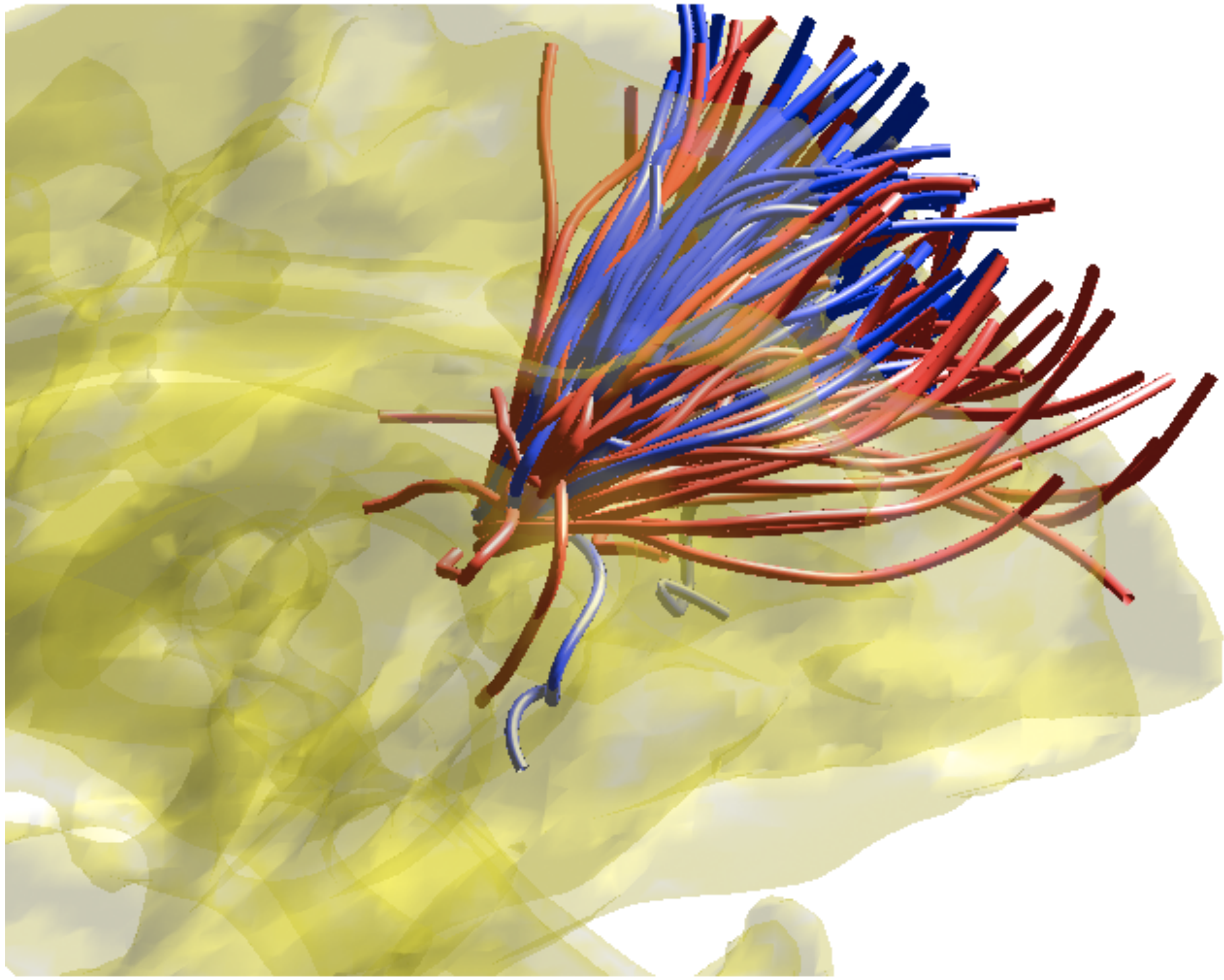

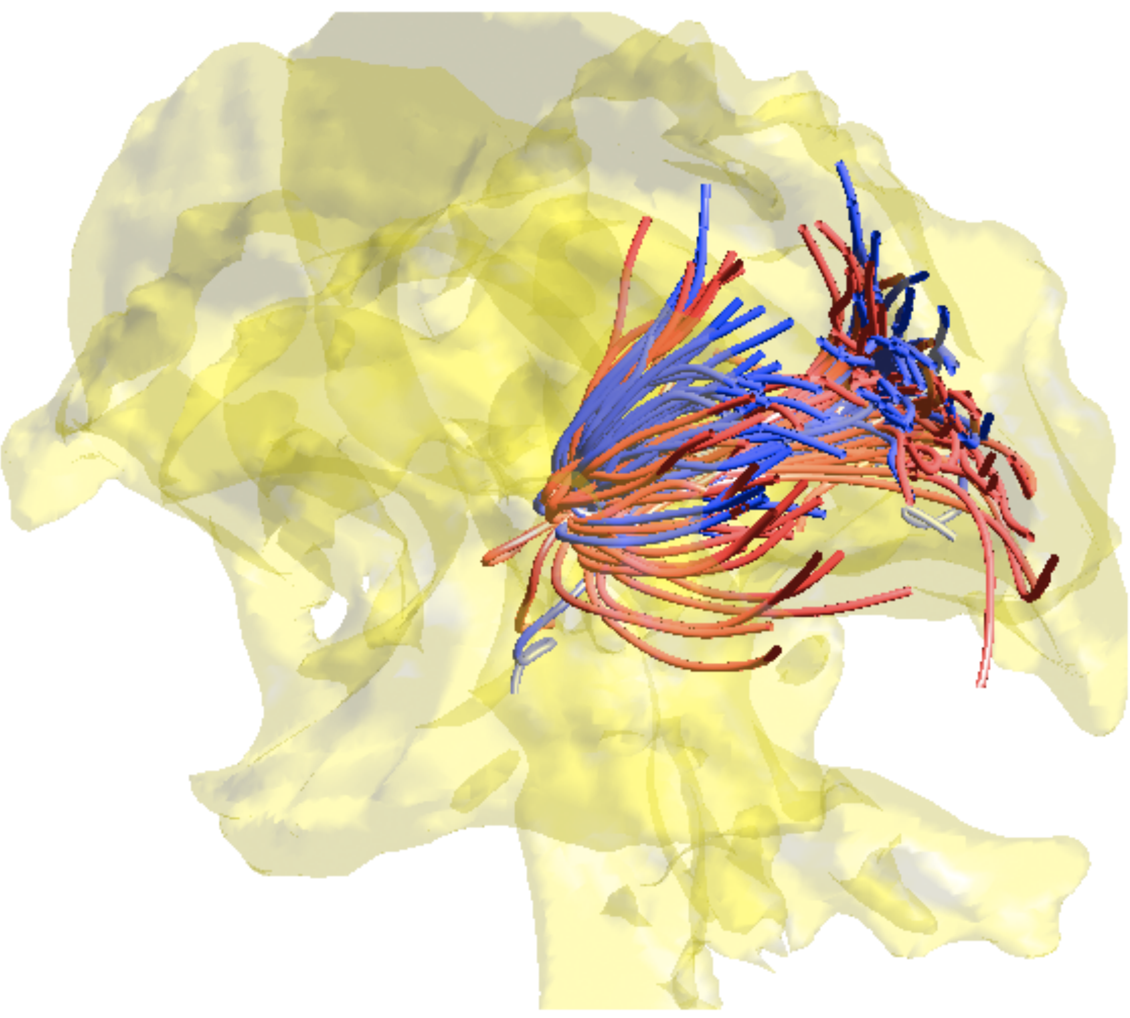

Average tracts across 74 subjects. Averaged within each subject (42 autistic 32 control)

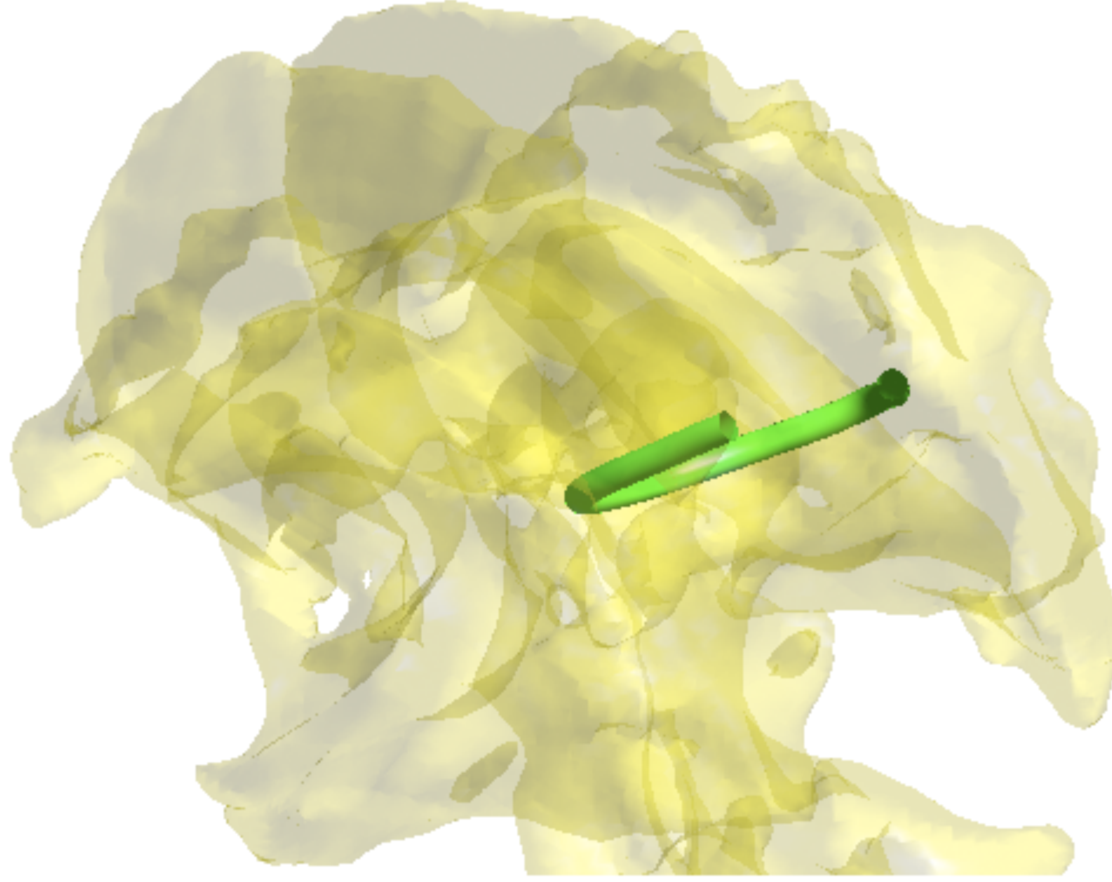

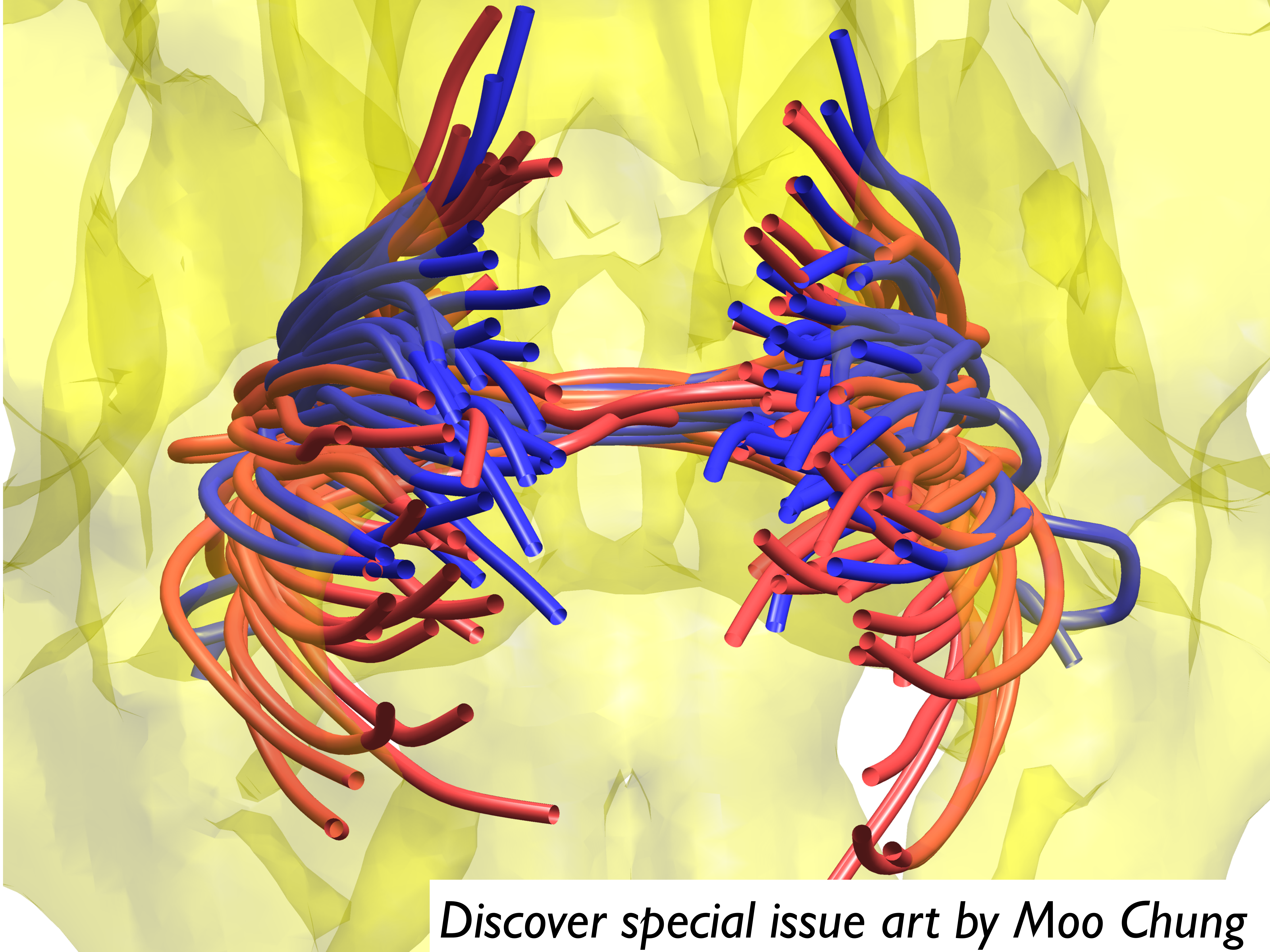

Discover special issue art by Moo Chung

Fiber concentration analysis using cosine series representation

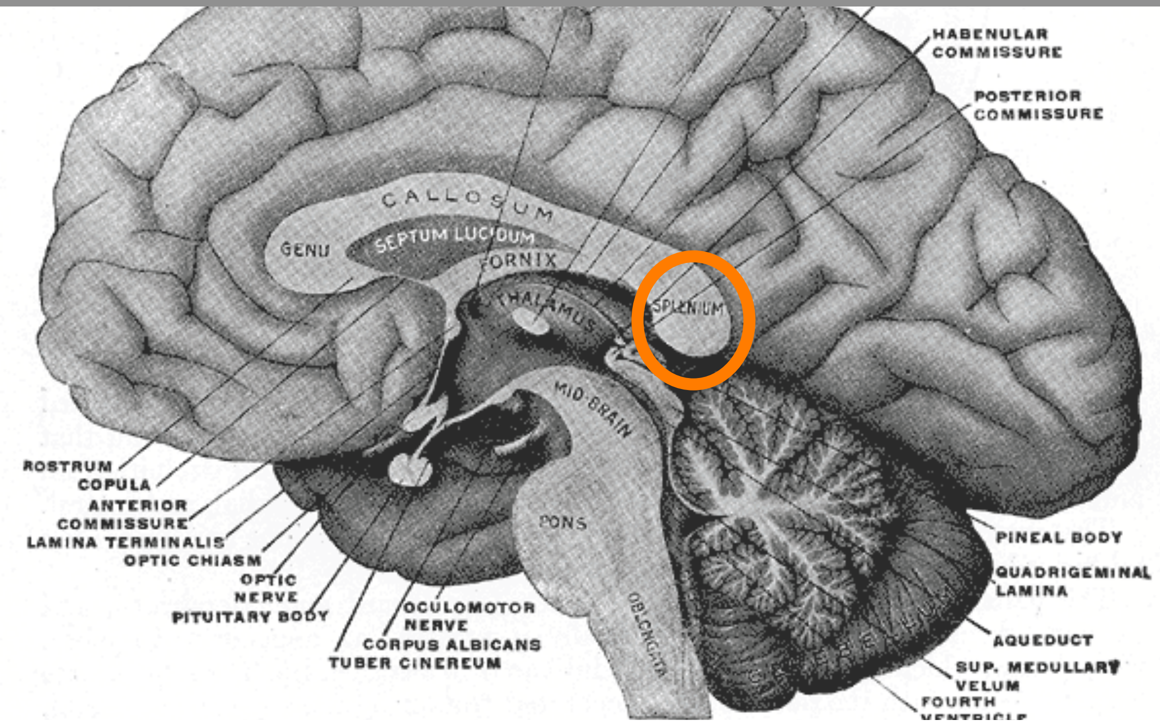

tracts passing through spleninum

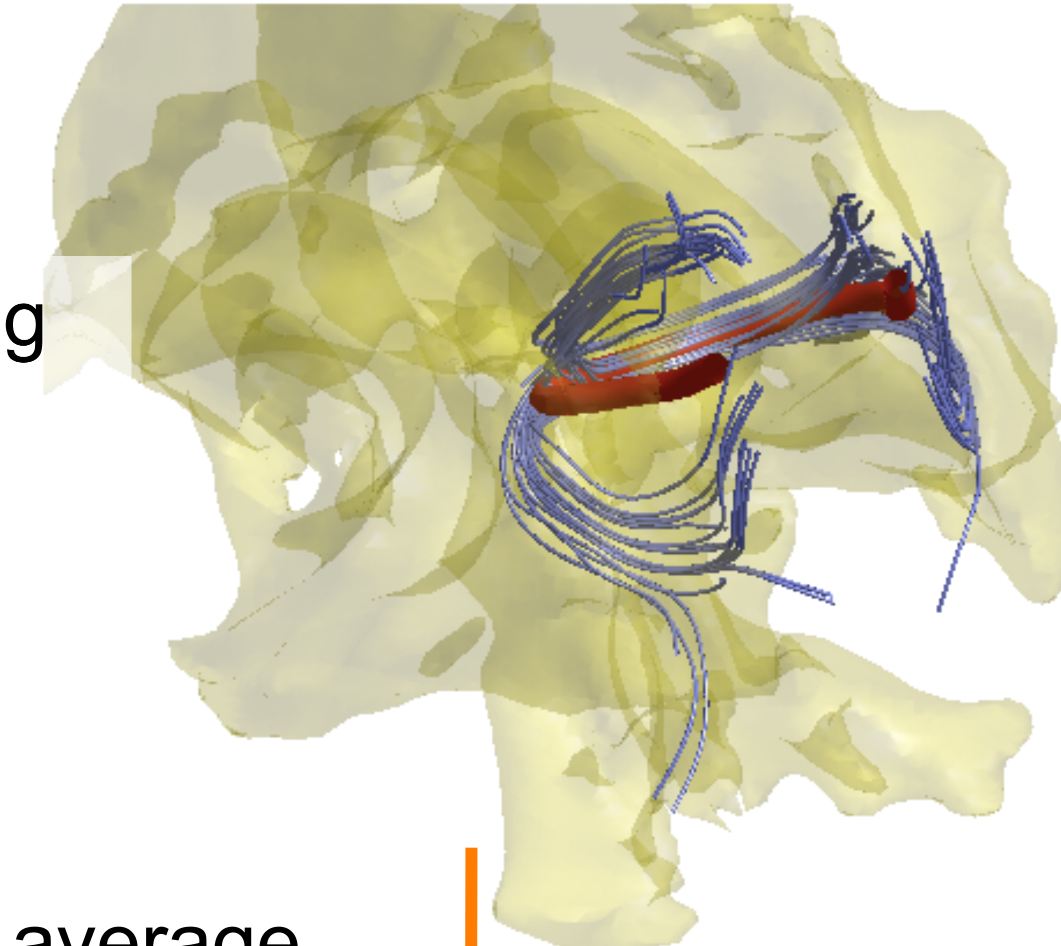

average tracts

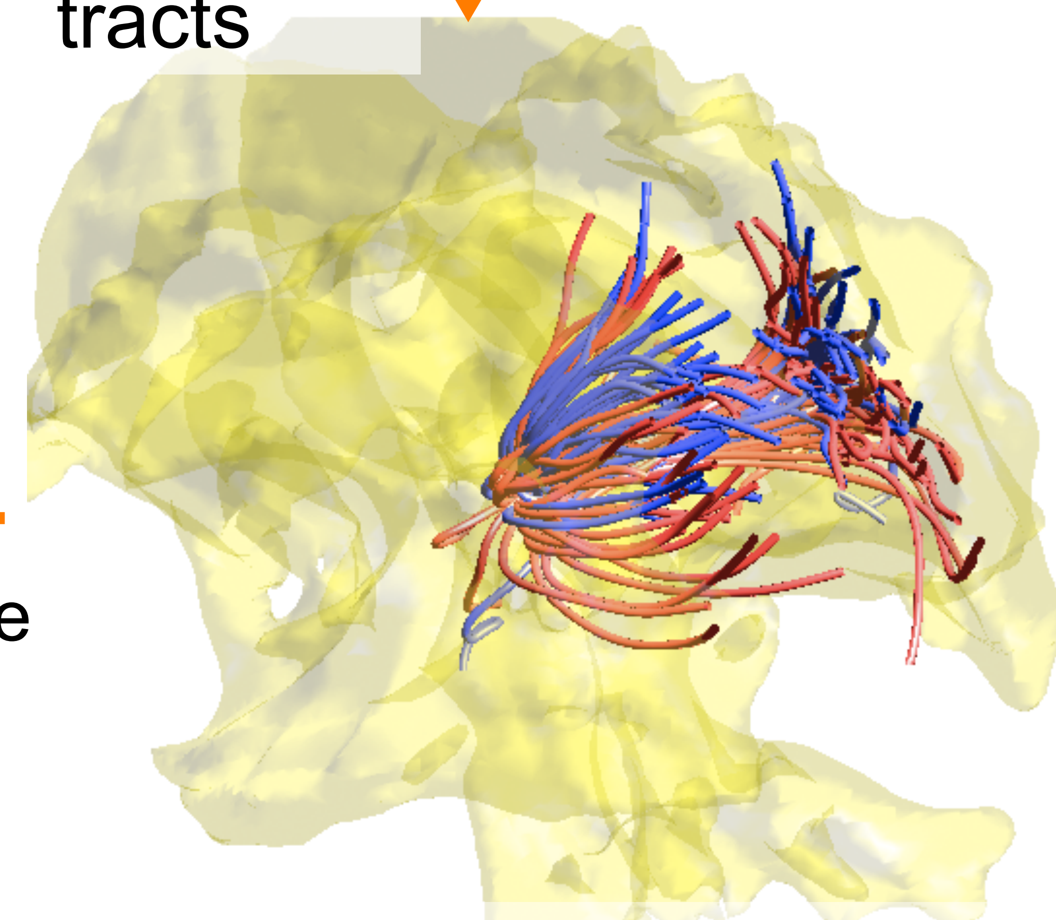

42 autistic & 32 control

two sample t-test

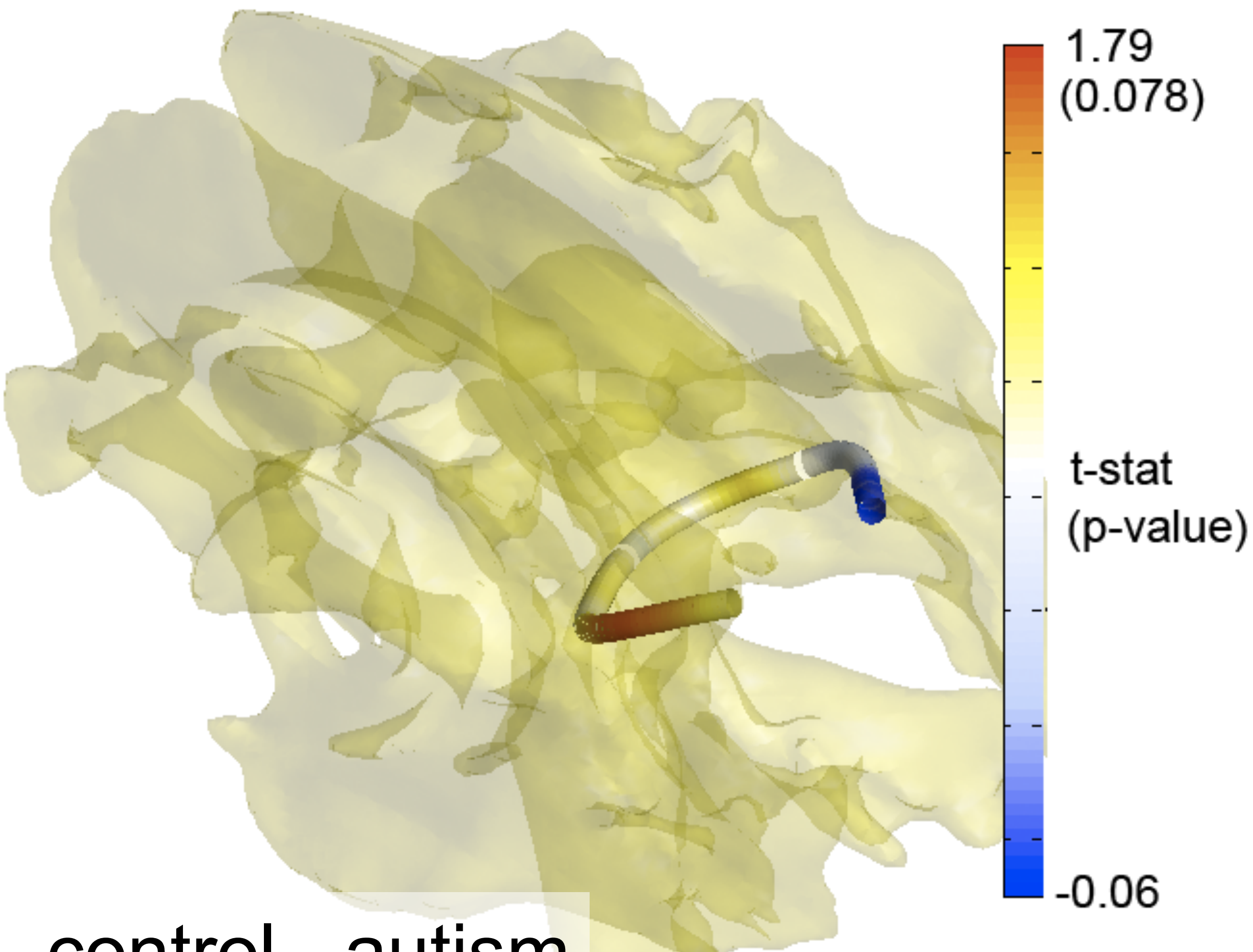

control - autism

Inference on representation

Compare tract shapes between the groups

$$\boldsymbol{\zeta}^1, \cdots, \boldsymbol{\zeta}^m \longleftrightarrow \boldsymbol{\eta}^1, \cdots, \boldsymbol{\eta}^n$$

This is done by testing the equality of mean tracts between the groups

$$H_0 : \overline{\boldsymbol{\zeta}} = \overline{\boldsymbol{\eta}}$$

Equivalent hypothesis

$$H_0' : \overline{\boldsymbol{\zeta}}_1 = \overline{\boldsymbol{\eta}}_1, \cdots, \overline{\boldsymbol{\zeta}}_k = \overline{\boldsymbol{\eta}}_k$$

Two cosine representations are equivalent if and only if the coefficients match

Two sample T-test and Hotelling's T-square result

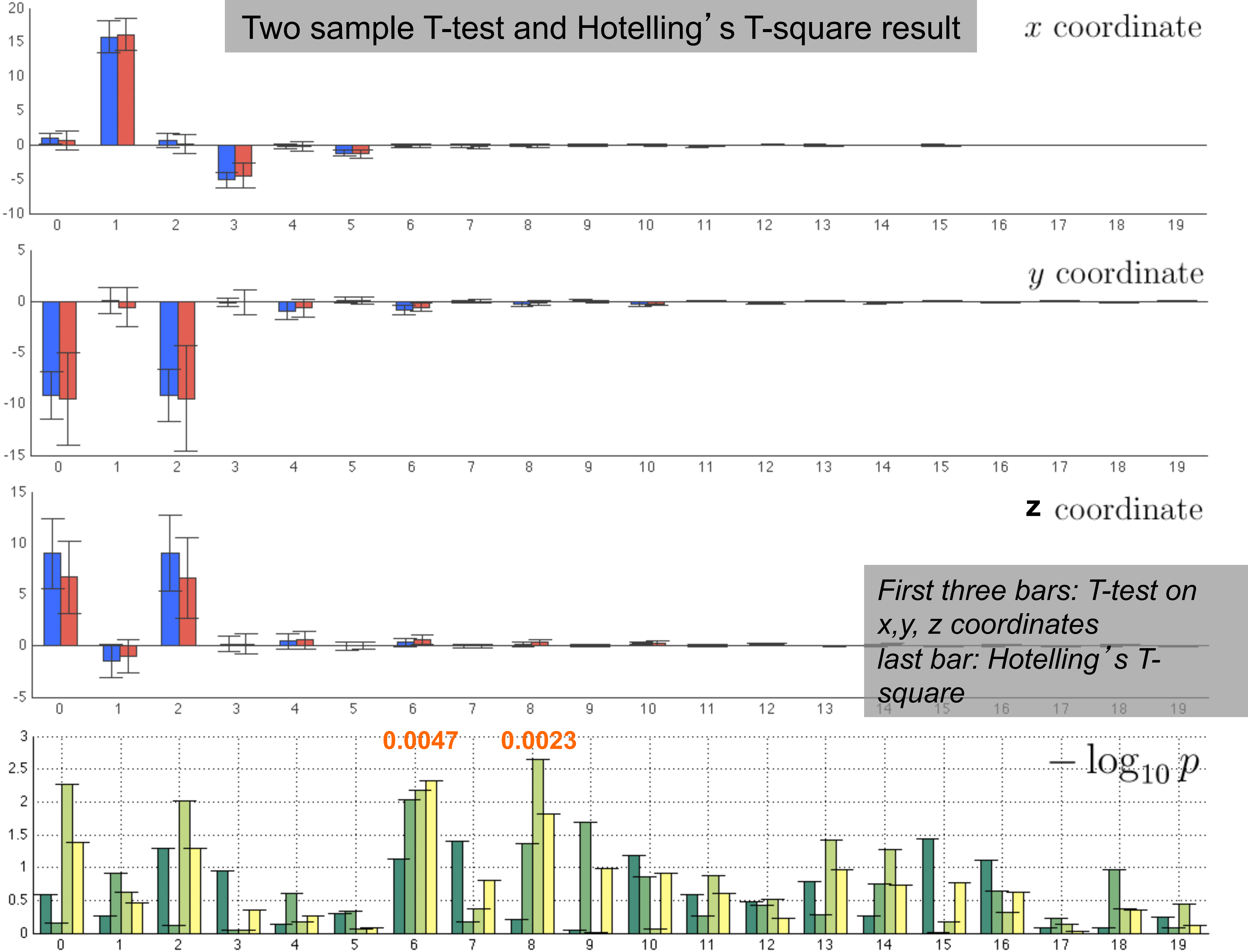

Validation via Random Simulation

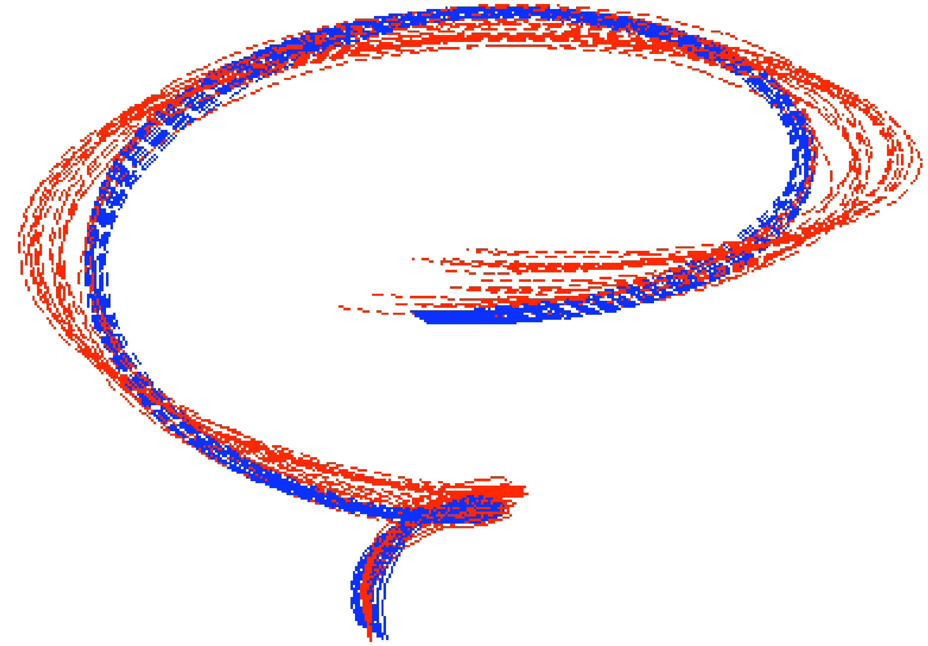

We have performed a simulation study to
proposed framework can detect small tract
between two collection of similarly shaped
the parametric curve

$$(18) \qquad (x, y, z) = (s \sin s, s \cos s, s), s \in [0, 10]$$

as a basis for simulation, we have generated two groups of random curves. This gives a shape of a spiral with increasing radius along the z-axis. The first group consists of 20 curves generated by

$$(x, y, z) = (s \sin(s + e_1), s \cos(s + e_2), s + e_3),$$

where $e_1, e_2, e_3 \sim N(0, 1)$. The second group consists of 20 curves generated by

$$(x, y, z) = ((s + e_4) \sin(s + 0.1), (s + e_5) \cos(s - 0.1), s - 0.1),$$

where $e_4, e_5 \sim N(0, 0.2^2)$. The non-additive noise is given

Forward model selection framework

$$\zeta_i(t) = \sum_{l=0}^{k} c_{li}\psi_l + \epsilon_i(t)$$

When do we stop the expansion?
Why did we choose degree 19?

optimal degree = 13.94 ± 7.02
upper 80 percentile = 19

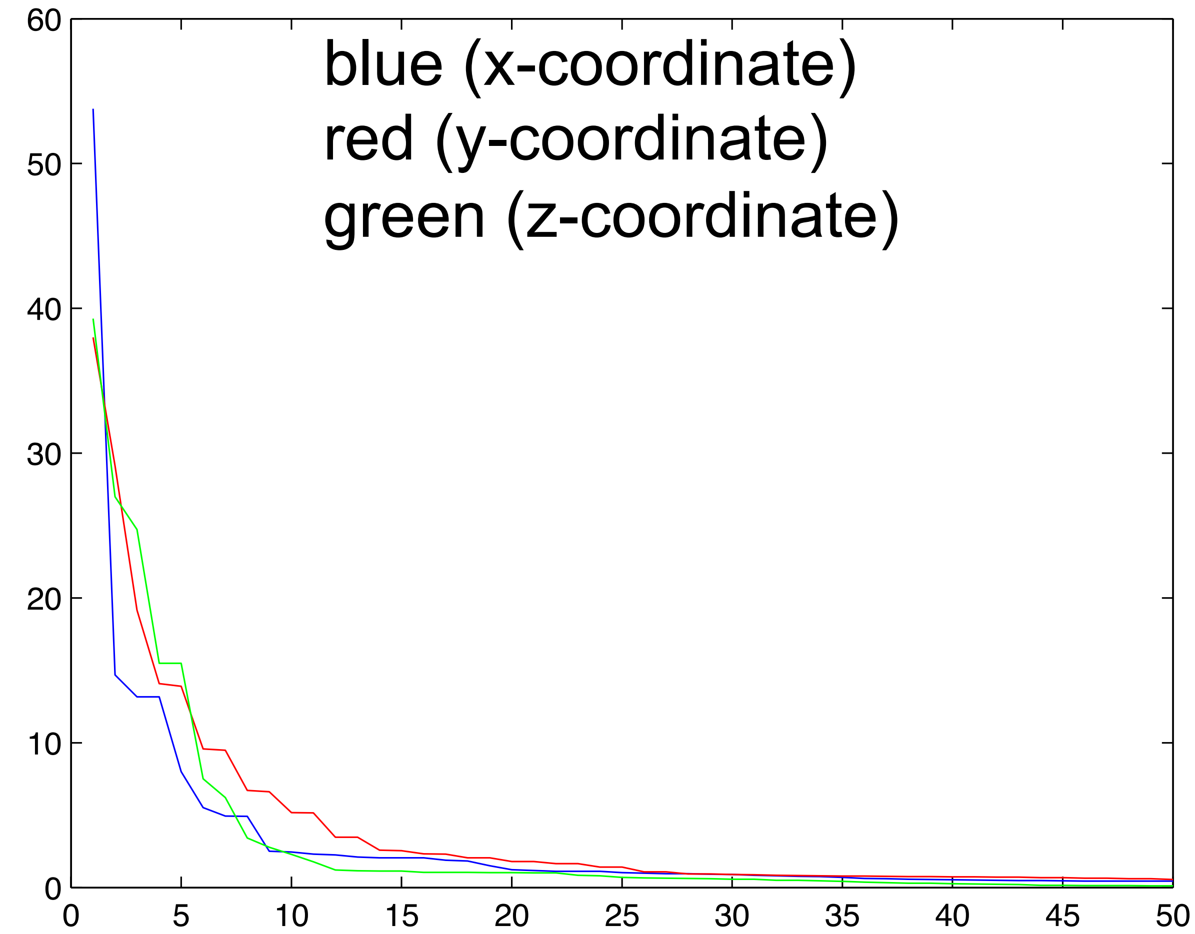

$$SSE_k = \sum_{j=1}^{n} \left(\varsigma_i(t_j) - \sum_{l=0}^{k} \hat{c}_{li} \psi_l(t_j) \right)^2$$

Figure 3. As the degree k increases, SSE decreases until it flattens out. So it is reasonable to stop the series expansion when the decrease in SSE is no longer significant. Under H_0, the test statistic F follows

$$F = \frac{\mathrm{SSE}_{k-1} - \mathrm{SSE}_k}{\mathrm{SSE}_{k-1}/(n-k-2)} \sim F_{1,n-k-2},$$

the F-distribution with 1 and $n-k-2$ degrees of freedom. We compute the F statistic at each degree and stop increasing the degree of expansion if the corresponding p-value first becomes bigger than the pre-specified significance $\alpha = 0.01$.

Thank you

Most MATLAB codes used for this lecture can be obtained from www.stat.wisc.edu/~mchung